Chesapeake Civil Transport Rotorcraft

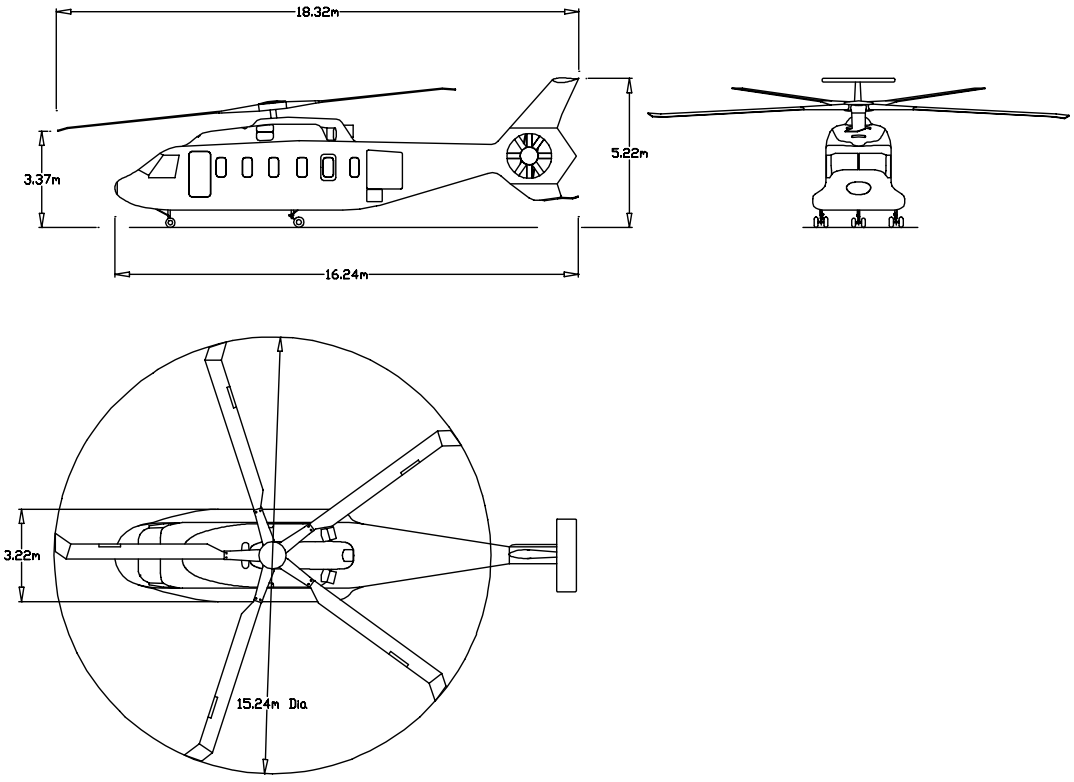

Department of Aerospace Engineering
University of Maryland
College Park, Maryland 20740

May 29, 1998

University of Maryland

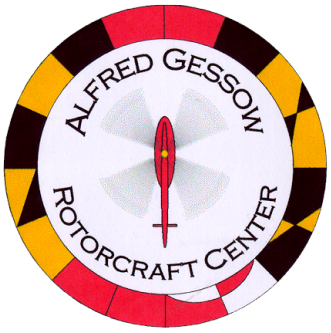

Alfred Gessow Rotorcraft Center
Department of Aerospace Engineering
University of Maryland, College Park
Maryland, 20742

Chesapeake Civil Transport Rotorcraft

In response to the 1998 Annual American Helicopter Society
Student Design Competition - Graduate Category
29 May 1998

Andreas P.F. Bernhard - Team Leader

Dr. Inderjit Chopra - Faculty Advisor

Jason Kiddy

Jayant Sirohi

R. Clifton Moody

Mao Yang

Jinwei Shen

Hyeonsoo Yeo

ACKNOWLEDGEMENTS

The design team would like to express its sincerest thanks to Dr. Marat Tishchenko and Dr. V.T. Nagaraj for their valued guidance with this design project. It was a privilege and an honor to attend the Spring 98 design lectures offered by these two renowned and accomplished helicopter designers. We would like to thank Dr. Inderjit Chopra for re-establishing the helicopter design course at the University of Maryland. The team also extends its gratitude to Prof. Alfred Gessow for his wise advice and recommendations.

Contents

List of Figures

List of Tables

EXECUTIVE SUMMARY

Introduction

The *Chesapeake* is a helicopter that has been designed in response to the Request for Proposal (RFP), issued for the 1998 *American Helicopter Society* Student Design Competition (sponsored by Boeing). The RFP identified the need for a civil short-haul VTOL aircraft. The primary market is expected to be the Northeast Corridor of the USA. It is envisaged that the VTOL infrastructure will be developed and integrated into the regional fixed wing flight operations. In particular a network of vertiports will be established, linking outlying areas with regional fixed wing hubs.

Specified Mission Requirements

The aircraft is to be optimized to maximize cost effectiveness. The standard mission consists of an un-refueled, two-leg roundtrip, with each leg a maximum of 200 nm. The standard version is a 19-seat aircraft, with launch in 2012. As a "lead-in" product, to be launched in 2007, a 12-seat derivative is required. This variant is to have commonality of all dynamic systems (including the rotor and transmission) and substantial commonality of subsystems. The fleet is sized to meet an initial requirement of 700,000 passenger miles per day, increasing to 1,100,000 passenger miles per day. The design is constrained by a stringent one-engine-inoperative (OEI) requirement that stipulates a OEI hover out of ground effect (HOGE), at mean-sea level, ISA+20, with a full passenger load and 60% fuel.

Aircraft Configuration Trade-Off Study

Both a conventional helicopter and a tiltrotor/tiltwing were considered as suitable candidates for this design, whereas compound helicopters, ABC and X-Wing were eliminated because of their poor cost effectiveness for the short-haul civil commuter mission. The trade study shows that a triple engine helicopter (with the option for switching-off one engine in cruise to improve the cruise efficiency) is more economical than a twin- or triple-engine helicopter (cruising on three engines) or a tiltrotor/tiltwing. In fact, the direct operating cost per air-seat-mile of the helicopter is 10% lower than that of a tiltrotor, for a typical 2x150 nm mission. The helicopter also offers several operational advantages, including: a lower disk loading (with associated lower downwash and reduced BVI noise during take-off and landing) and a lighter/more compact apron footprint.

The Chesapeake at a Glance

The Chesapeake is a 19 seat, triple engine helicopter with a fan-in-fin. The aircraft is designed to offer the passenger a "jet-smooth" ride, and the operator an affordable aircraft that is cost-competitive in the civil short-haul market. The spacious cabin is one of the largest in its class and with active vibration and noise-control offers a flight experience rivaling that of fixed wing turbojets.

- Advanced technologies are used to improve cost effectiveness. The Chesapeake has a low disk loading, five-bladed bearingless rotor. The composite rotor blades exhibit tip sweep and anhedral to improve performance

and incorporate smart trailing edge flaps for automatic in-flight tracking and vibration control. It is anticipated that future versions will use multiple flaps to address both vibration control and and BVI noise reduction.

- A fully integrated health and usage monitoring system (HUMS) is used to oversee the status and direct on-condition maintenance of flight-critical dynamic components (including the transmission, rotor hub and rotor blades and the fan tail). The Chesapeake is powered by three IHPTET 930 kW (1250 hp) turboshaft engines, that have a 30 second, 125% emergency rating. The engines are controlled via a full authority digital engine control (FADEC) system, that offers advanced engine diagnostics and also reduces the pilot workload during one-engine-inoperative (OEI) operations. The aircraft exceeds the stipulated OEI requirements to the extent that hover out of ground effect, with one engine inoperative, in ISA+20, with full passenger load and 60% fuel can be sustained at 5500 ft. This performance increase is derived from the engines, which are sized to meet the requirement to cruise on two engines, rather than the baseline OEI requirement. The cost of the more powerful engines is offset by the improved cruise fuel consumption and the resultant lower take-off weight.

- A fan-in-fin anti-torque system is used to improve safety of ground operations. An asymmetric arrangement of the fan blades is used to reduce noise levels.

- Based on a preliminary cost analysis, it is expected that the Chesapeake will cost $9.03 million (1997) and will have a direct operating cost per air-seat-mile of $ 0.86 (this includes depreciation, financing, insurance, maintenance, fuel and crew).

The Chesapeake 12-Ne

The 12 seat derivative version is the Chesapeake 12-Ne. This is a narrow-body version, with the seating reduced from three in-a-row to two in-a-row (in both configurations there is a an aisle). The 12-Ne has the same rotor, transmission system, empennage, fan-in-fin and undercarriage as the 19 seat aircraft. In addition, there is complete commonality of the electrical and hydraulic systems. In order to improve the cost-effectiveness of the 12-Ne, it is fitted with three smaller 745 kW (1000 hp) engines, and the aircraft range is limited to one 200 nm mission leg. Although the different engines will require separate certification, the lower installed power reduces the acquisition and direct operating costs. The 12-Ne is designed to meet the same mission requirements and performance criteria as the 19-seat version (except for the reduced mission range). The 12-Ne will have a purchase price of $7.61 million (1997) and a DOC/asm of $1.15. The DOC/asm is 34.5% more expensive than that of the 19-seat version.

Chesapeake Mission

Customized for the NE-corridor, the Chesapeake has a nominal cruise of 150 knots at 4000 ft, with a bad weather cruise altitude of 8000 ft. Maximum cruise speed is 160 knots. Based on flight operations below 8000 ft, the Chesapeake is offered with an unpressurised cabin. For marketing of aircraft in higher elevation regions, a pressurized cabin can be offered. The conversion from an unpressurised to a pressurized version is accommodated within the 2.5% take-off weight growth factor that has been incorporated into the baseline design.

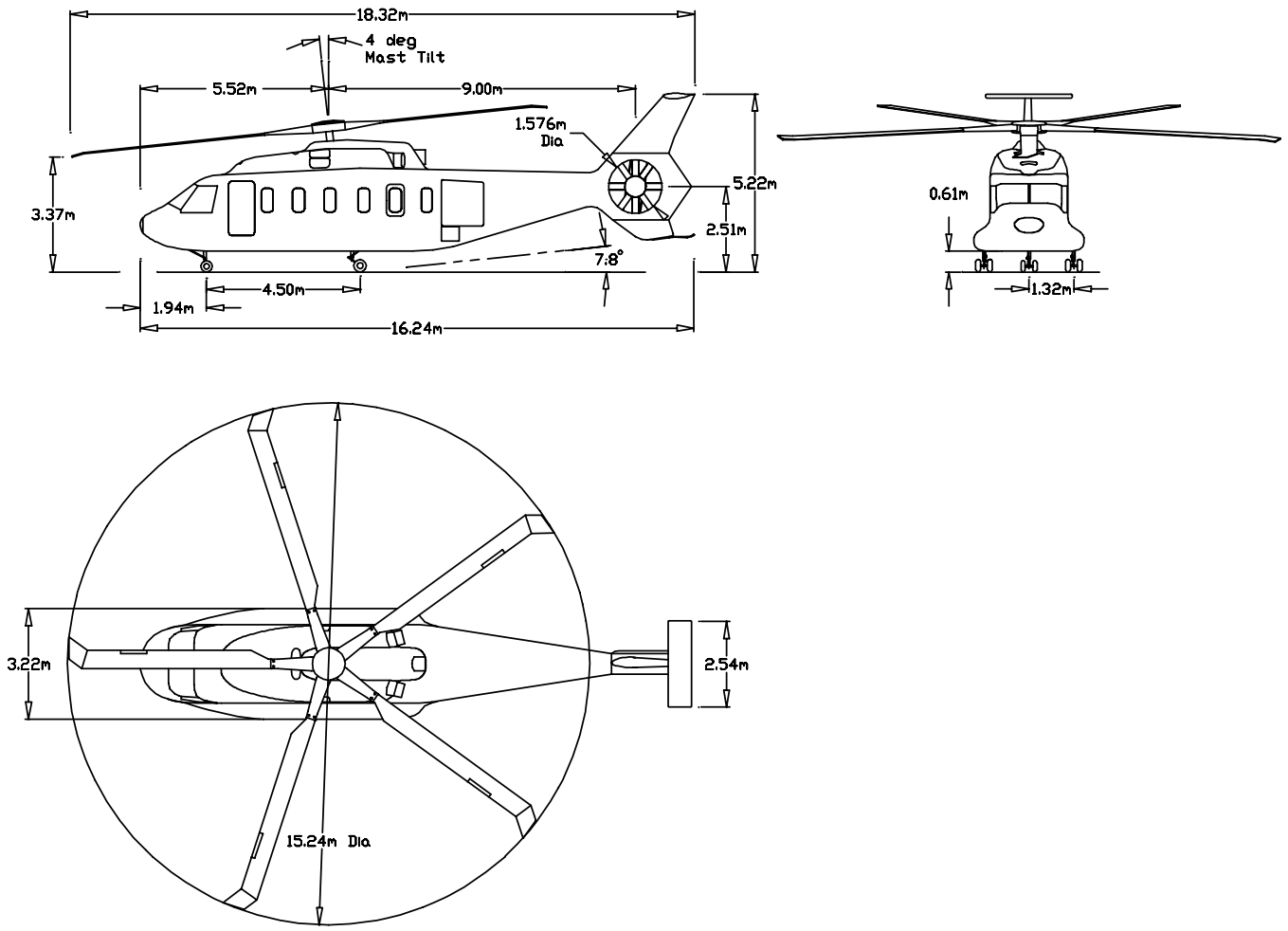

The Chesapeake 19-seat civil short haul helicopter

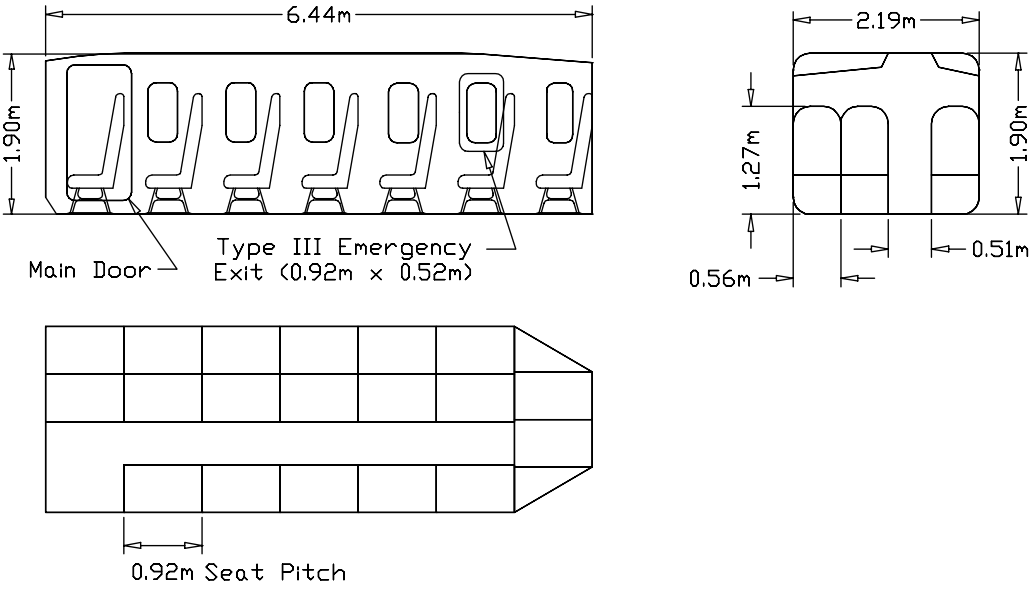

19-Seat Cabin layout

The triple-engine Chesapeake derives a significant performance benefit from the twin-engine cruise configuration (with one engine switched-off). First, the engines operate closer to the most efficient maximum power setting, thereby reducing the fuel consumption and overall take-off weight. Second, the engines are sized for the twin engine cruise requirement and in this case exceed the OEI requirements. It is shown in the trade-study that the improved fuel-efficiency and lower aircraft weight offset the additional cost of the larger engines. The Chesapeake is thus capable of full payload performance under hot-and-high conditions, while meeting the OEI requirement to sustain hover out of ground effect. For example, in ISA+20 and with a full 19 passenger load, it is possible to complete the un-refueled two leg 2x200 nm mission, if take off is below 1500 ft. If the fuel is reduced to complete one 200 nm leg instead, take-off elevation can be as high as 5500 ft. In contrast the RFP only requires a single leg (1x200 nm) range for ISA+20 conditions, and take-off from sea-level. This design offers the operator an aircraft capable of sustaining on-time operations even under hot-and-high conditions, without having to curtail range or payload. This performance increase is derived primarily via the engines sized for twin-engine cruise.

Furthermore, although the aircraft is designed to fly two un-refueled, 200 nm mission legs, a survey of the existing airports in the North-East corridor indicates that the average flight leg will be approximately 150 nm.

Approach and Methodology

The University of Maryland design was conducted in conjunction with the Spring 1998 Helicopter Design Course (ENAE634), from February to May 1998. The design was aimed at exposing the team members to the different aspects of an engineering design endeavour. To this end, no commercial design codes or analysis tools were used. In order to develop an understanding and an overview of the fundamental aspects of the aircraft-configuration trade-off study, an in-house code was developed based on Dr. Tishchenko's lecture notes [Tish98]. This code employs first order models for simplicity and insight. The performance analysis is based on a rigid blade model (incorporating equivalent hinge offset and root-springs) with a linear inflow model. The University of Maryland Advanced Rotor Code (UMARC) was used for the detailed rotor design (including stability analysis, estimation of hub loads and active vibration control)

Down-load Document from WWW

This document can be down-loaded from the following internet address:
http://www.enae.umd.edu/AGRC/Design98/chesapeake.html

Notes for the Aircraft Table (on page 5)

1) DOC (direct operating cost) includes: depreciation, financing, insurance, maintenance, fuel and crew costs.
2) Fleet sizing and DOC are based on an average mission leg of 150 nm and an annual utilization of 2000 flight hours.
3) Climb, descent is on 3 engines, cruise in ISA+20 is on 3 engines.
4) 19-seat fleet size based on 1,100,000 passenger miles/day, 12-seat fleet size based on 700,000 passenger miles/day (both with a 70% load factor).

CHESAPEAKE DESIGN FEATURES AND PERFORMANCE SUMMARY

	19 PASSENGER		12 PASSENGER	
General Specifications	**Metric**	**English**	**Metric**	**English**
Gross Take-Off Weight (GTOW)	7000 kg	15432 lbs	5375 kg	11850 lbs
Empty weight	3856 kg	8502 lbs	3513 kg	7745 lbs
Payload + 2 Crew	2078 kg	4580 lbs	1379 kg	3040 lbs
Usable fuel capacity	1066 kg	2350 lbs	483 kg	1065 lbs
No. of engines	3		-same-	
Type of engines	RFP IHPTET		-same-	
Unit price (1997 $)	9.03 million		7.61 million	
Total DOC[1,2] per flight hour (1997 $)	2089		1777	
Total DOC per seat-mile (1997 $)	0.86		1.15	
Overall length (rotors turning)	18.32 m	60.10 ft	- same -	
Overall height	5.22 m	17.13 ft	- same -	
Max. fuselage width	3.22 m	10.56 ft	2.66 m	8.73 ft
Performance Specifications	All data is in ISA, at GTOW		(unless otherwise specified)	
Engines used in cruise[3]	2		-same-	
Nominal cruise altitude	1220 m	4000 ft	- same -	
Nominal cruise speed	278 km/h	150 knots	- same -	
Max cruise speed (4000 ft)	296 km/h	160 knots	287 km/h	155 knots
Max rate of climb (sea level, MCP)	17.8 m/s	3500 ft/min	20.3 m/s	4000 ft/min
HOGE	4877 m	16000 ft	6360 m	20860 ft
Range (with standard reserves)	980 km	529 nm	482 km	260 nm
OEI ceiling (ISA +20, 60% fuel)	1674 m	5491 ft	1910 m	6270ft
Engine Specifications	dry, un-installed, each			
Emergency power, 30 s	1165 kW	1563 hp	932 kW	1250 hp
Take-off (nominal) power, 2 min (TOP)	932 kW	1250 hp	746 kW	1000 hp
Intermediate rated power, 30 min (IRP)	861 kW	1155 hp	689 kW	924 hp
Max. continuous power (MCP)	737 kW	989 hp	590 kW	791 hp
Rotor Specifications	common for both the 19 and 12 seat version			
Number of blades	5		-same-	
Diameter	15.240 m	50.00 ft	-same-	
Chord	0.533 m	1.75 ft	-same-	
Tip speed	213.4 m/s	700 ft/s	-same-	
Twist	-10 deg (linear)		-same-	
Sweep	35 deg from 95% radius		-same-	
Anhedral	10 deg from 95% radius		-same-	
Shaft tilt	4 deg (forward)		-same-	
Root cut-out	30%R		-same-	
Airfoils	root to 65% :	RAE 9648	-same-	
	65% to 87.5% :	VR-7	-same-	
	87.5% to the tip:	VR-8	-same-	
Fan	common for both the 19 and 12 seat version			
Diameter	1.576 m	5.17 ft	-same-	
No. of blades	8		-same-	
Twist	-7 deg		-same-	
Tip Mach number	0.55		-same-	
Asymmetric blade spacing	35/55 deg		-same-	
Solidity	0.63		-same-	
Airfoil	NACA 63A312		-same-	
Cabin Specifications				
Interior length	6.44 m	21.13 ft	- same -	
Interior height	1.90 m	6.23 ft	- same -	
Interior width	2.19 m	7.19 ft	1.63 m	5.35 ft
Seat Pitch	0.92 m	3.02 ft	- same -	
Overhead baggage space per passenger	0.072 m^3	2.54 ft^3	0.069 m^3	2.44 ft^3
Baggage compartment	1.345 m^3	47.5 ft^3	0.869 m^3	30.7 ft^3
Fleet Sizing[2,4]	121		122	

1 INTRODUCTION

The Chesapeake helicopter has been designed to meet the requirements set out in the 1998 AHS International Request For Proposal, [RFP98], for a commercial commuter VTOL aircraft. This RFP is based on the scheduled VTOL transport requirement linking outlying vertiports with regional fixed-wing airport hubs in the Northeast Corridor of the United States. The RFP stipulates a 19 seat vehicle, capable of flying two 200 nm legs without refueling (see Figure 1.1 for the specified mission profile). In addition to the 19 seat aircraft, a 12 seat version is required as a lead-in variant. Substantial commonality of dynamic systems (rotor, drive, propulsion and control systems) is required to minimize additional investment and qualification/certification costs. Complete commonality of other systems (electrical and hydraulic), but excluding the fuselage structure is desired.

It has long been recognized that helicopters, and more recently VTOL aircraft in general, can offer significant savings in travel time by directly linking downtown vertiports in nearby metropolitan areas or by acting as a feeder line, linking downtown and outlying vertiports to regional fixed wing hubs. The earliest commercial helicopter services included Los Angeles Airways, New York Airways and others, which operated in the 1950s and 60s, using Sikorsky S61 helicopters. Ever since, there have been more or less successful attempts at establishing civil short haul transport lines. Recent advances in VTOL technology and associated realization of reduced operating costs, coupled with ever increasing congestion around fixed wing airports, are making it more attractive to firmly establish a VTOL commuter service industry. In addition to improving the aircraft performance and reducing operating costs, a key factor for the success of these endeavors is the development of the VTOL infrastructure. This includes: integrating VTOL operations with traditional fixed wing airspace management, and secondly, developing urban/suburban community acceptance and support for VTOL activity. The 1998 American Helicopter Society Forum devoted a special session to the development of VTOL infrastructure.

In terms of the RFP, the issues of VTOL infrastructure development, and the market study defining the passenger capacity and fleet sizing are beyond the scope of this design project. Instead, the aircraft sizing and fleet requirements are stipulated.

It follows that the primary objective of the present design study, is to define a VTOL aircraft that meets the RFP requirements and maximizes operating cost effectiveness (including both direct operating costs per air seat mile and the premium a passenger is prepared to pay for shorter travel times). Based on these considerations, it is imperative to note that pure aircraft performance is not, by itself, the driving factor; hence any new technologies and aircraft configuration concepts have to "buy their way" onto the aircraft.

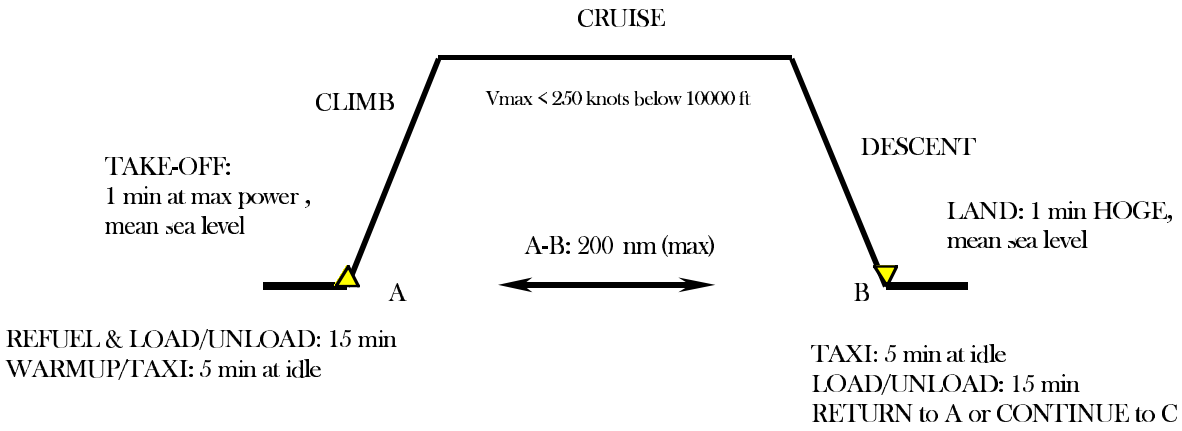

Figure 1.1: Civil short-haul mission profile: each mission consists of a 2 leg, un-refueled roundtrip

2 AIRCRAFT CONFIGURATION TRADE OFF STUDY

2.1 INTRODUCTION

The primary operation of this commercial aircraft is as a scheduled commuter line between outlying vertiports and main airport hubs in the US North-East Corridor. The main design objective is to optimize the commercial operation cost effectiveness of the aircraft. In order to meet the VTOL and the nominal 2x200 nm range requirements, several candidates can be considered: conventional helicopter, compound helicopter (with lift and/or thrust compounding), a tiltrotor/tiltwing, X-wing, and ABC vehicle. In considering these aircraft configurations, it must be pointed out that economic feasibility, and not mission performance alone,is the primary consideration for the commercial transport operation. Consequently, the high speed and long range X-wing and ABC concepts will not be considered. The X-wing (with cruise speeds in excess of 350 knots) employs an exotic and expensive rotor system that can be stopped in forward flight, using pure jet-thrust for cruise propulsion. In contrast the ABC helicopter uses a high stiffness, complex, coaxial rotor system. Despite the high cruise speeds, these systems, with high installed power requirements and expensive rotor systems, are not economically viable compared to the more affordable single rotor helicopter or tiltrotor options, especially for the relatively short 200 nm maximum mission leg. The compound helicopter offers an attractive increase in the cruise speed into the 250 knot region, compared to the helicopter. However, the increased empty weight fraction and complexity of lift- and thrust- compounding negate the speed advantage in terms of cost effectiveness [Tish98].

For this preliminary trade study, the candidate aircraft configurations are: a conventional helicopter and a tiltrotor. (Considering that this is a first order analysis, the performance differences between a tiltwing and a tiltrotor are expected to negligible, and these two are considered as a single concept.) Furthermore, a only a fixed diameter tiltrotor is considered. A variable variable diameter rotor offers the advantage of a reduced hover disk loading during VTOL and lower tip speed in forward flight. However, these advantages are offset by the added complexity and cost

and reduced efficiency associated with the non-optimum the blade twist for extended-rotor hover and contracted-rotor forward flight, and consequently only a fixed-diameter tiltrotor configuration is investigated.

It should also be noted, that in this trade-off study, the feasibility of a STOL short-haul fixed-wing turboprop/jet will not be considered, as a competitor to the VTOL candidates.

2.2 HELICOPTER vs. TILTROTOR

In comparison to a helicopter, the tiltrotor can achieve 2 to 3 times higher lift to drag ratios and double the cruise speed (in conjunction with higher cruise altitudes), [Tish90]. The presence of the tiltrotor wing and the dual rotor system has two implications: first, in order to prevent an excessive wingspan the tiltrotor typically has a high disk loading (for example 73.5kg/m^2,15.1 lb/ft^2 for the BB-609 and 117.8 kg/m^2, 24.1 lb/ft^2 for the V-22). Second, for the same payload capability, the presence of the wing and a dual rotor system results in a higher empty weight. These two factors lead to a higher power/weight ratio and a higher unit price. The helicopter, thus, has a lower operating cost per flight hour, whereas the faster tiltrotor can achieve a lower cost per air-seat-mile, especially as the mission range increases [Gmel89]. However, for short flight distances, the impact of the fixed ground turn-around time and the climb to cruise altitude reduces the speed advantage and cruise efficiency of the tiltrotor. Thus, there is a range below which the helicopter has a lower cost per air-seat-mile compared to the tiltrotor.

Now, cost effectiveness is defined in terms of a cost index that incorporates both the cost per air-seat-mile and the premium the customer is prepared to pay for shorter travel time. Gmelin *et al* [Gmel89] proposed a rentability index, which effectively includes the cost per air-seat-mile and the observation that the customer is willing to pay 30% more to halve the travel time. However, a high fidelity definition of such a cost effectiveness index requires a detailed market study which is beyond the scope of this preliminary design analysis.

For the purpose of this trade-off study, the aircraft's cost effectiveness will be quantified using both the rentability index and the cost per air-seat-mile.

2.3 HISTORICAL DATA

Prior to starting the trade-off study, a survey of helicopters in the same category (12-19 passengers and 2x200 nm un-refueled range) was undertaken. For completeness, the two existing tiltrotors are included in this comparison, see Table 2.1.

For the listed helicopters the average empty weight fraction (empty weight/total weight) is 0.569 (tiltrotors: 0.630) and the fuel weight fraction is 0.182 (tiltrotors: 0.120). Considering that the stipulated useful load (19 passengers plus baggage and 2 crew) is 2078 kg (4580 lb), it is to be expected that a conventional helicopter will have a take-off weight of 7980 kg (17600 lb).

2.4 MISSION PROFILE STUDY

In order to define the mission profile, it is necessary to consider the RFP requirements for the expected average trip distance in the North-East corridor and to select appropriate cruise altitudes.

2.4.1 Typical Mission Distances

The RFP indicates the "opportunity for a fleet of short to medium-range VTOL passenger rotorcraft, capable of departing from small, less-congested airports and arriving at main hub airports using adjacent vertiports",[RFP98] In order to estimate the expected typical trip distance, a survey of existing airports in the North-East corridor, amenable for scheduled flight operations, was made. The main selection criteria were: the airport must have a control tower, be located in Class B, C or D airspace and Jet-A fuel must be available.
51 airports, meeting the above criteria, were selected using the Airport Facilities Directory[NOAA98]:

Albany County
Atlantic City International
Baltimore Washington Intl
Barnstable Municipal
Belmar Farmingdale
Binghamton Regional
Charlottesville - Albermarle
Chester County
Dulles International
Dutchess County
Francis Gabreski
Frederick Municipal
General Lawerence Logan International
Greater Cumberland Regional
Groton - New London
Harrisburg International
Hartford Brainard
John F Kennedy International
La Guardia
Lancaster County
Laurence G Hanscom Field
Lawerence Municipal
Leesburg Municipal - Godfrey Field
Lehigh Valley International
Long Island MacArthur
Mannassas / Harry Davis Field
Nantucket Memorial
New Bedford Regional
New Castle County
Newark International
Newport News/Williamsburg Intl
Northeast Philadelphia
Oneida County
Petersburg Municipal
Philadelphia International
Pittsfield Municipal
Republic
Richmond International
Robert Miller Airpark
Salisbury-Ocean City Wicomico Reg.
Schenectady County
Stewart International Norfolk Intl
Syracuse Hancock International
Theodore Francis Green State
Trenton Mercer
Vinyard Haven
Washington County Regional
Washington National
Westchester County
Westover ARB/Metropolitan
Worchester Regional

Using the longitude and latitude coordinates of each airport, the total distance between each location was calculated. All distances beyond the 200 nm RFP limit and all distances below 50 nm (where the aircraft would not be competitive with surface-based transport) were ignored. The resultant geometric average of all remaining trips was 126 nm. This brief analysis of the average VTOL commuter service distance does not account for the development of a vertiport feeder-network (independent of existing airports) nor does it account for weighting factors associated

Table 2.1: Civil Helicopter and Tiltrotor Survey

Aircraft	GTOW lb	$W_{payload}$ lb	W_{empty} lb	$\frac{W_{fuel}}{GTOW}$ lb	Disk Load'g lb/ft^2	Power Load'g lb/SHP	V_{cruise} knots	Range nm	$\frac{W_{empty}}{GTOW}$
Bell 212	11200	3762	5997	.129	6.14	8.68	107	238	0.535
Bell 412 HP	11900	3031	6625	.189	7.16	8.69	124	328	0.557
Bell 430	9000	3735	5265	.178	6.50	6.30	130	440	0.585
S-76 B	11400	2969	6548	.165	7.5	7.1	140	357	0.574
S-76 C	11700	3535	6282	.161	7.69	7.29	150	430	0.537
S-92	22220	4604	13730	.177	9.82	7.86	155	400	0.618
AS 332L1	18960	5665	9745	.189	9.22	6.33	138	473	0.514
NH 90	20062	4409	11905	.209	8.93	6.5	140	650	0.593
EH101	31500	4815	19220	.237	10.77	6.06	150	785	0.610
BB 609	16000	5500	10500	-	15.1	-	275	750	.656
V-22	55000	20000	33140	.120	24.3	5.66	275	2100	.603

with higher traffic on certain main routes (for example Washington to Philadelphia, or New York to Boston). Nevertheless, this shows that while the helicopter has to be designed for the maximum 2x200 nm roundtrip, the fleet sizing and cost optimization should be based on the shorter average yearly round-trip distance. For the purpose of this design study, and taking into account the weighting of primary flight routes, it is estimated that the average flight will be 2x150 nm.

2.4.2 Typical Mission Altitudes

The design cruise altitude is predominantly a function of aircraft configuration and terrain. A tiltrotor/tiltwing, for example, needs to cruise at 18000-25000 ft to achieve its optimum cruise efficiency. Consequently, terrain and weather issues are generally not significant for tiltrotor cruise profiles. In contrast, the helicopter's optimum cruise is significantly lower.

In order to determine the typical flight cruising altitude of the proposed helicopter service, the weather in the North-East Corridor was investigated, using Aviation Routine Weather Reports (or METAR's). The METAR reports contain information concerning any significant weather, surface conditions, as well as the cloud cover at different altitudes.

For our investigation, the weather reporting station at Philadelphia's International Airport was chosen as representative of the North-East Corridor. Figure 2.1, based on hourly METAR reports for 1996 and 1997 (down-loaded from the Internet), shows the percentage of time that the cloud cover was below a particular altitude.

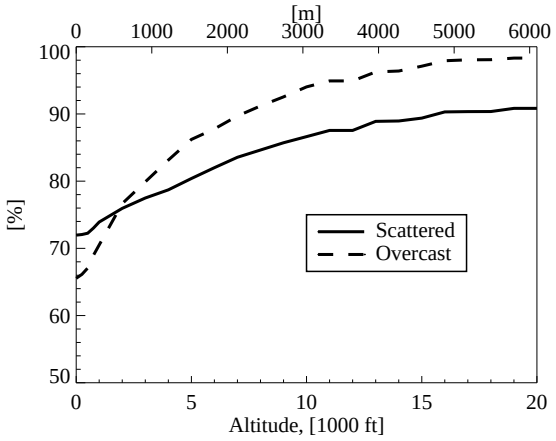

Figure 2.1: Meteorological data: percentage of time that a given cloud pattern exists at or below a certain altitude (scattered = 3/8-5/8 cloud cover)

The solid line represents the most significant overcast cover. For example, a helicopter with a low level cruise altitude of 4000 ft, will fly above overcast conditions 83% of the time and with a "weather avoidance altitude" of 8000 ft will clear the bad weather 91% of the time. In contrast a tiltrotor, with a cruise altitude of 18000 ft, will fly over the cloud cover 98% of the time.

2.5 TRADE-OFF STUDY METHODOLOGY

A preliminary design study was conducted to evaluate whether a helicopter or a tiltrotor configuration is more cost effective for the RFP requirements. The objective of the analysis is to minimize both the total operating cost per air-seat-mile and the travel time. The study is based on the 19 seat aircraft and 1,100,000 passenger mile requirement per day. (The economics of the 12-seat "lead-in" variant will not be considered in this investigation.) The trade-off study flow chart is shown in Figure 2.2.

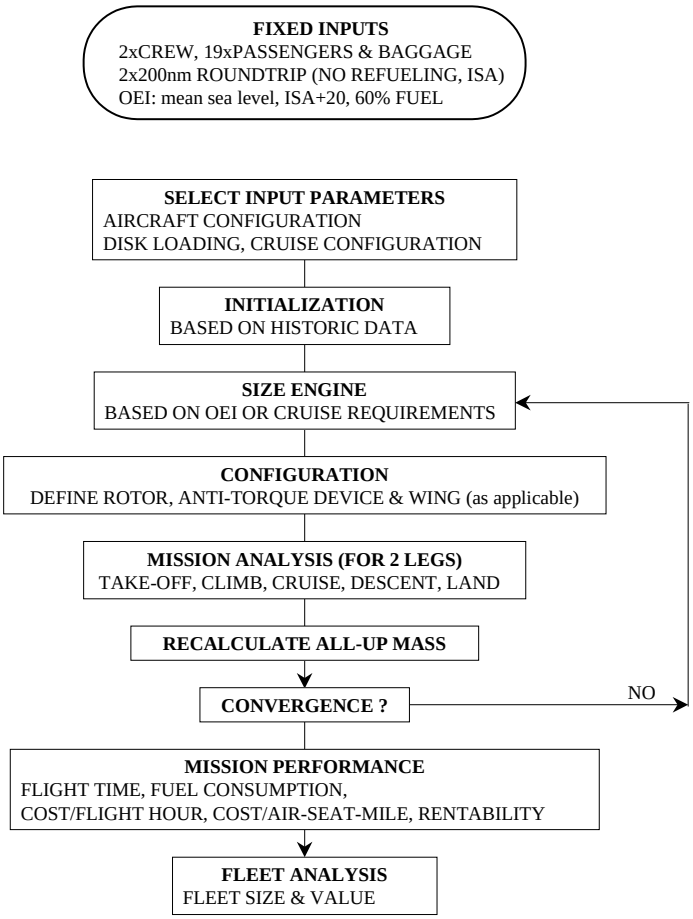

Figure 2.2: Trade-off study flow chart

The input parameters comprise the aircraft configuration (helicopter or tiltrotor), number of engines and number of engines used in cruise, disk loading, cruise speed and altitude and climb/descent schedules. The weight of the crew and passengers plus baggage are specified in the RFP and do not enter the trade study as an independent variable. The analysis modules are briefly described below. A first order analysis is performed, because the objective is to select between a conventional helicopter and a tiltrotor for subsequent detailed study. Simple models are used for take off weight, engine performance and aerodynamics in conjunction with empirical cost relationships. These models are easy to implement and give an overview of general performance trends. In contrast, detailed "bottom up"

performance, weight breakdown and cost models require a high degree of aircraft definition which is not available at this stage.

2.5.1 Engine, Aerodynamic and Weight Models

Table 2.2 summarizes the engine, aerodynamic and weight breakdown approach used in this initial design iteration.

Table 2.2: The Trade-Off-Study Performance Models

Model	Description	Input Parameters
Engine	IHPTET	power
Hover	momentum theory	disk loading, aircraft weight
Forward flight	lift/drag ratio	aircraft weight, flight speed
Weight	empirical model	weight efficiency, payload

The scalable IHPTET engine model provided in the RFP was selected, with appropriate corrections for effects of altitude, ISA+ condition, ram effect and installed power losses. This engine was selected, because it outperforms current engines (incorporating the 25% SFC improvement and the 40% power/weight improvement[RFP98]). Hover performance is analyzed via momentum theory, taking into account figure of merit, vertical drag and transmission efficiency correction factors. Forward flight (for both helicopter and tiltrotor) is modeled using empirical cruise lift/drag ratios. Take-off weight is calculated using empirical relations for empty weight fractions along with payload (passengers and baggage), crew weight and estimated fuel. These empirical formulae are obtained from curve fits to weight trends of existing VTOL aircraft and are defined separately for conventional helicopters and a wing-borne configurations[Tish98]. For example: the cruise lift to drag ratio for the helicopter varies from 4.2 (at 2000 kg take off weight) to 4.4 (at 8000 kg). In contrast, for the tiltrotor the lift to drag ratio varies from 8.5 (at 2000 kg) to 9.5 (at 15000 kg).

This first order analysis ignores two important features. First, the empty weight fraction is assumed to be a function of only the take-off weight, whereas it is also significantly influenced by the disk loading. Second, the empirical cruise performance based on lift to drag ratios fails to capture the effects of the detailed rotor parameters (including solidity, planform, tip geometry) and wing configuration. These cruise lift to drag ratios, derived from data on existing aircraft, are not directly amenable for investigating the effects of varying cruise speed and altitude, and the climb schedules on aircraft performance.

2.5.2 Economic Model

The helicopter cost analysis is based on historical data and empirical models. All cost calculations are in fiscal year 1997 Dollars ($FY97). The economic model is presented in detail in Section 15.1. The aircraft price [Harr97] is estimated via an empirical model based on a multivariable linear regression analysis of historical aircraft price data (including both twin and triple turbine engine helicopters and the V-22 tiltrotor). The primary cost drivers are shown to be the aircraft empty weight and the total installed power. Considering that commercial commuter helicopters are not subject to the traditional strict size constraints of military aircraft, it follows that a lower disk loading, with associated lower power requirements, will result in a lower price [Harr97].

It will be assumed that the tiltrotor incurs the same maintenance costs per flight hour (fh) and empty weight as the helicopter. Olson [Olso93] reports an average maintenance cost of \$0.067/fh/lb(empty) for helicopters and \$0.008/fh/lb(empty) for turboprop aircraft. It may be argued that the tiltrotor spends most of its life in the airplane mode where the rotor and airframe loads are lower than in a helicopter. This leads to lower dynamic loads, longer life and reduced maintenance. However, the added complexity of the tilting mechanism, dual rotors, a cross-coupling drive system and the additional wing structure required for the heavy engines and rotors at the wingtips offset these advantages. Scott [Scot96] derived a maintenance model based on historic data on civil, turbine-engine helicopters and fixed wing aircraft. In this model the maintenance cost per flight hour is based on the empty weight, the weight of the dynamic components, total installed engine power, the landing gear type and the number of units. Scott showed that a 40 seat, 600 nm tiltrotor will have expected maintenance costs of \$0.066/fh/lb(empty), compared to \$0.063/fh/lb(empty) for a 40 seat, 400 nm helicopter. These values correlate well with the \$0.067/fh/lb(empty) quoted by Olson [Olso93].

The aircraft's cost effectiveness will be evaluated in terms of two parameters: first the direct operating cost per air-seat-mile (DOC/asm) and second, the rentability index. The DOC/asm (which includes depreciation, financing, insurance, maintenance, fuel and crew compensation) is a measure of the expenses incurred by the operator per air-seat mile and does not account for the value of the passenger's time.

The rentability index (RI) is a cost-measure that is defined to quantify the premium the passenger is prepared to pay to shorten the effective flight time by a certain percentage. Gmelin *et al* [Gmel89] indicted that the customer is willing to pay 30% more to double the effective speed and proposed the following definition:

$$\mathrm{RI} = \frac{(V_{\mathrm{Peff}})^{0.4}}{\mathrm{DOC/asm}}$$

where V_{Peff} is the effective flight speed, based on the passenger's total travel time from boarding to disembarking. The higher the rentability, the more cost effective the aircraft.

For improved fidelity, a detailed market survey of the North-East corridor is required to establish what premium business travelers are prepared to pay to shorten their point-to-point travel time by a certain percentage (say 25 or 50%).

This first order economic model, in conjunction with the simple performance analysis, is useful for analyzing the overall mission performance and fleet operating costs for a variety of design and cruise profile concepts. The above economic model has several important limitations (see Section 15).

For a VTOL aircraft, the fuel and crew costs are secondary, compared to the aircraft ownership costs (depreciation, insurance, financing and the maintenance), [Olso93]. It follows that the primary VTOL cost drivers for the DOC/asm and the rentability index are the aircraft empty weight, installed power and cruise speed. This is in stark contrast to turboprop/turbojet operating costs, which are dominated by fuel and crew costs [Olso93].

2.5.3 Aircraft and Cruise Configurations

The most cost effective aircraft design will tend to optimize the cost drivers identified above: maximize cruise speed and minimize weight and installed power. From the mission profile, it is evident that the envisaged commercial

commuter aircraft will operate primarily in the cruise mode. Consequently, the aircraft is designed for high-speed cruise, rather than for maximum vertical flight efficiency. For the trade study, the following four aircraft/cruise configurations will be considered:

Table 2.3: Aircraft and Cruise Configuration

Aircraft	Target Cruise
Twin engine helicopter	4000 ft, 150 knots
Triple engine helicopter	4000 ft, 150 knots
Triple engine helicopter	4000 ft, 150 knots, cruise on 2 of 3 engines
Twin engine tiltrotor	18000 ft, 300 knots

The un-pressurized helicopter is envisaged to take advantage of the North-East-corridor's low-level flight routes, with a nominal and maximum cruise altitude of 4000 and 8000 ft respectively. The low-level cruise offers several distinct advantages. First, traffic conflicts with the faster fixed wing commercial air traffic are avoided. Second the need for aircraft pressurization is eliminated, resulting in a weight and power reduction. And third, considering that each mission leg is a maximum of 200 nm, the low cruise altitude reduces the climb segment. The main disadvantage of the low level cruise is that flight operations will be affected if the bad weather extends above 8000 ft. However, in Section 2.4.2 it is shown that increasing the cruise altitude from 8000 to 18000 ft does not significantly improve the opportunity to over-fly bad weather. The en-route climb rate is limited to 1250 ft/min, because the cabin is un-pressurized. In contrast, the tiltrotor has to climb to a high cruise altitude of 18000 ft to achieve efficient flight at the maximum lift to drag ratio. However, the pressurized tiltrotor can achieve higher en-route climb rates. The helicopter cruise speed of 150 knots, is based on the 150 knot cruise speed of the EH101 and the 155 knots of the S-92. The tiltrotor cruise speed is taken as 300 knots. This is faster than the BB-609 (257 knots) and the V-22 (275 knots) and accounts for advances in both engine performance and tiltrotor technology. In the climb and descent analysis, the tiltrotor speed is limited to 250 knots below 10000 ft as required by the RFP.

Furthermore, it is stated in the RFP mission profile that the cruise leg is to be flown at V_{minDOC}, the speed corresponding to the minimum air-seat-mile based direct operating cost. Typically this speed will be close to the best range speed. However, in the discussion pertaining to the value of the travel time (see Section 2.5.2), the aircraft should be flown at the speed that maximizes the rentability, V_{maxRI}. Considering that the rentability is heavily weighted by the flight speed, it is evident that $V_{maxRI} > V_{minDOC}$. Consequently, the nominal cruise speeds have been set, based on maximum cruise speeds of comparable aircraft.

The OEI requirement at ISA+20 and 60% fuel weight results in a very high power/weight requirement. Consequently the engines operate well below the optimum continuous power setting in cruise, resulting in poor fuel economy. It is evident that for the same OEI condition, a three-engine helicopter will require a lower power/weight ratio than a twin engine helicopter. The power, weight and fuel savings translate into a lower operating cost. In order to further optimize engine performance in cruise, a third helicopter variant is proposed: this is a triple engine helicopter, with the facility to switch-off one engine in cruise, with the remaining two engines operating close to maximum continuous power. This improves the fuel efficiency. (The cruise with one engine shut down raises a number of operational issues that will not be addressed at this stage). In the trade-off study, the engines for the

triple engine helicopter (with one engine off cruise) are sized such that the helicopter meets both the OEI and the desired cruise requirements. It is assumed that a different engine is switched off for each cruise leg. Thereby the engines accumulate only 2/3 of the flight time on average, reducing the time between overhauls. This is included in the maintenance costs, assuming that the engines contribute 33% of the total maintenance burden.

It should be noted that at this stage a triple engine tiltrotor variant is not considered. The reason for this is that the third engine will require a separate (crash-worthy) mount and gearbox in the wing/fuselage interface. The associated cost and weight penalty will negate the advantage of the OEI rating using three vs two installed engines.

2.5.4 Trade-Off Study Results

The algorithm was validated using a helicopter similar to the Sikorsky S-92 Helibus which has a 19 seat capacity, 400 nm range, take-off mass of 10000 kg, a disk loading of 47.5 kg/m^2, cruise speed of 140 knots and installed engine power of 2x1750 hp.

The S-92 purchase price [Heli98] is \$12.5-\$13 million. For the same disk loading, the present trade-off study algorithm (with the IHPTET engine) converges to a 140 knot helicopter of 9810 kg, with a price of \$14.5 million. The 16% higher price reflects a larger installed power, based on the restrictive RFP OEI requirement (0 ft, ISA+20, 60% fuel).

In this preliminary study, the disk loading was selected as primary input parameter. Figures 2.3-2.13 show the trade-off study results for take-off mass, fuel capacity, nominal engine power, purchase price, direct operating cost per flight hour and air-seat-mile, and rentability as a function of disk loading. The aircraft is sized to achieve the 2x200 nm roundtrip flight (without refueling) and fleet sizing is for the 1,100,000 passenger mile requirement.

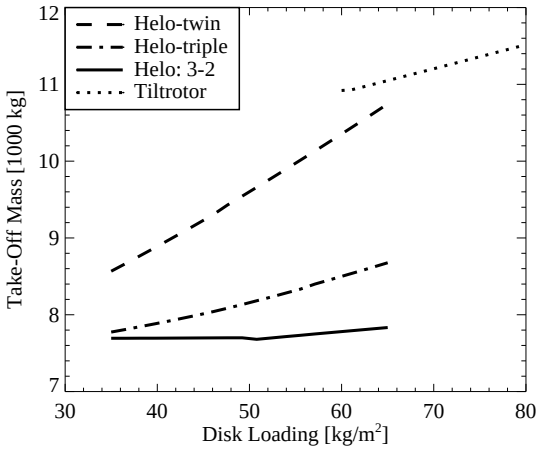

Figure 2.3: Take-off mass vs. disk loading, Helo-twin: twin engine helicopter, Helo-triple: triple engine helicopter helicopter, Helo 3-2: triple engine helicopter with one engine shut down in cruise

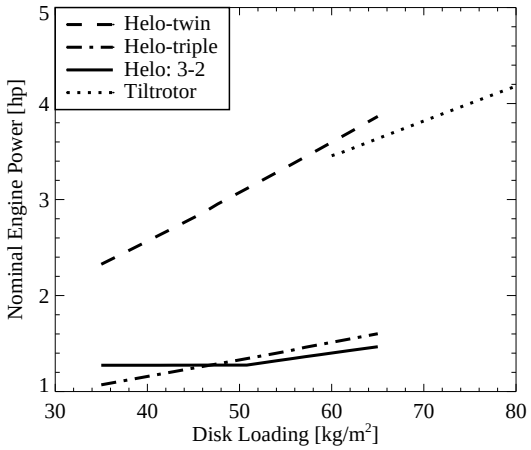

Figure 2.4: Nominal engine power vs. disk loading

The slope-discontinuity in the curves for the helicopter "Helo 3-2" (Figures 2.3-2.10) represents the point where the engine sizing switches from the cruise requirement to the OEI requirement. The aircraft power and weight

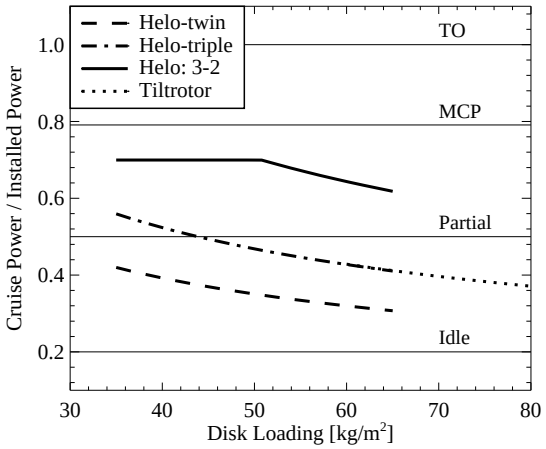

Figure 2.5: Cruise power relative to the nominal engine power: TO = take-off, MCP = max. continuous power, Partial = 50% of nominal power, Idle = 20% nominal

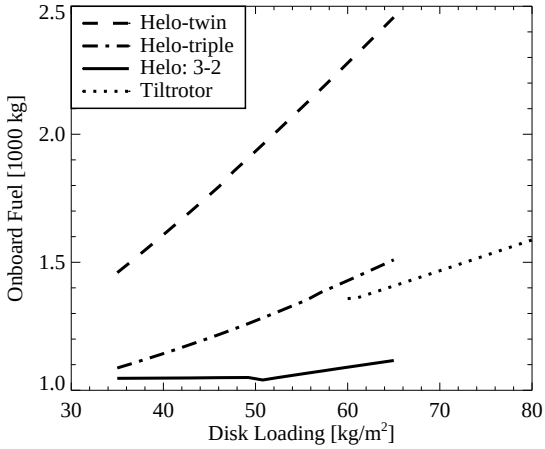

Figure 2.6: On-board fuel capacity vs. disk loading

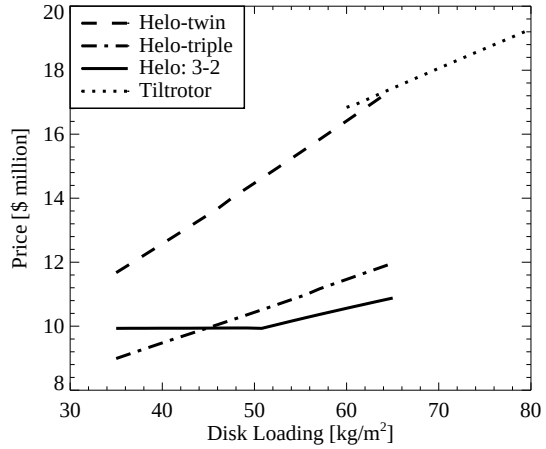

Figure 2.7: Aircraft price (1997 $) vs. disk loading

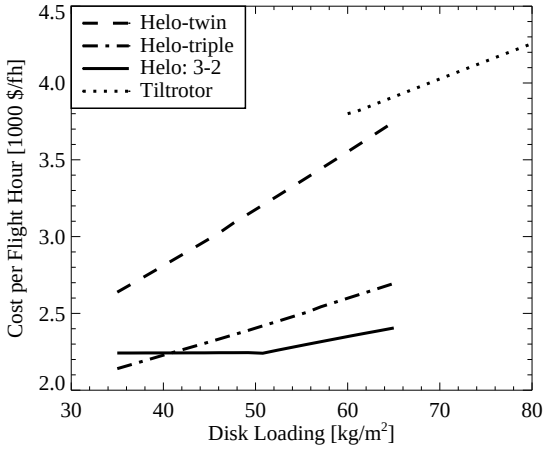

Figure 2.8: Direct operating cost (1997 $) per flight hour, DOC/fh, vs. disk loading, based on a 2x200 nm mission

are fixed to a large extent by the OEI power requirement, the empty-weight fraction and the hover disk-loading. The dominant trend in Figures 2.3-2.10 is that as the disk loading is increased, the VTOL aircraft power/weight ratio drops, which results in a lower cruise fuel efficiency. Compared to the triple engine helicopters, the twin engine helicopter is severely overpowered in order to meet the OEI requirement. This is reflected in its higher take-off weight, larger installed power and higher fuel consumption. Consequently, the twin engine helicopter is more expensive to purchase and to operate per flight hour and air-seat mile. Figure 2.5 shows that in cruise, the triple engine helicopter, with one engine shut down, indeed operates closest to the optimum maximum continuous power setting. This gives the lowest trip fuel consumption, as indicated in Figure 2.6. Comparing the tiltrotor and the triple engine helicopters, it is evident that the lower weight efficiency of the tiltrotor results in a higher take-off weight and higher power/weight ratio for a given disk-loading (Figures 2.3-2.4). Consequently, for the same payload

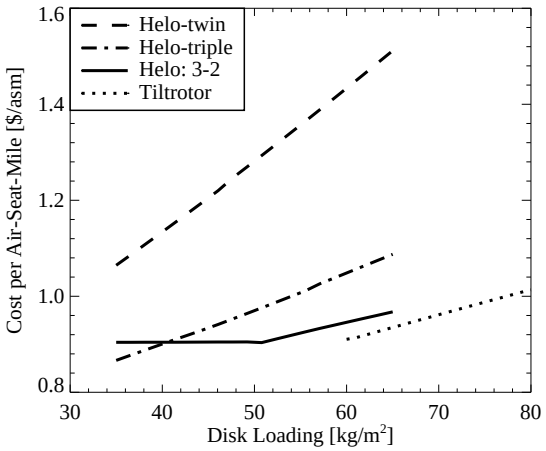

Figure 2.9: Direct operating cost (1997 $) per air-seat-mile, DOC/asm, vs. disk loading, based on a 2x200 nm mission and the total travel time (from boarding to de-boarding)

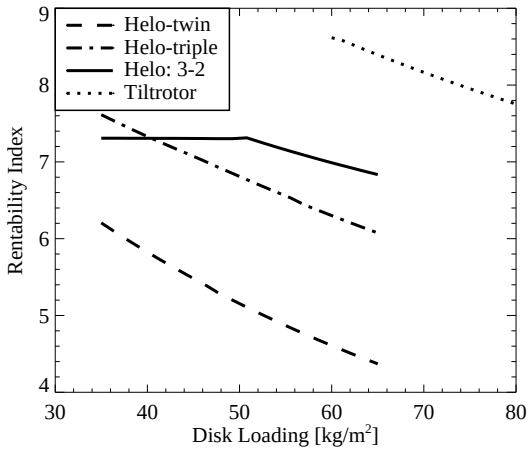

Figure 2.10: Rentability Index (RI) = $\frac{(V_{\text{eff}})^{0.4}}{\text{DOC/asm}}$

capability, the heavier tiltrotor will have a more expensive purchase price and total operating cost per flight hour (Figures 2.7-2.8). The higher DOC/fh is offset by the speed advantage, as shown in Figure 2.9 and 2.10 for DOC/asm and rentability index respectively. It should be noted, that even though the tiltrotor cruise speed is double that of the helicopter, the effective average mission speed (which includes ground turn-around time), is only 45% faster than that of the helicopter for the 200 nm mission leg.

In order to quantitatively discuss the differences between the various configurations, the following discussion is with reference to a helicopter disk loading of 40 kg/m^2 and tiltrotor disk loading of 70 kg/m^2, refer to Table2.4. The former is a compromise between selecting a low disk loading and maintaining a minimum rpm of 250 rpm, for a fixed tip speed; and the latter is based on the BB-609 (73.5 kg/m^2). The quoted flight time includes an allowance for aircraft taxi time, embarking and disembarking.

It should be noted that the stringent RFP OEI requirement (to maintain hover at mean sea level, ISA+20, 60% fuel, full passenger complement) results in the low power loadings compared to the helicopters and tiltrotors tabulated in Table 2.4.

The twin engine helicopter is not cost competitive with the triple engine variants or the tiltrotor. The reason for this is that in order to meet the stringent OEI requirement, the twin engine helicopter has a 31% higher power/weight ratio than the triple engine helicopter. This translates into larger engines, poor cruise fuel consumption and a larger take-off weight and consequently higher operating prices. The cost per flight hour is 26% higher than that of the baseline triple engine helicopter.

The two triple engine helicopter variants have similar characteristics and operating costs. In the case of only two cruise engines, the engines operate closer to the optimum maximum continuous power setting and thereby yield improved fuel efficiency. However, for a disk loading below 45 kg/m^2, the high-speed cruise requirement exceeds the OEI requirement for the engine sizing of the one-engine-off helicopter. The more powerful engines allow for the OEI requirement to be extended to a higher weight, altitude or ISA+ condition. For example, OEI hover is possible at

the maximum take-off weight, 1500 ft and ISA+20. The extra cost of the larger engines is offset by the improved fuel efficiency and associated lower take-off weight. In view of the fact that the economic models do not explicitly account for the number and size of the engines, and the contribution of the engine to the maintenance costs, it is not possible to definitively state that either of the 3 engine helicopters is more cost effective. The acquisition and operating costs of three smaller engines vs. two larger engines requires careful attention for a subsequent more detailed design study.

As expected, the tiltrotor has a higher take-off weight, because of the inherently higher empty weight fraction. The heavier take-off weight is associated with more powerful engines and a higher price [Harr97]. Consequently the operating cost per flight hour is 80% higher than that of the triple engine helicopters, while the speed based cost per air-seat-mile is only 7% higher. As a result of the high flight speed, the fleet size is 40% smaller, although interestingly the fleet value is of the same order as that of the 3 engine helicopter variants. The speed advantage of the tiltrotor, which completes the 200 nm 37 minutes faster, becomes evident in the rentability index, which is 12% higher than that of both the three engined helicopters.

As shown in Section 2.4.1, it is conceivable that the average yearly trip distance will be less than 200 nm. The geometric average distance between airports in the North-East corridor is shown to be approximately 125 nm. Figures 2.11-2.13 are added to show the impact of the shorter trip distance. For the tiltrotor results, the cruise altitude and cruise speed (which is limited to 250 knots below 10000 ft) are adjusted appropriately to reflect the shorter trip distance. As the trip distance is reduced, the contribution of the fixed ground time has a more significant impact on the tiltrotor, and the rentability drops faster than that of the helicopters. The figures show that the cross over point for DOC/asm lies beyond 200 nm and the rentability cross over point lies at 120 nm. Figure 2.13 shows the impact of reduced average flight distance on the fleet size needed to achieve the passenger-mile requirement. (Note that fleet size was based on the 2000 flight hour limit per aircraft per year, rather than the less restrictive 16

Table 2.4: Selected Data Points from the Trade Study

Description[1]	Units	Helo 2	Helo 3	Helo 3-2	Tiltrotor
Disk loading	kg/m^2 (lb/ft^2)	40 (8.19)	40 (8.19)	40 (8.19)	70 (14.3)
Cruise speed	knots	150	150	150	300
Travel time[2]	-	1 hr 47 min	1 hr 47 min	1 hr 47 min	1 hr 10 min
Rotor diameter	m (ft)	16.82 (55.2)	15.85 (52.0)	15.65 (51.3)	10.10 (33.1)
Take-off mass	kg (lb)	8890 (19600)	7890 (17395)	7700 (16975)	11200 (24690)
Fuel capacity	kg (lb)	1610 (3550)	1145 (2525)	1050 (2315)	1570 (3460)
Nominal power	kW (hp)	2x1916 (2x2570)	3x865 (3x1160)	3x950 (3x1275)	2x2850 (2x3820)
Power loading	kg/kW (lb/hp)	2.32 (3.81)	3.04 (5.00)	2.70 (4.44)	1.97 (3.23)
Engines sizing	-	OEI	OEI	2 engine Cruise	OEI
Price	million $	12.6	9.5	9.9	18.1
DOC per hour	$	2810	2230	2240	4030
DOC per air seat mile	$	1.13	0.90	0.90	0.96
Fleet size	-	116	116	116	69
Fleet value	million $	1455	1100	1150	1240
Rentability Index	-	5.82	7.33	7.31	8.17

1) Helo 2 = twin eng. helicopter, Helo 3 = triple eng. helicopter, Helo 3-2 = triple eng. helicopter, with cruise on 2 engines
2) Travel Time is for a 200 nm leg, from boarding to disembarking
3) All prices are in 1997 $

hours per day).

It is important to note, that for scheduled flight legs longer than 250-300 nm it will be difficult for the tiltrotor with a DOC/asm of $\$_{97}0.5$-0.95 to compete with regional turboprops/turbojets that have a DOC/asm of the order of $\$_{97}0.15$.

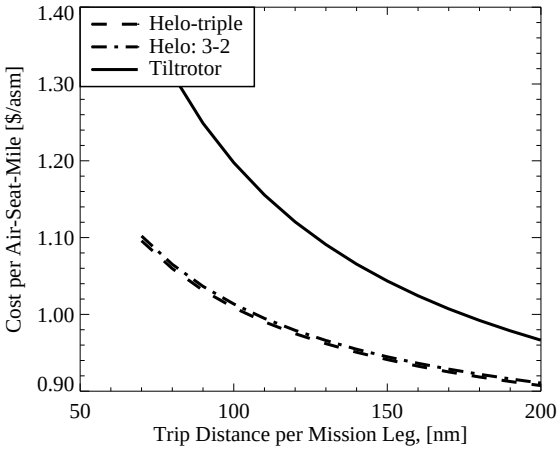

Figure 2.11: Direct operating cost per air-seat-mile, DOC/asm, vs. trip distance (1997 $)

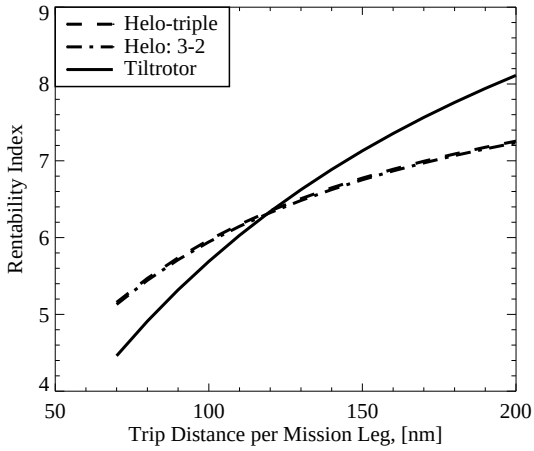

Figure 2.12: Rentability vs. trip distance

Table 2.5 shows the cost-effectiveness results, based on an average mission that consists of two 150 nm legs. This value lies between the maximum mission range of 200 nm, and the 125 nm geometric average distance between existing airports in the North-East corridor. Thus, for the 150 nm average trip distance, the triple engine helicopter has a 10% lower DOC/asm and essentially the same rentability as the tiltrotor.

It should be emphasized that the cost model used in this analysis is only a first order estimate. Small changes in the maintenance costs and aircraft price will have a significant impact on the relative economic merits of the triple engine helicopter vs. the tiltrotor, and the 2 vs. 3 engine cruise option. These cost per air-seat-mile results are

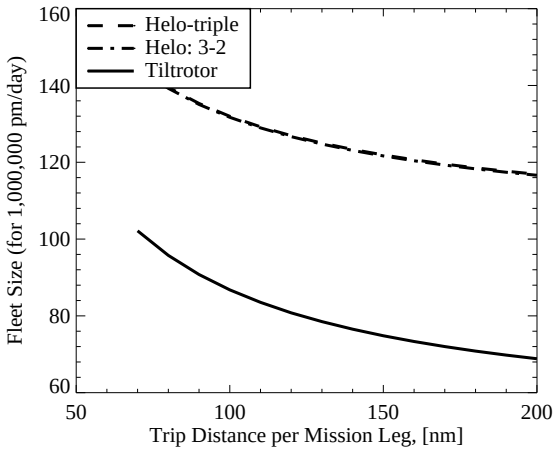

Figure 2.13: Fleet size vs. trip distance (based on 1,100,000 passenger miles/day)

Table 2.5: Cost-Effectiveness Based on an Average 2x150 nm Mission

Description	Units	Helo 3-2*	Tiltrotor
Disk loading	kg/m^2 (lb/ft^2)	40 (8.19)	70 (14.3)
Cruise speed	knots	150	300
Travel time** (for 150 nm)	-	1hr 28 min	1 hr
DOC per air seat mile	$\$_{97}$	0.94	1.04
Fleet size	-	122	75
Fleet value	million $\$_{97}$	1209	1351
Rentability Index	-	6.8	7.1

* triple engine helicopter, with cruise on 2 engines
**Travel time: form boarding to disembarking

in stark contrast with typical turboprop DOC/asm of $\$_{97}$ 0.15 [Olso93]. The commuter helicopter and tiltrotor are approximately 7-8 times more expensive than a turboprop, in terms of cost per air-seat-mile. From a marketing perspective, it is essential to establish that this premium for a VTOL feeder line from downtown vertiports to major airport hubs in the North-East corridor can be supported.

The three main factors that need to be addressed in a subsequent more detailed trade study are: first, quantify the extra cost the passenger is willing to incur to reduce the total travel time. Second, how severely congested is the fixed wing air traffic at 15-20000 ft, and how does this impact the flight scheduling of tiltrotor flights? And third: what is the expected average trip distance based on the actual number of flights versus the median distance?

2.6 Conclusions

The trade study thus shows that the two triple engine helicopters and the tiltrotor have a similar cost per air-seat-mile and rentability index. The helicopters are lighter and have a lower unit price, which is negated by the necessity for a larger fleet. Within the limited accuracy of the cost models, it is not possible to definitively discard any of the three configurations. It is clearly shown, however, that the cost effectiveness of the tiltrotor drops faster than that of the helicopter as the average roundtrip distance decreases from the maximum mission requirement of 2x200 nm.

Considering the following factors, the triple engine helicopter (with 2-engine cruise) is selected as suitable candidate for further detailed design (see Table 2.4 for the specifications).

- The helicopter can take advantage of uncluttered low-level flight routes. In contrast, the tiltrotor needs to fly at altitudes of 15-20000 ft in order to realize the flight speed and cruise efficiency advantages. This will require the tiltrotor to slot in to existing commercial fixed wing flight routes, which can negatively impact the deployment and schedule flexibility. In addition, on short flight routes the tiltrotor will not be able to climb to the optimum cruise altitude. The reduced lift/drag ratio at lower altitudes will result in in higher operating costs.

- The tiltrotor requires a significantly higher disk loading (to prevent an excessively large wingspan). This is associated with higher downwash velocities which will hamper vertiport ground operations near the tiltrotor. The high disk loading will also result in higher BVI related noise levels in the vertical flight mode. This external noise will require on-board active systems, in order to meet the stringent noise requirements, which add cost,

complexity and weight.

- As a result of high blade twist, a tiltrotor cannot autorotate effectively. This poses a risk during the unlikely event of multiple engine or transmission failure during transition flight, where the flight speed is below stall speed of the wing. In the event of an engine failure during cruise, the gliding tiltrotor will destroy its prop-rotors on landing. In contrast, in a correctly performed autorotation, no significant damage to the helicopter is expected.

- For the same payload the helicopter is 30% lighter than the tiltrotor. In addition, with blades folded, the helicopter will require less space than the tiltrotor (assuming the tiltrotor has only blade folding, but no wing folding). The larger apron footprint and take-off mass directly impact the cost of vertiport development, especially in downtown areas.

- The triple engine helicopter, with the option to switch-off one engine in cruise has several advantages over the baseline triple engine helicopter: first, the improved fuel efficiency and second the fact that the engines only accumulate 2/3 of the cruise flight hours. Combining these two effects results in a lower overall weight and operating cost. In addition, since the engines are sized for the cruise requirement and are slightly oversized for the stipulated OEI requirement, the one-engine-inoperative performance can be expanded to a higher take-off weight, altitude or ISA+ condition. As a result, the aircraft operation need not be restricted on hot summer days.

- The main disadvantage of this helicopter is the fact that it takes 88 minutes to complete a typical 150 nm mission leg, compared to the 60 minutes of the faster tiltrotor. This results in a 47% longer travel time for the customer and a a 63% larger fleet to meet the projected passenger-mile market. At this stage it will be assumed that the 10% cheaper total operating cost per air-seat-mile and the above operational advantages outweigh the drawbacks of the slower helicopter.

For the next design iteration it is recommended that more detailed aircraft aerodynamic, weight breakdown, aircraft price and extended empirical and maintenance cost models are used to improve the fidelity of the flight performance and cost analyses. With these models a multi-objective cost function can be established to optimize the design for maximum cost effectiveness. The cost effectiveness should take into account the total operating cost per air-seat-mile, the average yearly trip distance, the value of the customer's travel-time, the climb and cruise profile and the apron footprint. The key features of such an optimization study are summarized in Table 2.6.

Table 2.6: Second Level Trade Off Study Methodology Results

1) Aircraft characteristics	Mass breakdown, installed power, fuel capacity
2) Aircraft geometry	Rotor characteristics, wing characteristics (if applicable), fuselage dimensions
3) Mission profile performance	Cruise speed and altitude, climb schedule, total flight time and fuel consumption for the average flight distance
4) Economics	Aircraft price, cost per flight hour, cost per air-seat-mile and direct operating cost break down, rentability and fleet sizing

In this second level trade-off study it would be of interest to investigate the cost benefit of using advanced technologies to improve the cruise speed and cruise efficiency to maximize the rentability index. For example, using active vibration reduction mechanisms to extend the cruise speed of helicopter, or using active twist rotor-blades to improve the propulsive efficiency of the tiltrotor.

An important consideration in the development of a short-haul civil VTOL industry is that it is neither desirable, nor feasible, to compete head-on with fixed wing operations for flight legs beyond 250-300 nm. The primary reason is that the turboprop and turbojet aircraft have a direct operating cost per air-seat-mile (DOC/asm) on the order of 15% of current helicopter systems [Olso93]. Instead, it is envisaged that short range VTOL operations will complement the longer range fixed wing operations. The objective is to exploit the unique benefits of each aircraft type to optimize flight operations in terms of operating costs, airport congestion, passenger flight time and community acceptance [Flat91]. In this scenario, there are two potential missions for the VTOL aircraft:
First, VTOL aircraft perform short range (75 nm - 200 nm) direct downtown vertiport-to-vertiport scheduled services. Here the main advantage is the potential time saving since the ground-commute from downtown to an outlying regional airport is eliminated. This requires a careful market study, since several cities such as Washington, D.C., do have convenient airports near the central business district. Second, VTOL aircraft form part of a dual mode regional transport system. In this case, the focus is on a complete point-to-point travel package that is offered to the customer. The VTOL acts as feeder from vertiports to major regional fixed wing hubs, where the passenger connects to a fixed wing aircraft for a long-range (greater than 300 nm) or transcontinental flight leg.

Table 2.7 compares the 1997 statistics for the US regional fixed wing airline industry with the RFP specifications for the scheduled short-haul civil VTOL commuter market.

Table 2.7: U.S. Regional Airline Industry [Shif98] vs. the RFP

	US Regional Fixed Wing Industry	Proposed NE Corridor VTOL Fleets*
Carriers operating	104	8
Passengers carried (millions)	66.3	21.4
Average passengers carried per airline	637,533	-
Revenue passenger miles (billions)	15,30	3.212
Available seat miles (billions)	27.79	4.589
Average load factor (percentage)	55.04	70
Airports served in North America	766	NA
Average passenger trip length (miles)	231	150
Aircraft operated	2,104	1000-1500**
Average seating capacity (seats per aircraft)	25.9	19
Average seating annual utilization (hours per aircraft)	2,231	2000

* RFP data is based on 8 fleets, and 1,100,000 passenger miles per day
** 1000 tiltrotors or 1500 helicopters

It is evident that there is substantial overlap between the operating characteristics of the US regional fixed wing operators and the RFP proposed short-haul VTOL commuter line, supporting the argument for highly integrated VTOL and fixed wing operations.

3 PRELIMINARY DESIGN CONSIDERATIONS

Prior to commencing the detailed design iteration performed in Sections 5 to 15, several preliminary design aspects need to be considered, including operational and mission issues, the primary rotor parameters and the anti-torque device.

3.1 OPERATIONAL ASPECTS

The analysis (including engine sizing, weight breakdown and compliance with the OEI requirements and the stipulated mission profile) is iterated in order to achieve a design that meets the desired performance objectives. These are based on the RFP and the trade-off study (Section 2.5.4) and are listed in Table 3.1.

Table 3.1: Performance Objectives

cruise, nominal (ISA+0)	two engines, 150 knots, 4000 ft
cruise, weather avoidance (ISA+0)	two engines, 150 knots, 8000 ft
cruise, ISA+	three engines, 150 knots, 4000 and 8000 ft
OEI HOGE capability	full payload, 60% fuel, ISA+20, mean sea level
Max. cruise, two engines @ max. continuous power (MCP)	160 knots at 4000 ft

The above performance objectives are to be attained with a full payload, which is defined as the weight of the passengers, including baggage.

It should be noted that although the RFP stated mission profile is for two legs, flown in ISA+0 conditions, it is common to encounter performance limiting ISA+ conditions during hot and humid summer months. In order to improve the marketability of this aircraft, the performance criteria are selected such that the aircraft can complete the full payload mission profile in ISA+20 and bad weather conditions requiring cruise at 8000 ft (see Section 14 for further details on operational aspects). For the flight scheduling based on a nominal 150 knot cruise speed, the 160 knot maximum cruise speed allows for on-time arrivals, despite a 10 knot headwind.

In the trade-off study (Section 2) it is shown that the engine sizing is dictated by the twin engine cruise requirement, rather than the OEI condition. In fact, it is shown that the aircraft can maintain a one-engine inoperative hover (out of ground effect) at maximum take off weight and an altitude of 2000 ft (see Section 9). Fuel sizing is for an un-refueled roundtrip or a two-leg mission of 2x200 nm.

The 4000/8000 ft cruise altitudes are adequate for the Northeast corridor. First, the maximum airfield elevation is below 1000 ft; second the maximum terrain elevation is below 2000 ft; and third, as shown in Section 2.4.2, cruise above 8000 ft does not significantly improve the opportunity to fly above bad weather. The advantage of the 8000 ft maximum altitude is that pressurization is not required. Should the aircraft be subsequently marketed in regions requiring higher altitude capability, a pressurized variant can be developed. Aircraft pressurization will add 1% to the take-off weight, and slightly reduce available engine power (because cabin pressurization is via engine compressor bleed). The increase in weight and the reduced power available to the main rotor fall within the 2.5% weight growth allowance in the design (Section 7). Note also that pressurization has no impact on the OEI performance, in that pressurization is not required at take-off.

3.2 PRIMARY ROTOR PARAMETERS

Prior to starting the detailed design iteration, the primary rotor parameters are considered, including: disk loading, tip speed, and solidity. The airfoil selection is discussed in detail in Section 10.3

An important consideration in rotor design is to ensure that the rotor has sufficient thrust and power margin to meet the standard Rate 1 turn requirement at ISA+20, maximum take off weight, maximum speed and the maximum cruise altitude of 8000 ft. This ensures that the airline operator does not need to restrict the payload (i.e. reduce the number of passengers and/or on-board fuel).

Main Rotor Diameter: this is based on the 40 kg/m^2 (8.2 lb/ft^2) disk loading selected in Section 2. The final disk loading is slightly lower at 38.4 kg/m^2 (7.86 lb/ft^2).

Tip speed: there are four constraints on choosing main rotor tip speed: 1) advancing blade compressibility limit, 2) auto-rotation limit (lower limit), 3) noise limit (upper limit) and 4) retreating blade stall limitation. A high tip speed will delay retreating side stall, decrease transmission weight (as a result of lower torque levels), decrease blade weight (due to the high rotational kinetic energy). However, the maximum tip speed is limited by advancing side compressibility effects (transsonic flow and shocks) and associated high noise levels. A swept tip design can be used to delay the advancing side compressibility effects. The noise limit for rotor speeds is approximately 750 ft/s [Prou90]. In accordance with the RFP, the tip Mach number can not exceed 0.85. To meet these requirements, a compromise tip speed of 213.4 m/s (700 ft/sec) is selected.

Solidity: the solidity is determined by the rotor stall boundary. As flight speed is increased, an increasingly larger portion of the disk operates in the stall regime. This manifests itself as a rapid increase in the vibration levels (associated with the large changes in blade lift and pitching moment) and high power requirements (associated with the large drag). Increasing the solidity increases the thrust capability of the rotor at the expense of increasing the profile power. Evaluation for the helicopter flight envelope requires a detailed rotor, hub and control system design. As a first approximation of the rotor thrust boundary, the maximum C_T/σ curves presented by Prouty [Prou90] are used. These curves show the maximum rotor loading as a function of advance ratio for level flight, steady turns and transient maneuvers. The steady turn and transient maneuver limits in this reference allow for short term higher vibration levels. Considering that the ride quality is of paramount importance for a civil commuter operation, the rotor will be designed so as not to exceed the level-flight rotor-load boundary during a standard Rate 1 turn (180 deg/minute, corresponding to a 30 degree bank angle). This prevents undesirable increased vibrations during cruise course adjustments. For 160 knots, the C_T/σ is given as 0.095 - 0.105 (for low drag designs). The selected solidity of 0.111 gives an extreme-case rotor loading of $C_T/\sigma = 0.096$, at 160 knots, 8000 ft, maximum take-off weight, ISA+20 and a load factor of 1.16 (corresponding to a 30 degree bank turn). In contrast, for nominal cruise at 4000 and 8000 ft (ISA+0), the rotor loading, C_T/σ, is 0.069 and 0.078, respectively.

Twist: the blade twist is a compromise between the high blade twist desired for good hover performance and a low blade twist desired for forward flight. A high blade twist approximates the ideal twist, resulting in a uniform inflow and low induced power. However, in forward flight the high twist contributes to high vibration levels and negative angles-of-attack at the advancing side blade tip. Considering that typically the twist ranges from -8^o to -14^o a linear twist of -10^o is selected for the preliminary design.

Tip Geometry: advanced tip geometries including features such as tip sweep and anhedral offer distinct per-

formance enhancements.

Tip sweep has two important effects. First, the tip sweep improves the blade stall characteristics, resulting in lower pitch link loads. Conseqeuntly, the rotor thrust boundary can be extended [Amer92]. Second, the tip sweep delays the onset of compressability effects (such as Mach drag divergence) by reducing the free stream component normal to the tip. A tip sweep of 35 deg, from 95% radius is selected [Tish98]. Note that the swept tip also changes the incidence angle of blade vortex interactions, altering the acoustic signature.

It is necessary to demonstrate that the helicopter rotor does not exceed the RFP maximum tip Mach number limit of 0.85. Figure 3.1 shows the maximum permissible flight speed based on the Mach 0.85 limit, as a function of cruise altitude. This plot takes into account the fact that the maximum blade section Mach number is encountered just inboard of the sweep junction (at 95% radius) rather than at the tip. At 4000 ft (in ISA) the maximum permissible flight speed is 160 knots and at 8000 ft (in ISA) it is 153 knots. In ISA+ conditions the the speed of sound drops, and the above maximum permissible flight speeds are increased.

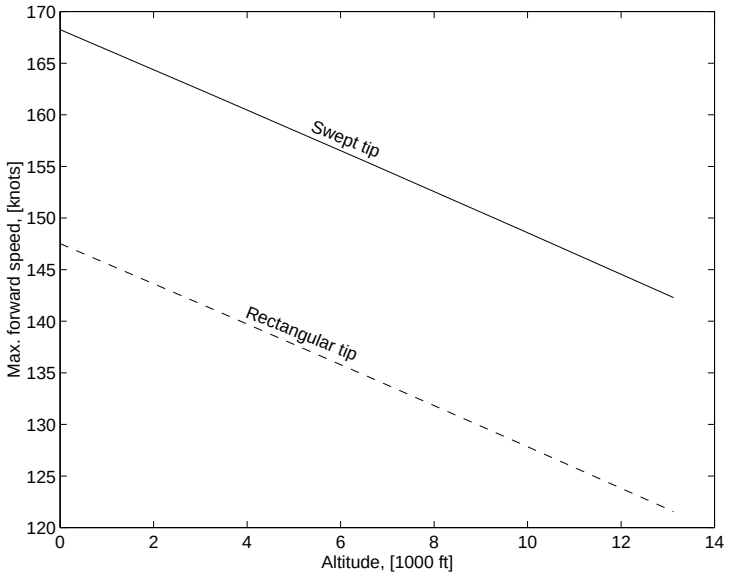

Figure 3.1: Maximum permissible flight speed (in ISA), based on RFP Mach 0.85 limit (V_{tip}= 213.4 m/s = 700 ft/sec)

The dominant effect of tip anhedral is to reduce the hover tip losses and thereby improve the Figure of Merit. The anhedral also increases the separation of the tip vortices from the rotor plane, reducing BVI induced noise. A 10 deg anhedral, from 95% radius is selected which is expected to yield a 2.5% improvement in the Figure of Merit. In conjunction with the tip sweep and anhedral a rectangular blade planform is selected.

In this intial design study a compund tip geomtetry, with non-uniform chord, sweep and anhedral, will not be considered.

Table 3.2 summarizes the primary rotor parameters.

3.3 ANTI-TORQUE DEVICE

A conventional tail rotor, a fan-in-fin and a circulation control tailboom (NOTAR) were considered. Both the fan-in-fin and the NOTAR system offer distinct advantages in terms of ground safety and lower noise. In the absence

Table 3.2: Rotor Parameters

Number of blades	-	5
Diameter	m (ft)	15.24 (50)
Chord	m (ft)	0.533 (1.75)
Tip speed	m/s (ft/sec)	213.4 (700)
Twist	deg	-10 (linear)
Sweep (from 95%R)	deg	35
Anhedral (from 95%R)	deg	10
Disk area	m^2 (ft^2)	182.5 (1964)
Airfoils	-	RAE 9648 (root to 65%radius),
	-	VR-7 (65% to 87.5%radius) and
	-	VR-8 (87.5% radius to the tip)
Blade aspect ratio	-	14.3
Root cut-out	%	30

of an exposed tail-rotor it is possible for ground personnel to safely move about the aircraft for rapid loading and unloading and potential hot refueling. In the case of the fan-in-fin the significantly reduced interaction of the main rotor wake with the fan lowers the noise level, while in the case of the NOTAR system, this interaction is completely eliminated. The circulation control tailboom was eliminated, because for a 7000 kg (15000 lb) helicopter the tailboom diameter would become prohibitively large. Consequently, a fan-in-fin is selected for the Chesapeake (see Section 11 for further details).

4 CHESAPEAKE DESIGN FEATURES & PERFORMANCE SUMMARY

This section presents the final design configuration for the 19-seat Chesapeake helicopter, which is the result of the detailed design iteration performed in Sections 5 to 15. The triple-engine helicopter (with twin engine cruise), identified in the trade-off study is used as starting point, refer to Table 2.4. A three-view schematic of the final helicopter is presented in Figure 4.1 and the 19-seat cabin layout is shown in Figure 4.2. Figure 4.3 shows a three dimensional wire frame model of the helicopter fuselage. Table 4.1 summarizes the design features and the performance of the 19 seat Chesapeake. The 12 seat derivative is briefly presented in Section 16.

Notes for the Aircraft Specification Table 4.1(next page)

1) DOC (direct operating cost) includes: depreciation, financing, insurance, maintenance, fuel and crew costs.

2) Fleet sizing and DOC are based on an average mission leg of 150 nm and an annual utilization of 2000 flight hours.

3) Climb, descent is on 3 engines, cruise in ISA+20 is on 3 engines.

4) 19-seat fleet size based on 1,100,000 passenger miles/day, 12-seat fleet size based on 700,000 passenger miles/day (both with a 70% load factor).

Table 4.1: Chesapeake Design Features and Performance Summary

	19 PASSENGER		12 PASSENGER	
General Specifications	**Metric**	**English**	**Metric**	**English**
Gross Take-Off Weight (GTOW)	7000 kg	15432 lbs	5375 kg	11850 lbs
Empty weight	3856 kg	8502 lbs	3513 kg	7745 lbs
Payload + 2 Crew	2078 kg	4580 lbs	1379 kg	3040 lbs
Usable fuel capacity	1066 kg	2350 lbs	483 kg	1065 lbs
No. of engines	3		-same-	
Type of engines	RFP IHPTET		-same-	
Unit price (1997 $)	9.03 million		7.61 million	
Total DOC[1,2] per flight hour (1997 $)	2089		1777	
Total DOC per seat-mile (1997 $)	0.86		1.15	
Overall length (rotors turning)	18.32 m	60.10 ft	- same -	
Overall height	5.22 m	17.13 ft	- same -	
Max. fuselage width	3.22 m	10.56 ft	2.66 m	8.73 ft
Performance Specifications	All data is in ISA, at GTOW		(unless otherwise specified)	
Engines used in cruise[3]	2		-same-	
Nominal cruise altitude	1220 m	4000 ft	- same -	
Nominal cruise speed	278 km/h	150 knots	- same -	
Max cruise speed (4000 ft)	296 km/h	160 knots	287 km/h	155 knots
Max rate of climb (sea level, MCP)	17.8 m/s	3500 ft/min	20.3 m/s	4000 ft/min
HOGE	4877 m	16000 ft	6360 m	20860 ft
Range (with standard reserves)	980 km	529 nm	482 km	260 nm
OEI ceiling (ISA +20, 60% fuel)	1674 m	5491 ft	1910 m	6270ft
Engine Specifications	dry, un-installed, each			
Emergency power, 30 s	1165 kW	1563 hp	932 kW	1250 hp
Take-off (nominal) power, 2 min (TOP)	932 kW	1250 hp	746 kW	1000 hp
Intermediate rated power, 30 min (IRP)	861 kW	1155 hp	689 kW	924 hp
Max. continuous power (MCP)	737 kW	989 hp	590 kW	791 hp
Rotor Specifications	common for both the 19 and 12 seat version			
Number of blades	5		-same-	
Diameter	15.240 m	50.00 ft	-same-	
Chord	0.533 m	1.75 ft	-same-	
Tip speed	213.4 m/s	700 ft/s	-same-	
Twist	-10 deg (linear)		-same-	
Sweep	35 deg from 95% radius		-same-	
Anhedral	10 deg from 95% radius		-same-	
Shaft tilt	4 deg (forward)		-same-	
Root cut-out	30%R		-same-	
Airfoils	root to 65% : RAE 9648		-same-	
	65% to 87.5% : VR-7		-same-	
	87.5% to the tip: VR-8		-same-	
Fan	common for both the 19 and 12 seat version			
Diameter	1.576 m	5.17 ft	-same-	
No. of blades	8		-same-	
Twist	-7 deg		-same-	
Tip Mach number	0.55		-same-	
Asymmetric blade spacing	35/55 deg		-same-	
Solidity	0.63		-same-	
Airfoil	NACA 63A312		-same-	
Cabin Specifications				
Interior length	6.44 m	21.13 ft	- same -	
Interior height	1.90 m	6.23 ft	- same -	
Interior width	2.19 m	7.19 ft	1.63 m	5.35 ft
Seat Pitch	0.92 m	3.02 ft	- same -	
Overhead baggage space per passenger	0.072 m^3	2.54 ft^3	0.069 m^3	2.44 ft^3
Baggage compartment	1.345 m^3	47.5 ft^3	0.869 m^3	30.7 ft^3
Fleet Sizing[2,4]	121		122	

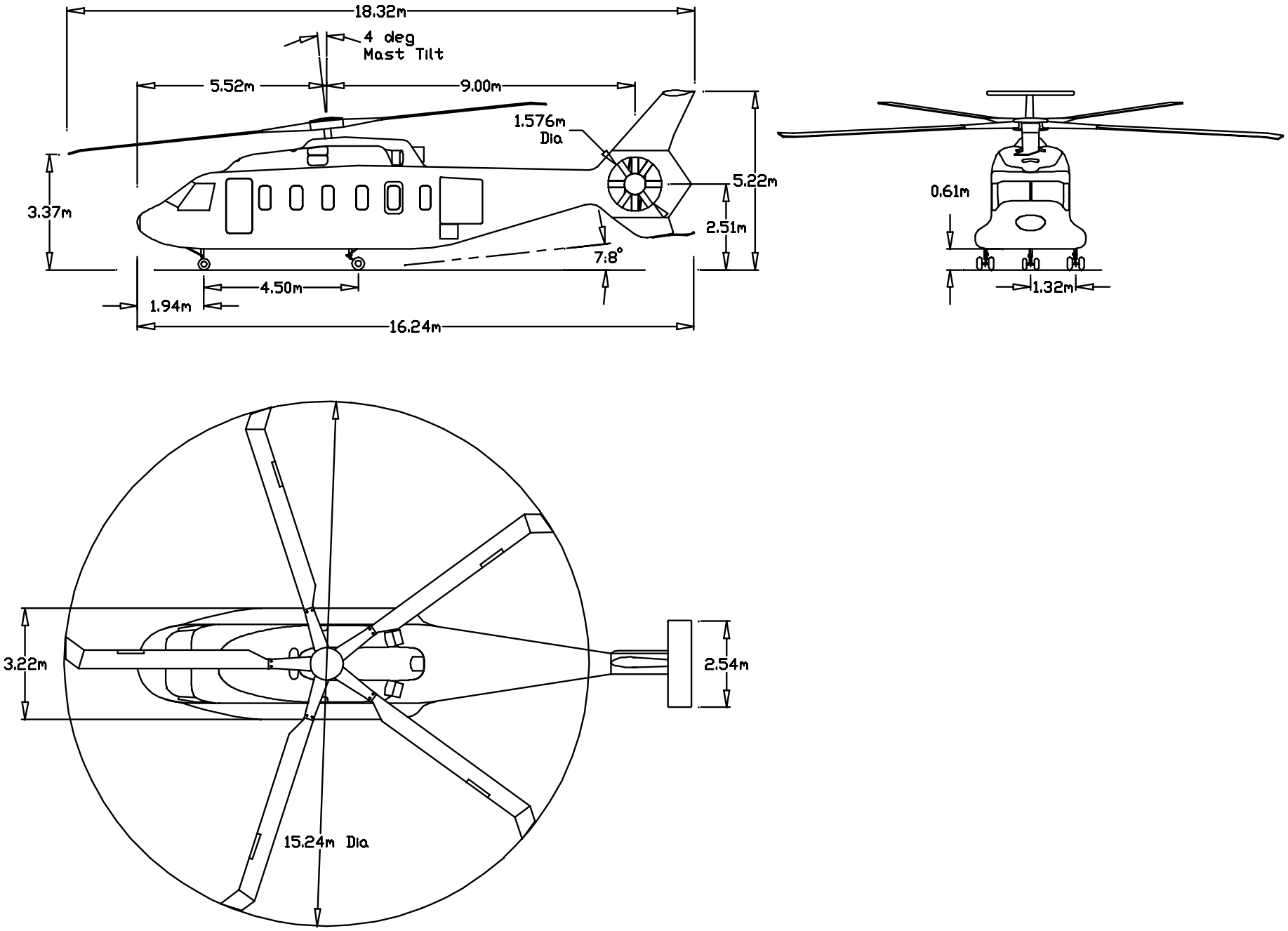

Figure 4.1: Three-view drawing of the Chesapeake 19-seat helicopter

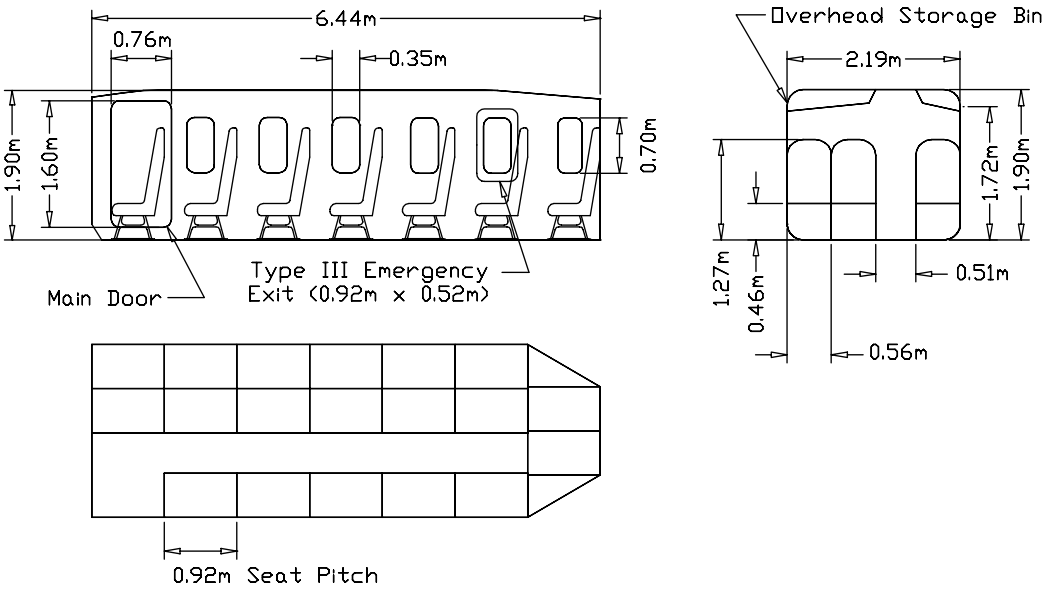

Figure 4.2: 19-Seat cabin layout

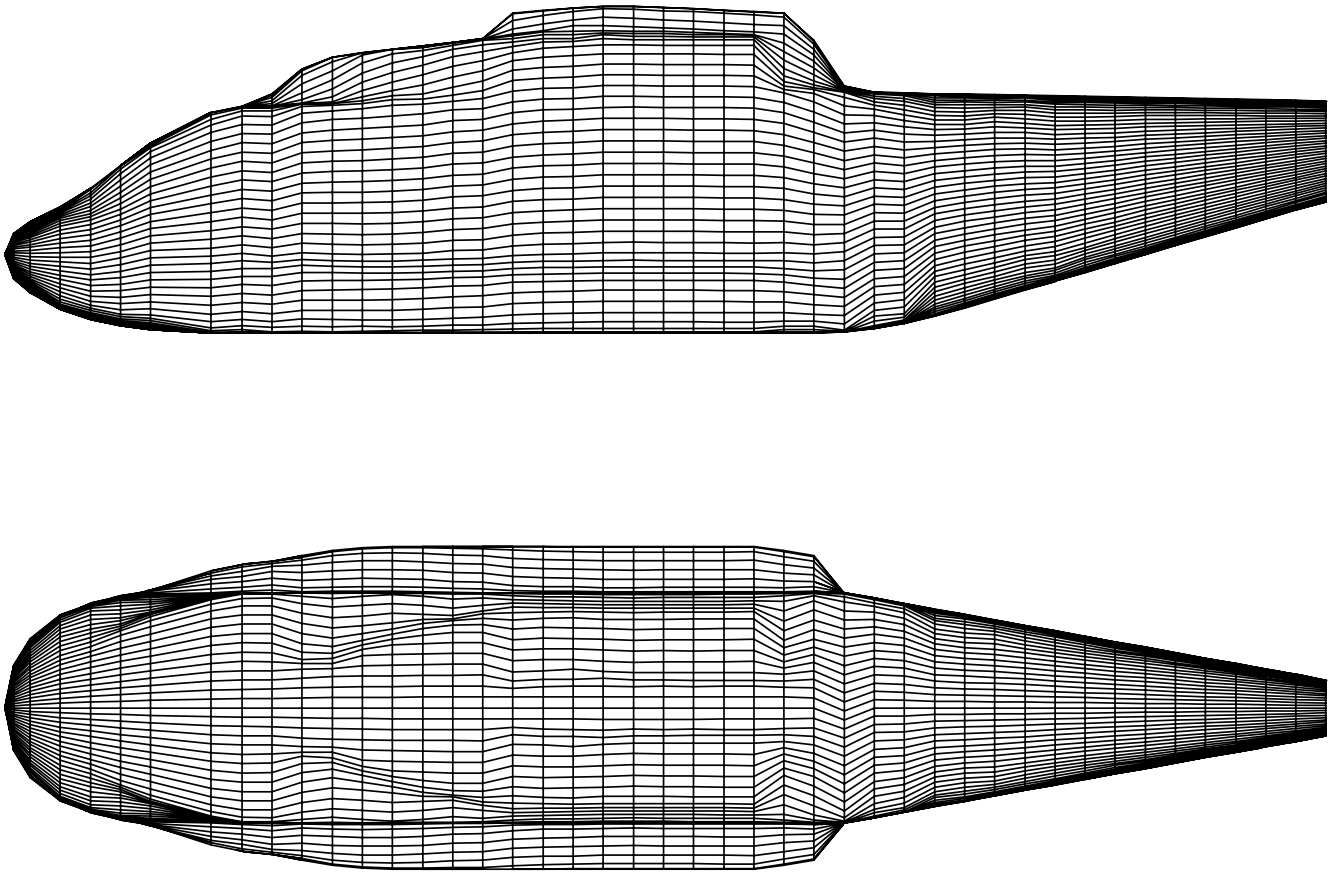

Figure 4.3: Fuselage wireframe model: side-view and top view

5 AIRFRAME & SYSTEMS

The fuselage and tail section of the Chesapeake will be predominantly manufactured from composites, with the exception of high temperature areas (near the engine exhausts) and very high stress areas. The main advantages of composites include a high stiffness/weight ratio, corrosion resistance and damage tolerant behavior. The structural concept for the fuselage is to meet both the FAR regulations, including crashworthiness, and to increase marketability, including low maintenance cost, high structural reliability/redundancy, long fatigue life, easy access to line-replacement-units (LRUs) and a high payload/weight ratio.

5.1 CABIN LAYOUT

For this commercial short haul commuter aircraft, the passenger cabin layout is a primary design driver. The 19-passenger layout is shown in Figures 5.1 and 4.2. Standard airline economy seating is chosen with the following dimensions: seat pitch = 92 cm, seat width = 56 cm, aisle width = 51 cm and aisle height = 190 cm.

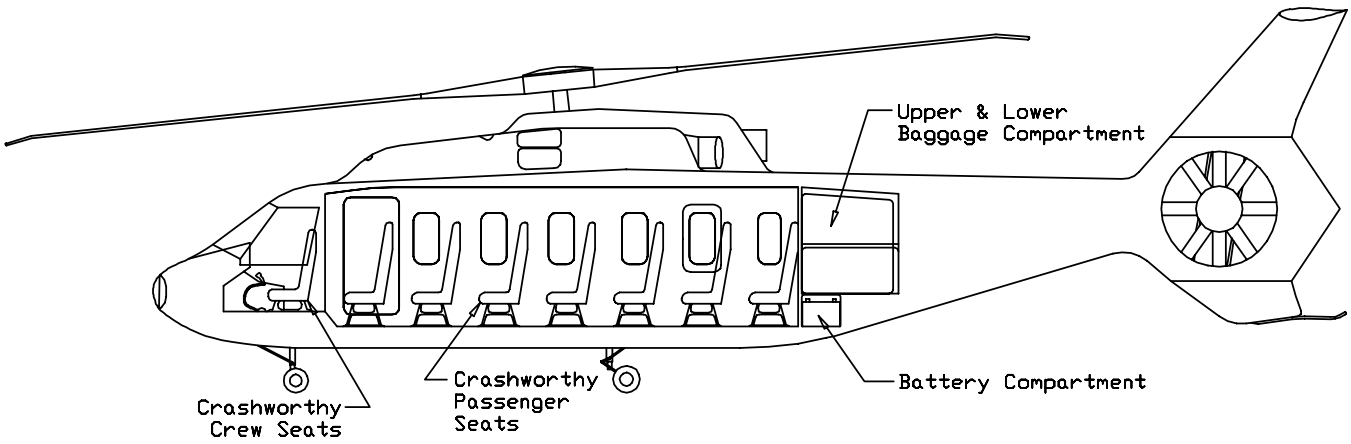

Figure 5.1: 19-Passenger cabin layout: side view detail

Overhead baggage space is provided over each row of seats. External baggage capacity is specified as 2.5 ft^3 per passenger. This gives a maximum external baggage volume of 47.5 ft^3 for the full load of 19 passengers. The cargo compartment is located aft of the passenger cabin, at the base of the tail section of the fuselage. This position was chosen to facilitate baggage handling. The CG travel resulting from variable amounts of baggage in the compartments was calculated and accounted for in the overall CG calculations.

5.2 AIRFRAME STRUCTURAL GROUP

The fuselage of the Chesapeake consists of four modules: cockpit, center fuselage, rear fuselage and tail section. These four modules can be produced separately and equipped with electrical wires, hydraulic lines and subsystems before final assembly. This modular concept also helps in transporting the helicopter by air or road. A schematic of the airframe structure is shown in Figure 5.2.

To illustrate the structural details, the center fuselage is described in more detail below (the cockpit and rear fuselage are similar in construction).

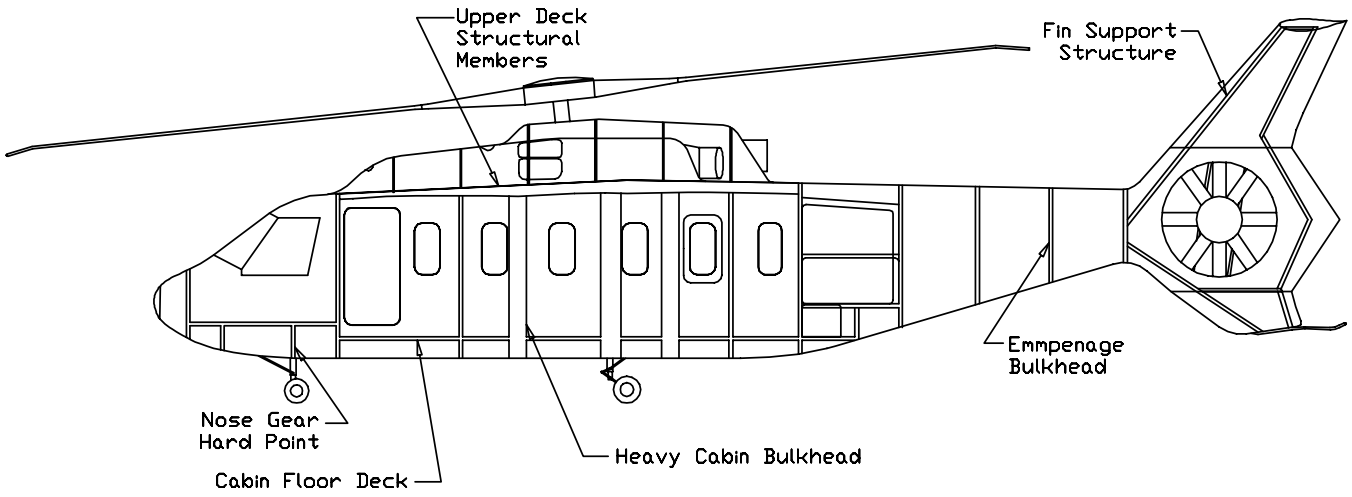

Figure 5.2: Schematic of the airframe structure

5.2.1 Center Fuselage

As a compromise between structural weight, manufacturing costs, and tooling effort, the module is divided into three main components; an upper deck, the side panels and a subfloor panel. Two 'D' shaped bulkheads are used to support and assemble the three components.

The upper deck is the primary structural interface for the main gearbox, engines, and hydraulic and electric lines. The heavy mass items (gearbox, engines *etc*) are mounted on the upper deck, which is designed to the FAR crashworthy design requirements. The upper deck is a Kev/Gr/Ep sandwich panel that is bonded to a 'D' shaped bulkhead. Titanium is used in the hot region around the engines for engine and transmission support fittings. The side panels are Kev/Gr sandwich panels with window openings. These panels are manufactured in one step by co-curing the Kev/Gr composite. The subfloor panel is also a component with many system interfaces, similar to the upper deck. More importantly, the subfloor panel includes a high energy absorbing capability to comply with crashworthiness requirements (section 5.2.3).

5.2.2 Cockpit and Rear Fuselage

The details of the cockpit and rear fuselage are similar to the center fuselage in structure. The cockpit module is characterized by a large front window and the shape of the nose design to decrease parasite drag in forward flight. The nose is produced as a monolithic part and attached to the first frame in the cockpit module. The remainder is similar to the center fuselage and is composed of an upper deck, side panels and subfloor panels.

The rear fuselage is designed to withstand the torsion, shear and bending forces arising from the tail rotor loads. It also provides the interfaces for the fan-in-fin drive shaft, controls and electrical wiring. The structure of the rear fuselage is also similar to the center fuselage.

5.2.3 Fuselage Crashworthiness Issues

For a commercial transport helicopter, crashworthiness issues are one of the most important aspects of the fuselage and passenger cabin design. There are three energy absorbing load paths for crashworthiness: first, the landing gear,

second the subfloor panel and third, the long stroke crashworthy seats. However, in light of the fact that the undercarriage is retractable, the subfloor structure and stroking seas are designed to provide the required crashworthiness. In the event that the landing gear is extended, it can provides additional crash-impact absorption. The crashworthy behavior of the subfloor panel depends on the materials used, the construction and shape of the structural elements, and the particular method of assembly of the elements.

Keel beams: from both static load and dynamic drop tests [Stit89], keel beam sections with the sine wave webs have been proven to exhibit good crash energy absorption characteristics. Two such keel beams are laid between the cabin floor and the 'D' shape bulkheads. The two keel beams run from the cockpit nose to the interface of the center fuselage and rear fuselage, and connected to the 'D' shape bulkheads by rivet joints.

Sponsons: the sponsons house both the crashworthy fuel tanks and the main undercarriage. This allows a wider main gear track, and also prevents the gear from penetrating the passenger cabin. The sponson fuel tanks eliminate the need to house fuel below the cabin, which constitutes a significant fire hazard in the event of a crash. Frangible fuel connectors are used, which automatically disrupt fuel delivery to the engines in the event of a crash.

Pilot and passenger seats: stroking pilot and passenger seats are fixed on the floor rails. In the event of a crash the seat absorbs the impact, thereby reducing the impact g-levels transmitted to the pilot/passenger. (For example, shock absorption can be via plastic deformation of the seat support tube over a mandrel, or using seat tubes with integral pistons and a thixotropic shock absorption material). A example of a suitable crashworthy seat is Martin-Baker crashworthy seat which is or will be used in EH101, NH90 and S-92.

Engines and transmission: engines and transmission assemblies are designed not to break away from the upper deck and to withstand the FAR stipulated impact acceleration levels and rates.

5.2.4 Empennage

The empennage comprises the fan-in-fin anti-torque system and the horizontal and vertical stabilizers.

Fan-in-fin blades: These are composed of Graphite/Fiberglass skins and spar, over a dual density foam core, with a leading-edge nickel erosion cap and a fiberglass trailing edge.

Stabilizers: a hybrid sandwich structure, using Kev/Gr face sheets and a honeycomb core is used in the design of the tail section (primarily for weight reduction). The spars, for both the vertical and horizontal stabilizers, are made from Kev/Gr.

5.2.5 Manufacturing and Assembling Concepts

The subsystem packaging and supportability were kept in mind when designing the structure of fuselage. This results in four main modules that are pre-assembled with local components and hydraulic and electrical through-passes. This facilitates ease of final assembling and has results in low maintenance requirements, because of fewer parts (in particular fasteners).

5.2.6 Conclusions

Composite materials are used extensively in the Chesapeake fuselage design in order to meet performance and cost requirements. Design innovations, composite materials and improved manufacturing technology are applied to the

structural design to achieve performance goals, weight savings, damage tolerance, and reliability, maintainability and cost goals.

5.3 SYSTEMS

The primary helicopter systems are shown in Figure 5.3:

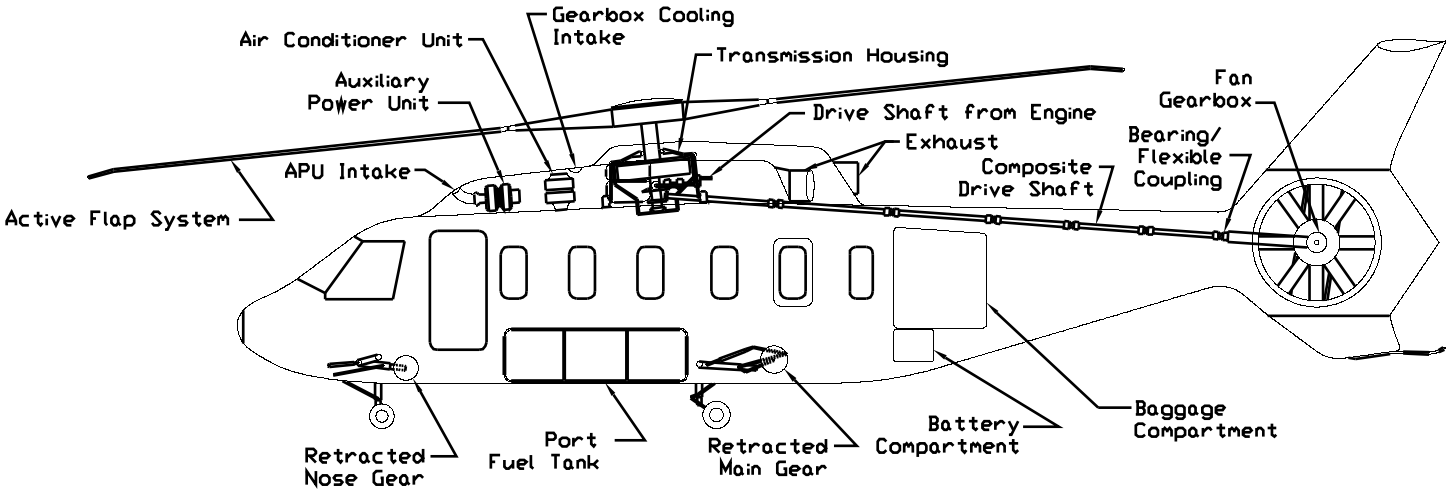

Figure 5.3: Aircraft Systems

5.3.1 Auxiliary Power Unit

An Auxiliary Power Unit (APU) is located in the foremost part of the central cowling. It is mounted directly on the transmission deck. The main purpose of the APU is to provide power for starting the main engines. It therefore satisfies the self-starting requirement of the helicopter specified in the RFP. Another function of the APU is to run the cockpit electronics and the air-conditioning plant while the vehicle is on the ground prior to take-off. The APU intake is located in the front of the main cowling and an exhaust duct carries hot gases to the exhaust duct of the central engine. This prevents ingestion of APU exhaust by the main engines during startup. Batteries are carried in a compartment below the main baggage compartment primarily for starting the APU. The use of an APU for starting the main engines results in much smaller and lighter batteries.

5.3.2 Air Conditioning System

An air conditioning plant is located just behind the APU in the central cowling. Power to run the plant is taken from the APU before take-off and from the main engines after take-off. The AC plant provides ventilation and regulate the temperature and humidity of the cabin. The cooling air for the AC plant radiator is delivered from the main gear box cooling system which is located just forward of the rotor shaft fairing (see Section 5.3.6).

5.3.3 Hydraulic System

The hydraulic pumps are run from the auxiliary gearbox and are located just aft of the AC plant. There are three independent hydraulic systems, two main units for operation of the swashplate actuators and an auxiliary unit for

the operation of the landing gear. Since the hydraulic pumps are connected to the auxiliary gear-box, hydraulic power is not lost during an engine failure. Each of the main hydraulic units can cater to 75% of the total demand, to ensure flight safety in the event of a failure of one of the main hydraulic systems.

5.3.4 De-Icing Systems

There are three on-board de-icing/anti-icing systems, for the rotorblades, the engine intakes and the cockpit front windows. The rotorblade de-icing system is comprised of a set of spanwise heating elements, located between the leading edge erosion strip and the rotorblade main spar. The heating elements are activated sequentially to reduce the overall power consumption of the system. The power for the de-icing systems is supplied by the electric generator located next to the main gearbox. An alternative system that may be considered in a subsequent design iteration is a hybrid anti-icing / de-icing system, proposed Kamel *et al* [AlKh98]. This system is designed to minimize power consumption and includes a leading edge thermal pad anti-icing subsystem, a downstream electro-mechanical de-icing system and a controller.

Engine intake anti-icing is achieved via an oil heating system, which is an integral part of the engine installation. The forward cockpit windows use electrical heating strips to prevent ice-accretion.

5.3.5 Main Generator

The helicopter has two electric generators located at the main gearbox. The generators supply power to the on-board electronics as well as the de-icing systems. Since each generator is directly coupled to the main gearbox, it will continue producing power as long as the main rotor rotates. It is therefore unaffected by engine failure.

5.3.6 Gearbox Cooling System

The main gearbox is cooled by a fan which takes in outside air from an intake located on the top of the central cowling. This cooling system also cools the radiator of the AC plant.

5.3.7 Doors and Emergency Exits

The cabin and cockpit are normally accessible via the main door which is aft of the cockpit on the port side of the aircraft. A section of the port sponson, below the main door, is hinged to fold downward. This hinged section has a set of three built in steps, for passenger-cabin entry and exit, as shown in Figure 5.4. Note that the bottom step folds into a vertical position during storage to prevent it from intruding into the cabin area.

Requirements (FAR 29:29.807) for emergency exits are exceeded with 3 Type III emergency exits located in the passenger cabin. Two exits are located in the rear of the cabin and the third is opposite of the main door. Emergency break-out side windows on both sides of the fuselage provide evacuation of the cockpit. The baggage compartment is accessible via a door on the port side of the fuselage aft of the main cabin.

5.3.8 Accessibility Features

In order to reduce the time and costs required for maintenance, special attention has been given to the accessibility of the mechanical systems. Access to the transmission deck (engines, gearbox, APU, etc) is possible by removing the

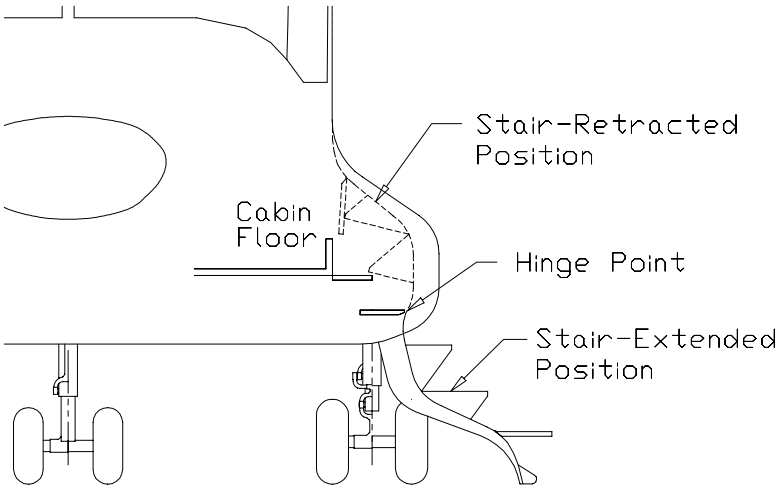

Figure 5.4: Integral stairs/sponson assembly

3 separate non-structural cowlings above the main fuselage. This will allow total access to all sides of the mechanical systems in this area. The batteries are located at ground level and can be reached using a hatch in the rear of the fuselage. The avionics and radar systems are also easily accessed at ground level via hatches in the nose area of the vehicle. Fuel systems and landing gear retraction mechanisms are located behind ground level hatches in the sponsons. Steps and grips (that recess into the aircraft) are provided on both sides of the fuselage for quick access to the mechanical spaces and to allow for preflight inspections.

5.3.9 Fuel Systems

Fuel is contained in tanks located in the side sponsons each containing 185 gallons total, 181 gallons usable (the tanks are sized for JP-4 at 100 F). The tanks are located near the longitudinal CG so that fuel distribution management is not required. Each main tank, with frangible couplings, is divided into three smaller tanks with baffles to control the effects of sloshing. The center tank is the distribution tank with fuel pumps and lines to the engines. The forward and after tanks have dual pumps to fill the center distribution tank. In accordance with the FAR, each engine has a separate fuel system of pumps and lines. The tanks are lined with a crash resistant flexible bladder. The tanks are filled using a common fuel filler port on the starboard side of the aircraft. The filler port is suitable for hot-refueling, which is required for the 15 minute turn around time between missions.

5.3.10 Landing Gear

A retractable, tricycle landing gear configuration is selected. The advantage of the tricycle arrangement, compared to a tail-wheel arrangement, is that the possibility of dangerous ground loops when taxiing or landing with forward velocity is eliminated.

The landing gear is fully retractable to reduce the parasite drag area of the helicopter and maximize cruise performance. The nose and main gear are located such that 80% of the static ground load is carried by the main gear. This facilitates good ground handling qualities of the vehicle. Because of limited space for the retraction of the landing gear, both the nose and main gear will consist of dual wheels with low tire pressures. The low tire pressure

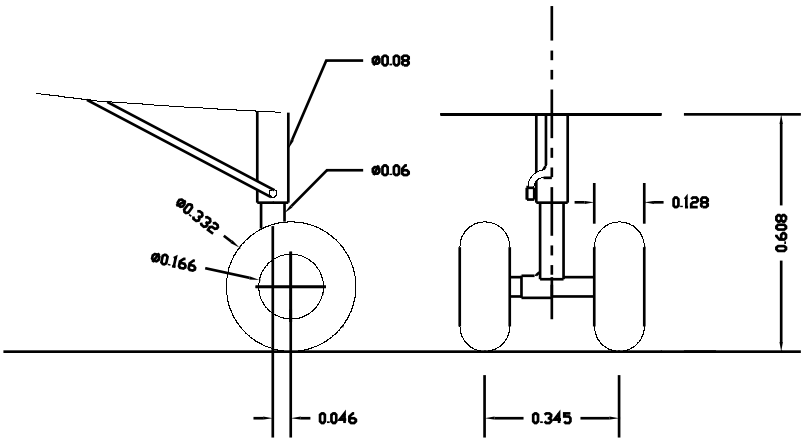

Figure 5.5: Nose gear dimensions

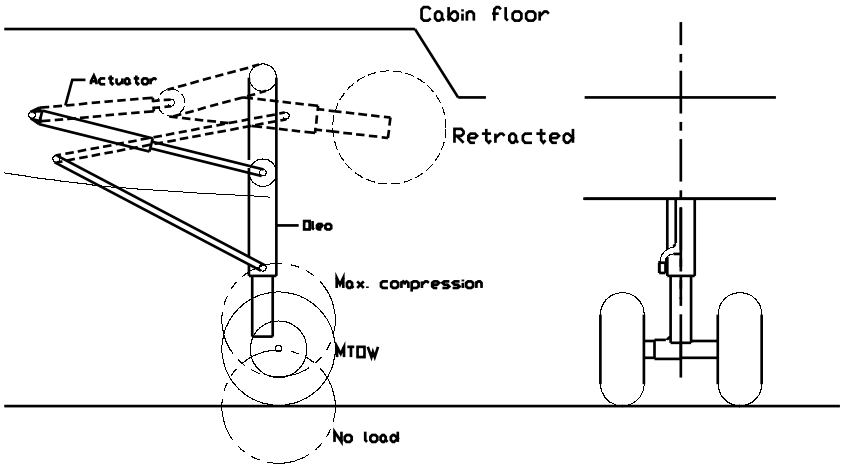

Figure 5.6: Nose gear retraction mechanism

also allows for the use of less prepared landing zones. Tire sizes are small enough so that they can be retracted into the fuselage and large enough to support the weight of the helicopter with low tire pressures. These tire pressures will allow the helicopter to be operated from medium sized airports. The tire specifications are: Nose Gear: 13 in x 5-5.5 in - 100 psi, Main Gear: 14.5 in x 5.5-6 in - 120 psi

Oleo-pneumatic shock absorbers are used for the main and nose gear. The stroke of the oleo is determined by the FAR 29.727 requirement that the shock absorbers must be able to withstand a drop test of 12 in. This corresponds to a drop velocity of 2.45 ft/sec. Using recommended values for the tire stroke (1/3 tire radius) and oleo and tire shock absorber efficiency (tire=0.47 and oleo=0.85) resulted in a stroke requirement of 15.2 cm. The stroke is increased to the recommended minimum of 25.4 cm [Raym92].

The diameter of the shocks was determined using a typical oleo internal pressure of 1800 psi and an external diameter of 1.3 times the internal diameter [Raym92]. The nose gear oleo diameter is controlled by the dynamic loading corresponding to a coefficient of friction of 0.8 (FAR 29.493). Oleo length is typically 2.5 times the required stroke [Raym92]. The oleo dimensions were calculated as: Nose Gear Oleo Diameter x Length: 8.9 cm x 63.4 cm, Main Gear Oleo Diameter x Length: 7.62 x 63.4 cm.

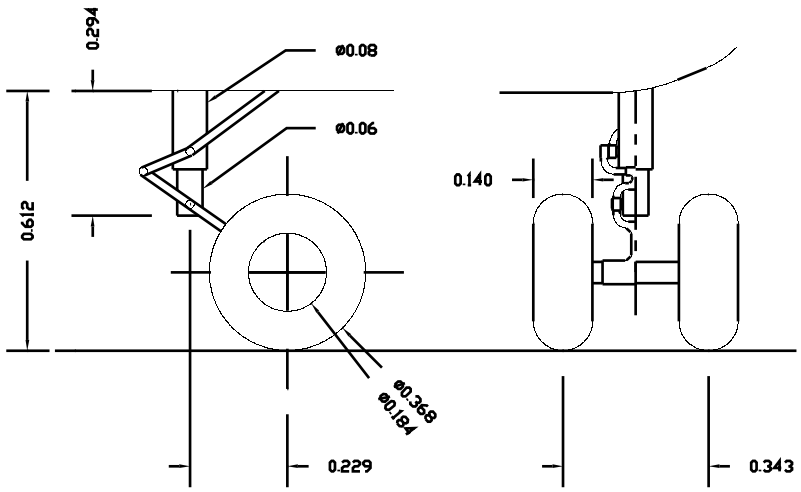

Figure 5.7: Main gear dimensions

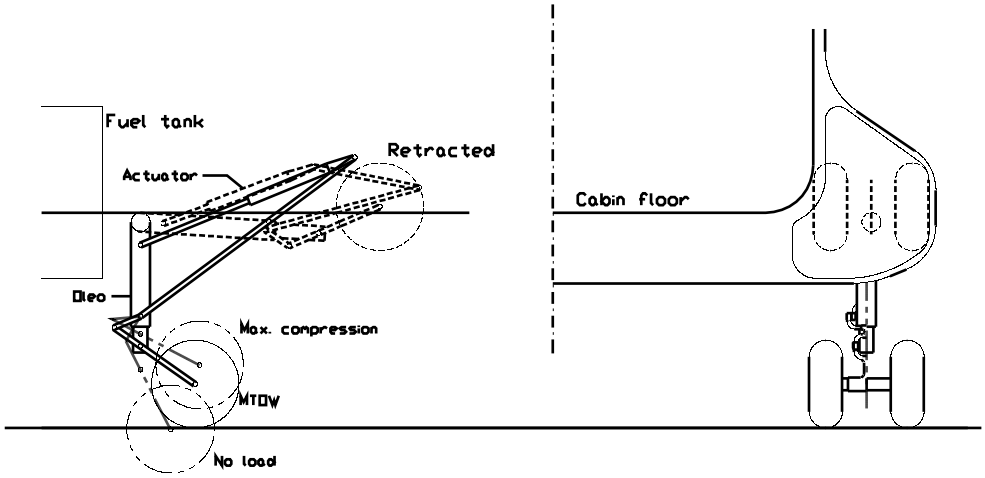

Figure 5.8: Main gear retraction mechanism

The gear retraction mechanisms are designed to be accommodated in the limited space available in the fuselage. The main gear retracts into the sponson behind the fuel tanks. The nose gear retracts into the fuselage below the cockpit.

The locations of the landing gear have been chosen to contribute to the crashworthiness of the vehicle. The main gear is located so that in the event of a crash landing, the gear will not penetrate the passenger cabin. The nose gear is situated so that the gear will penetrate the crew compartment between the two pilots seats.

Ground handling considerations are important in the layout of the landing gear. The horizontal overturning angle of the helicopter is calculated to be 63 deg (when the vehicle is empty) and 59 deg (when the helicopter is at maximum take-off weight). This is within the recommended limit of 63 deg [Raym92]. The tip back angle is 7.8 deg. An additional support arm has been added to the bottom of the tail, to protect the fin in the case of an extreme tail down landing. The minimum clearance distance between the ground and the rotor (with a -10 deg flap angle) is 2.26 m (7'-5") and occurs directly in front of the vehicle. This minimum clearance height is adequate to allow for safe baggage loading/unloading, re-fueling, pre-flight inspection, and passenger movement below the rotor.

6 ADVANCED ACTIVE SYSTEMS

The Chesapeake helicopter incorporates advanced active systems to achieve the "jet-smooth flight" design goal and to improve the aircraft cost-effectiveness. The active systems below are integrated with the aircraft software, and combine to form a smart-helicopter to enhance the handling and the ride-quality, to improve reliability and safety and reduce maintenance. Figure 6.1 shows a schematic of the HUMS and active vibration reduction system.

6.1 Active Vibration Control

An active trailing flap, with a discrete piezo-ceramic stack actuator mechanism is used for active vibration control. The adaptive time-domain control unit uses inputs from a set of rotor hub and cabin sensors to determine the flap deflection on-line. The flap actuation is independent of the primary flight controls. The active vibration control is discussed in detail in Section 10.10. In addition, with the rapid advances in smart rotor technology, it is foreseeable that the active flap system can be used to simultaneously attack rotor-borne noise and vibration reduction (most likely using a multi-flap configuration on each blade).

6.2 Active Interior Noise Control

In order to reduce noise in the cabin, a combined active/passive system is used. The passive system, in the form of an interior trim panel treatment, is most effective for broadband high frequency noise (associated primarily with the transmission system). The active noise cancellation will focus on the low frequency noise, dominated by the tonal rotor noise. The acoustics within the cabin are determined by the complex interaction of the rotor, rotor wake, engines and transmission (and associated support structure) and the cabin structure. For example, trim panels with surface bonded piezo-ceramic patch elements can be used to effect active noise reduction within the cabin. The acoustic analysis and details of the noise reduction systems will be addressed in the next detailed design iteration.

6.3 HUMS (Health and Usage Monitoring

The rotor blades, rotor hub and transmission are instrumented for on-line health and usage monitoring, see Figure 6.1. The key aspect of the HUMS system is that it uses advanced adaptive algorithms to monitor and track the integrity of the rotor and transmission system. The HUMS warns the pilot in the case of imminent flight critical failure, and for routine maintenance operations supplies an on-condition monitoring down-loadable database. The HUMS systems is briefly presented in Section 13.

6.4 FADEC (Full Authority Digital Engine Control)

The FADEC system controls the engine settings under the different flight conditions. In particular the FADEC is an essential element in reducing pilot workload during one-engine-inoperative situations. The FADEC is linked with the HUMS to provide an on-condition monitoring down-loadable database. The FADEC is briefly discussed in Sections 8 and 14.

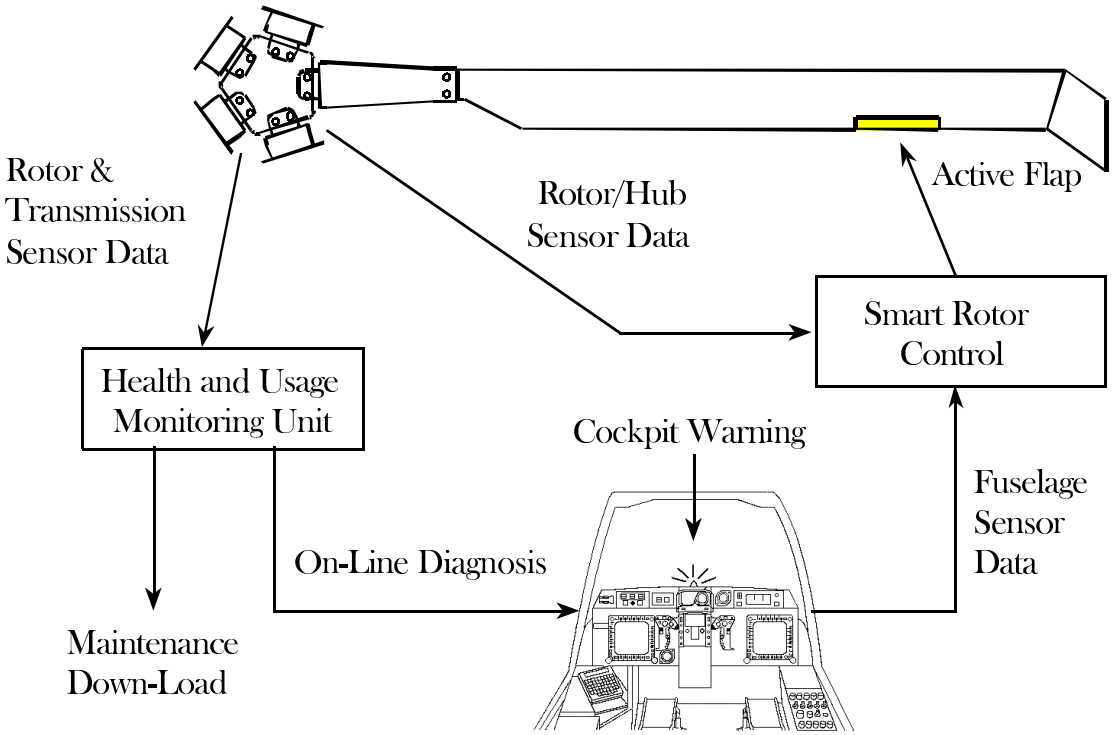

Figure 6.1: Schematic of the HUMS & active vibration reduction system

7 MASS AND BALANCE

7.1 WEIGHT ESTIMATION

The preliminary helicopter weight breakdown estimate is calculated using historical trends and taking into account advanced technologies. Prouty's empirical formulas [Prou90] are used as a starting point to determine the weights of components in the vehicle. The Chesapeake features several advanced low weight systems that that are accounted for in the weight estimation [Tish98], for example the composite fuselage and the bearingless hub. In addition, special consideration is given to components that are specific to the commercial passenger transport role, such as crashworthy-cabin design features, long-stroke passenger seats, increased structure associated with a roomy passenger cabin, interior furnishings and passenger cabin air-conditioning. The weights of these components are also included in the preliminary weight estimation. Note, that empty weight is defined as the dry-empty weight plus the unusable fuel and trapped transmission oil.

The vehicle weight is divided into groups conforming to MIL-STD-1374. The center of gravity (CG) locations are with reference to the ground plane and a virtual datum point 0.246 m ahead of the current nose. The detailed MIL-STD-1374 Weight Breakdown is presented in Appendix A.

Table 7.1: Weight Breakdown

	Mass,kg	% GTOW	Long. CG, m	Vert. CG, m
Gross	7000	100.0%	5.261	2.334
Empty	3856	55.1%	5.365	2.804
Ferry	5104	72.9%	5.143	2.419
19 Passengers and crew, no fuel	5934	84.8%	5.385	2.556
Passengers & Crew	2078	29.7%	5.484	2.081
Fuel (usable)	1066%	15.2	4.580	1.142
Engine and trans. oil	52	0.7%	5.296	3.484
Rotor group	433	6.2%	5.283	4.533
Engine nacelle	11	0.2%	5.050	3.550
Air induction	8	0.1%	3.296	1.169
Tail group	55	0.8%	13.715	4.028
Body group	794	11.3%	6.423	2.064
Alighting Gear group	174	2.5%	5.632	1.196
Propulsion	817	11.7%	5.784	3.451
Flight controls	148	2.1%	4.848	4.209
Auxiliary power	68	1.0%	3.281	3.430
Instruments	28	0.4%	0.874	1.854
Hydraulic & pneumatic	38	0.5%	4.651	3.572
Electrical	205	2.9%	6.742	2.732
Avionics	295	4.2%	0.351	1.674
Furn & equipment	396	5.7%	5.081	1.994
Air conditioning	49	0.7%	3.973	3.518
Anti-Icing	28	0.4%	5.283	4.533
Load & handling	40	0.6%	5.525	1.654
Manufacturing variation	28	0.4%	6.750	2.063
Weight growth	175	2.5%	5.05	2.063
Empty Weight Fraction $= \frac{\text{empty weight}}{\text{gross weight}}$			55.1%	
Weight Efficiency $= 1 - \frac{\text{empty weight}}{\text{gross weight}}$			44.9%	

7.2 FACTORS IN THE WEIGHT ESTIMATION

7.2.1 Crew, Passengers and Baggage

As specified in the RFP, each crew member is estimated to weigh 91 kg (200 lb) and each passenger with baggage is estimated to weigh 100 kg (220 lb). From the RFP, passenger baggage stowage capacity should include 1.5 ft^3 cabin stowage and 2.5 ft^3 external stowage, each at 10 lb/ft^3. The preliminary weight estimation assumed the average passenger to weigh 82 kg (180 lb), with 6.8 kg (15 lb) for a single carry on item (to be stowed in overhead bin) and 11.4 kg (25 lb) checked luggage (to be stowed in the cargo compartment behind the cabin).

7.2.2 Fuel Capacity

Total fuel capacity of the vehicle is sized to allow two mission legs at an altitude of 4000 ft, ISA+0 conditions and a cruising speed of 150 knots. Total fuel required for the mission is 1080 kg (2381 lb, 366 US gallons) of JP4. The fuel estimate includes an additional 1.3% to account for any unusable fuel in the system. The fuel is to be stored in two tanks, one in the port and another in the starboard sponson.

The vehicle carries 36 kg of engine oil (including 7.1 kg of trapped oil) and 16.4 kg of transmission oil (including 3.3 kg of trapped oil). These oil requirements were determined by comparing the oil-capacities of existing helicopters with similar horsepower ratings [Bell98].

7.2.3 Rotor Group

The weight of the rotor blades is estimated to be 313 kg (687 lb) [Prou90] and includes the weight of the rotor folding modifications. The weight of the titanium and composite bearingless rotor hub is estimated to be 120 kg (265.2 lb) [Prou90, Tish98].

7.2.4 Tail Group

The total weight of the tail group is estimated to be 55.4 kg (122 lb) using historical data [Prou90] with consideration given to the reduced weights of composite construction and a fan-in-fin installation [Tish98].

7.2.5 Fuselage

The Army/Bell Advanced Composite Airframe Program (ACAP) [Reis86] demonstrated that the use of composite materials can reduce the airframe weight by 22% without sacrificing crashworthiness or other strength concerns. Considering advances in the use of composite materials since the 1986 ACAP program, a reduction factor of 25% was applied to Prouty's estimate. The fuselage weight was increased by 80 kg (177 lb) to account for the additional structure required for a comfortably sized passenger cabin. In addition, 1.5% of the gross vehicle weight (105 kg) was added to the fuselage structural weight to account for any additional structural components used to enhance crashworthiness of the cockpit and passenger cabin.

7.2.6 Landing Gear

The weight of the landing gear was estimated to be 174 kg (384 lb) using historical data [Tish98]. The main gear, supporting the majority of the landing loads, is estimated to account for 80% of the total landing gear group weight (139 kg).

7.2.7 Propulsion

The engine weight is determined directly using the IHPTET scalable engine model [RFP98]. Based on a nominal engine power rating of 1250 hp, each engine is estimated to weigh 104 kg (230 lb). The drive train weight is estimated to be 399 kg (882 lb), based on historical data [Tish98] and is approximately 20% lower than that indicated by Prouty's empirical estimate. The propulsion subsystems weight is estimated to be 53 kg (117 lb), taken directly from Prouty's methods. The fuel subsystems were estimated at 5% of the total fuel weight (54 kg) [Tish98].

7.2.8 Flight Controls

The weight of the flight controls is estimated to be 148 kg (328 lb) based on Prouty's method (15.6 kg cockpit controls and 133 kg systems controls).

7.2.9 Auxiliary Power Unit

The weight of the auxiliary power unit is estimated to be 68 kg (151 lb) using data from existing helicopters.

7.2.10 Instruments

The instruments group weight reflects the incorporation of a "glass cockpit". These types of displays are significantly lighter than the traditional analog gages. Prouty's empirical equations were used to determine the weight of the required analog instruments. A reduction factor of 50% was used to account for the use of a glass cockpit. Total estimated weight of the instrument group is 28 kg (62 lb) including 14 kg (31 lb) for the glass instruments and 14 kg (31 lb) for the cockpit computers.

7.2.11 Hydraulic and Pneumatic Systems

The hydraulic and pneumatic system weights are estimated at 38 kg. Weight saving in this area can be realized by the use of titanium hydraulic and pneumatic lines and by giving special attention to the routing of these lines.

7.2.12 Electrical Systems

In the electrical group, a 15% weight reduction is realized. Because the design includes an on board APU to start the main engines, the cold start load requirements of the batteries will be reduced, allowing lightweight batteries to be used. The lightweight aviation batteries are estimated to weigh 50 kg (111 lb) and are located in an accessible compartment aft of the cabin to aid in CG control. Fiber optic cables will be used to reduce the overall weight of the required electrical cables. Additional weight savings can be realized by giving special consideration to the routing of these cables. The electrical cables are estimated to weigh 67 kg (148 lb). Two generators, with a total weight of 89 kg (197 lb), will be used to power the electrical systems from the main gearbox.

7.2.13 Avionics

As specified in the RFP, the avionics are taken to weigh 295 kg (650 lb).

7.2.14 Furnishings and Equipment

Furnishings and equipment contribute 396 kg (873 lb) to the total weight of the vehicle. This group includes crashworthy crew and passenger seats (10 kg) and miscellaneous items including: carpeting, reading lights and trim panels estimated to weigh 7.3 kg/m^2 (1.5 lb/ft^2) over the interior walls, ceiling and floor of the passenger cabin and cockpit. The construction of the overhead stowage bins is estimated to add 31 kg (68 lb) to the weight of the vehicle. Additional components to aid in the noise abatement are also included in this section and estimated to weigh 1% of the gross vehicle weight (70 kg).

7.2.15 Air Conditioning Systems

The weight of the air conditioning system was estimated to be 49 kg (108 lb) using Prouty's method and including an additional 75% to account for the climate control of the large passenger cabin.

7.2.16 De-Icing System

The rotor blade de-icing system is estimated to weigh 28 kg (62 lb) [Prou90].

7.2.17 Load and Handling Group

The load and handling group contributes 40 kg (88.4 lb) to the total weight and includes items such as checked baggage handling components, aircraft towing points and jack hard points.

7.2.18 Manufacturing Variation

Manufacturing variations are estimated at 0.4% (28 kg) of the gross weight [Prou90].

7.2.19 Weight Growth

In order to account for the potential weight growth of the vehicle during future design phases or construction, 2.5% of the gross weight (175 kg) was added to the total vehicle weight [Raym92]. This weight growth can allow for changes in the vehicle requirements or other design changes (such as the addition of a cabin pressurization system). At present this weight growth is included in the empty weight.

7.3 WEIGHT EFFICIENCY

Based on the initial weight estimations, the predicted empty weight fraction (empty weight/ gross weight) is 55.1%, leaving 44.9% for fuel, crew and payload. This compares favorably with the current trend in helicopters approaching an empty weight fraction of 50%.

7.4 WEIGHT AND BALANCE

The CG locations of the main components of the vehicle are shown in Figure 7.1.

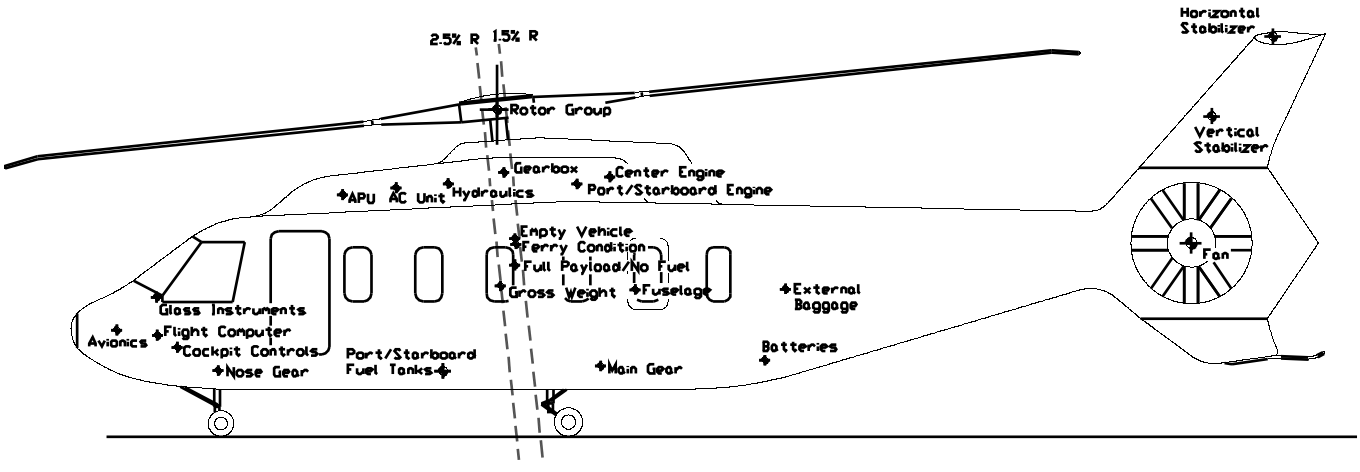

Figure 7.1: Center of gravity locations

The configuration of the Chesapeake fuel tanks is such that there is minimal CG travel throughout the mission. Figure 7.2 shows the worst case longitudinal center of gravity envelope (for all conceivable combinations of number of passengers, seating arrangement, carry-on and checked luggage and on-board fuel).

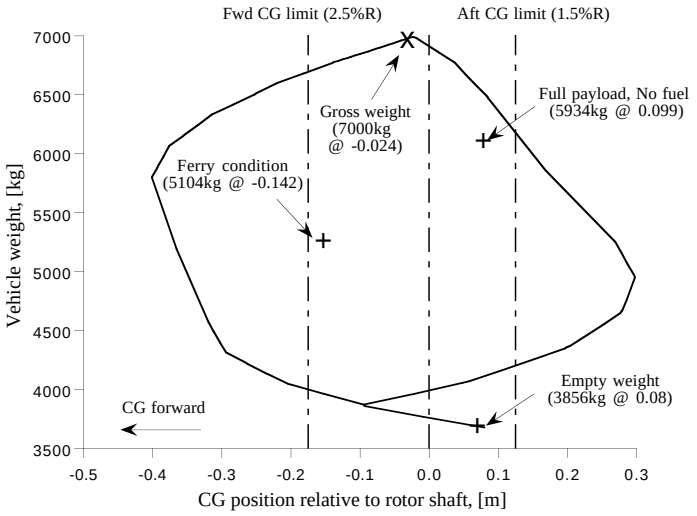

Figure 7.2: Longitudinal CG travel

The total CG travel under all possible design loading conditions is 71 cm (9.3% of the rotor radius). For stability and control reasons it is desirable to limit the CG travel to 2.5% of rotor radius forward of the shaft and 1.5% aft [Tish98]. The longitudinal bounds of the CG envelope are shown in Figure 7.1. The center of gravity locations for empty weight, gross weight, and full payload/no fuel conditions all are within the specified limits. There exists, for each loading condition (depending on the number of passengers, and the carry-on and checked baggage per passenger), a passenger seating arrangement that will result in a vehicle CG that is within the acceptable CG envelope. As is standard practice, it is the responsibility of the pilot in command to ensure that the CG limits are not exceeded under the various passenger and baggage loading combinations.

8 ENGINE

8.1 ENGINE SELECTION

In order to meet the performance objectives (see Section 9) three scalable Integrated High Performance Turbine Engine Technology (IHPTET) engines are selected, each with a nominal 932 kW (1250 hp) rating (dry un-installed). Table 8.1 lists the pertinent parameters for suitable existing engines (including the RFP stipulated SFC and power/weight ratio improvements) and the IHPTET engine, specified in RFP. The IHPTET engine offers three distinct advantages: it has the lowest specific fuel consumption, the highest power to weight ratio and most importantly, it offers a very high short period emergency setting of 125% for 30 s. This high ratio of emergency to nominal (take-off) power allows the helicopter to meet the stringent OEI requirements, without sacrificing cruise fuel efficiency.

Table 8.1: Existing Engine Data (incorporating the IHPTET Improvements)

Manufacturer	Model	Power, shp			SFC, lb/h/shp			Weight, lb
		T.O.	MCP	Emergency	T.O.	MCP	Emergency	
P&WC	PT6T-3D Twinpac	2520	1876	-	-	-	-	690
Turbomeca	TM 333	1401.4	1244.6	1479.8	0.397	0.407	0.392	345
	Turmo IIIx	2072	-	-	0.452	-	-	655
	(C3)	-	-	-	-	-	-	-
	Makila	-	1314.6	2627.8	-	0.422	0.361	535
	1A1	-	-	-	-	-	-	-
Klimov	TV3-117	2100	1680	2347.8	0.455	0.512	-	745
Rolls-Royce	Gem 42	1400	1246	1484	0.488	-	-	404
	RTM 332-01	2940	1764	3236.8	-	0.360	-	538
	Mk1017	-	-	-	-	-	-	-
	Gem 60-3/1	1584.8	1542.8	1584.8	-	-	-	407
	Mk 530	-	-	-	-	-	-	-
	Gnome H.1400-1	2149	1750	2324	-	-	0.456	326
GE	T700-700	2270.8	1853.6	-	-	0.353	-	437
	T700-401	2366	2011.8	2412.2	-	0.353	-	434
	T700-701C	2520	2326.8	2646	-	0.344	-	456
	T700-401C	2520	2326.8	2716	-	0.344	-	458
	CT7-2A	2275	-	2415	-	0.355	-	442
LHTEC	T800-LHT-800	1867.6	1453.2	1958.6	0.337	0.351	0.336	315
Textron/ Lycoming	T5311A	1540	-	-	0.510	-	-	496
IHPTET (scalable)	1250	1250	989	1563	0.305	0.328	0.302	229

The IHPTET program was started in 1988 by a consortium of government and industry representatives with the aim of greatly increasing the performance of turbine engines. With this in mind, the IHPTET program has three milestones for rotorcraft engines:

Phase I (completed): +40% Power/Weight, -20% SFC
Phase II (by 1997): +80% Power/Weight, -30% SFC
Phase III (by 2003): +120% Power/Weight, -40% SFC

Technological innovations found in IHPTET engines include advanced materials, innovative structural designs, and improved aero-thermodynamics. The IHPTET engine settings and associated specific fuel consumption are tabulated in Table 8.2. Figure 8.1 shows the curve fit used in the engine model, for performance analysis.

8.2 ENGINE PERFORMANCE

Figures 8.2 and 8.3 show the variation of the available engine power with flight speed, altitude and ISA+ condition (where the available power takes into account the power losses due to engine installation (1%), the gearbox (3.5%), compressor bleed (2.5%) and engine accessories (2.0%)). The engine model includes intake ram-effect (due to flight speed, [RFP98]), a 1.15% power drop per degree Kelvin ISA+ [Tish98] and a 1.5% power drop per 1000 ft altitude [Prou90].

Table 8.2: IHPTET Engine Data (static, ISA, mean sea level) [RFP98]

Setting	Time Limit	Power Ratio*	Power kW (SHP)	SFC/$\sqrt{\theta}$ kg/kW/hr (lb/hr/SHP)
Emergency	30 s	1.25	1165 (1563)	0.184 (0.302)
Take-Off (TOP) / Contingency	2 min	1.00	932 (1250)	0.186 (0.305)
Intermediate (IRP)	30 min	0.924	861 (1155)	0.188 (0.309)
Max. continuous (MCP)	-	0.791	737 (989)	0.200 (0.328)
Partial	-	0.5	466 (625)	0.243 (0.400)
Idle	-	0.2	186 (250)	0.608 (1.000)

*The power ratio is defined with respect to the nominal, un-installed, dry engine power.

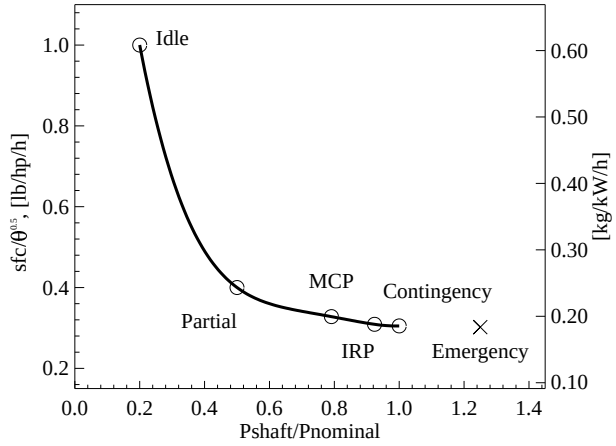

Figure 8.1: Specific fuel consumption

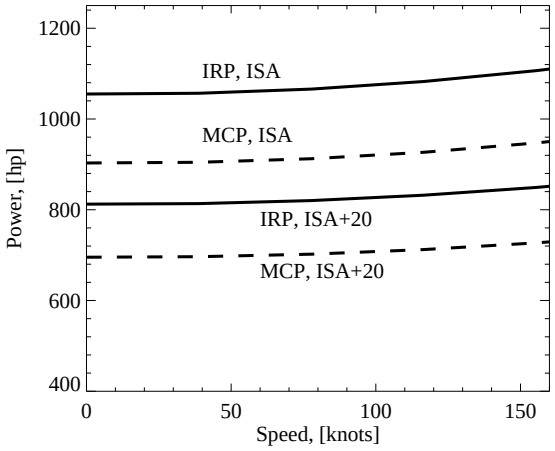

Figure 8.2: Available engine power vs. flight speed

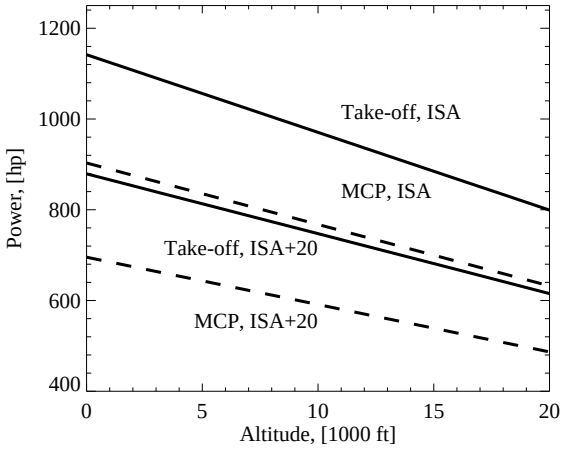

Figure 8.3: Available engine power vs. altitude

8.3 ENGINE WEIGHT AND DIMENSIONS

The size and weight of the scalable engine is given by the RFP leading to a weight of 104.2 kg (229 lbs). It was found that the formula for engine diameter given in the RFP is questionable. Application of this formula, assuming a length to diameter ratio of 2.25, yields an engine with a specific gravity of approximately 9, which clearly is not

possible. A more realistic specific gravity of 4.5 will be assumed in the present design study in order to obtain a more realistic size for the engine. This enlarges the dimensions of the final engine to 1.25 m length and 0.5 m diameter.

8.4 ENGINE INTEGRATION

The physical arrangement of the three-engines on the upper structural deck is shown in Figure 8.4

In addition, the engine will be integrated into the aircraft flight control system via a full authority digital engine control (FADEC) system. The FADEC controls the engine settings, monitors engine parameters for the health and usage monitoring system (HUMS) and automatically accelerates the remaining engines to the appropriate limit settings during an OEI situation (see Section 14.2).

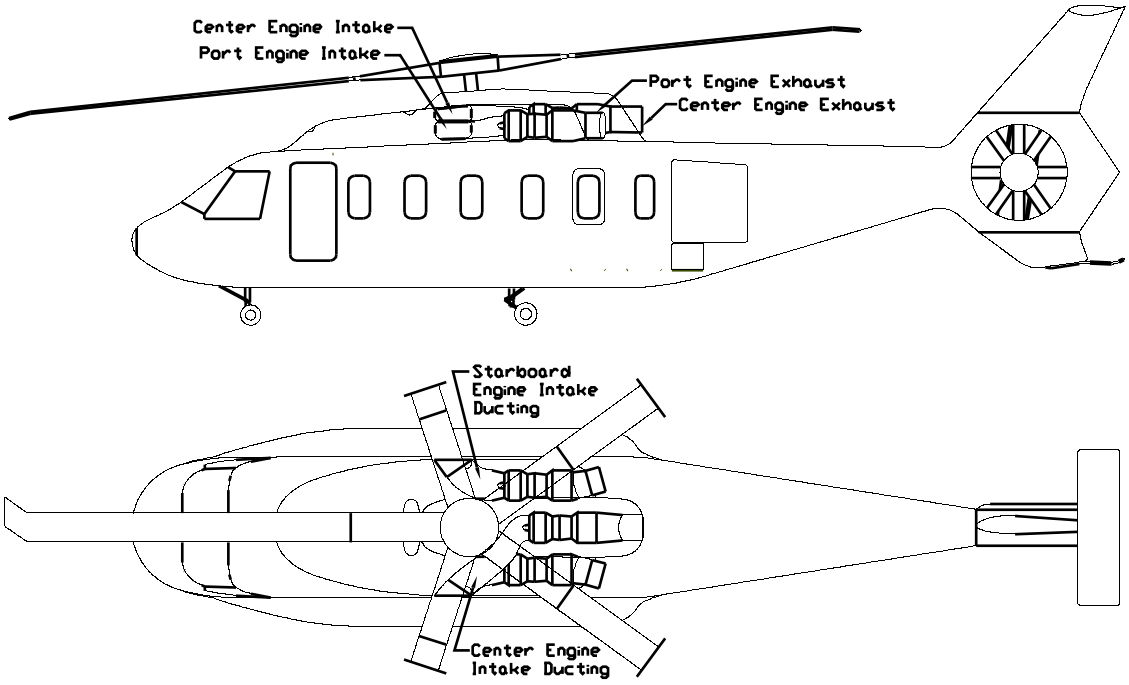

Figure 8.4: Engine installation

9 PERFORMANCE

For this first design iteration, the performance analysis focuses on hover, forward flight and one-engine-inoperative, for different ISA+ and altitude conditions. The engines and rotor are sized so as to meet the performance objectives listed in Table 3.1. The primary parameters that are investigated include: maximum flight speed, hover ceiling, OEI performance, fuel consumption, range, endurance, trim control settings and the fuselage attitude in cruise.

The current analysis for main rotor power uses a rigid flap blade (with an equivalent offset hinge and bending spring), linear inflow dynamics and a coupled non-linear trim model. Figure 9.1 shows main rotor power estimates using the rigid blade model, an elastic blade model and a comprehensive rotorcraft code, viz, UMARC (University of Maryland Advanced Rotor Code). This code incorporates a fully coupled elastic blade model and detailed aerodynamics (including unsteady aerodynamics and a free wake model). As expected, for performance calculations, the

rigid blade model results agree very well with the UMARC results. Consequently, the faster rigid blade model is used for the subsequent performance analysis. Based on the detailed rotor/hub design in Section 10, an equivalent hinge offset of 4% and a flap frequency of 1.06/rev are used in the rigid blade performance model.

The following abbreviations are used for the engine settings (see Table 8.2): TOP = take-off power, IRP = intermediate rated power, MCP = maximum continuous power; and for the atmosphere model: ISA = international standard atmosphere, ISA+ = uniform temperature increase above ISA (in Kelvin).

Table 9.1: Performance Summary: Max TOW, ISA, unless otherwise specified

Max. Take-Off Weight (TOW)	kg (lb)	7000 (15430)
Nominal cruise speed	km/h (knots)	278 (150)
Max. cruise speed (4000 ft)	km/h (knots)	296 (160)
Max. cruise speed (8000 ft)	km/h (knots)	283 (153)
Nominal cruise altitude	m (ft)	1219 (4000)
Bad weather cruise altitude	m (ft)	2438 (8000)
Engines used in cruise*	-	2
HOGE ceiling: ISA (3 eng. @ take-off power)	m (ft)	4877 (16000)
HOGE ceiling: ISA+20 (3 eng. @ take-off power)	m (ft)	2610 (8550)
Max. climb rate (sea level, 80 knots, MCP)	m/s (ft/min)	17.8 (3500)
Max. climb rate (sea level, ISA+20, 83 knots, MCP)	m/s (ft/min)	11.31 (2227)
Max. vertical climb rate (sea level, MCP)	m/s (ft/min)	7.2 (1427)
Best range speed	km/h (knots)	260 (140)
Best endurance speed	km/h (knots)	148 (80)
Range (w. standard reserves, 150 knots)	km (nm)	980 (529)
Max. range (w. standard reserves, 140 knots)	km (nm)	1033 (558)
Endurance (w. standard reserves, 80 knots)	hours	4.37
One Engine Inoperative: TOW with 60% fuel	kg (lb)	6570 (14484)
HOGE ceiling: ISA (2 eng. @ emergency)	m (ft)	4540 (14895)
HOGE ceiling: ISA+20 (2 eng. @ emergency)	m (ft)	1670 (5491)

* Climb, descent is on 3 engines, cruise in ISA+20 is on 3 engines

9.1 DRAG BREAKDOWN

Empirical data is used to evaluate individual contributions to the parasite drag of the helicopter. In order to improve the cruise performance and to reduce the fuel consumption, special attention has been given to reducing the parasite drag of the vehicle. Table 9.2 shows a breakdown of the parasite drag areas.

Table 9.2: Drag Breakdown

Component	Drag Area (m^2)	%
Main rotor hub and shaft	0.65	47.4
Fuselage	0.51	37.3
Rotor-fuselage interference	0.070	5.1
Exhaust drag	0.052	3.8
Fan-in-fin	0.041	3.0
Miscellaneous (instruments, door handles *etc*)	0.021	1.5
Horizontal stabilizer	0.015	1.1
Vertical stabilizer	0.011	0.8
Total	1.37	

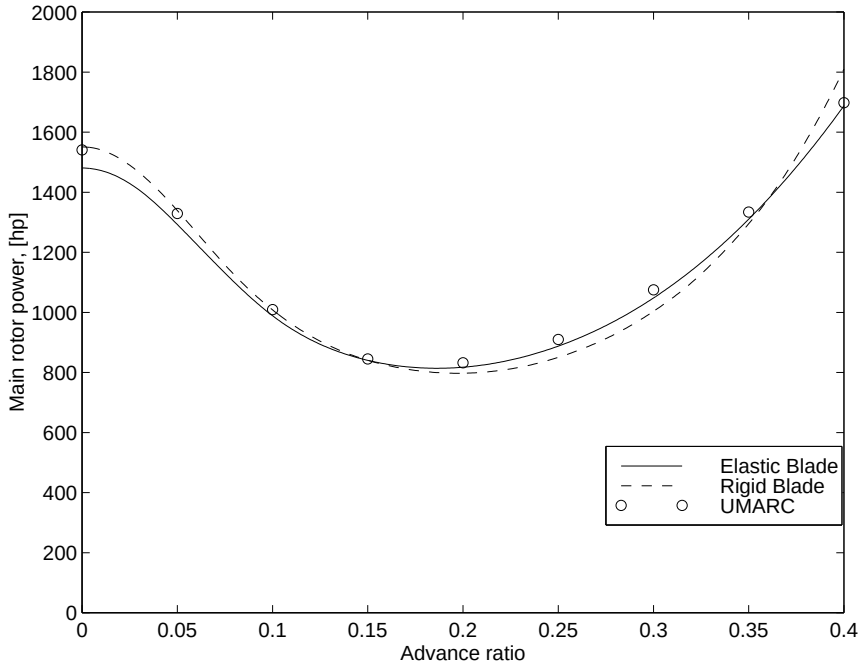

Figure 9.1: Comparison of rigid blade, elastic blade and UMARC model for main rotor power at sea level

The fuselage has been designed so that the shape is smooth and has no abrupt changes that would cause flow separation. Attention has been given to the design of the sponson and engine compartments so that the transition to the main fuselage is gradual, resulting in a low drag design. The bearingless rotor hub with fairing incorporates fewer parts and contributes less to the drag area than a traditional rotor hub. The fan-in-fin design reduces the drag loss associated with a traditional tail rotor. The total parasite drag area of 1.37 m^2 corresponds to 0.75% of the main rotor disk area. This value is appropriate for helicopters with clean aerodynamic designs [John80].

It should be noted that fuselage aerodynamics play an important role in the overall aircraft performance. In particular, in order to minimize the fuselage drag in cruise, it is desirable to have a low fuselage angle of attack. In addition a near-zero fuselage pitch attitude (in cruise) is desirable for passenger comfort. Based on subsequent trim results, the shaft incidence angle, relative to the fuselage, is set at 4 deg (see Figure 9.4) so that the fuselage is horizontal in cruise.

9.2 PERFORMANCE ANALYSIS

The nominal engine power for the scalable engine is defined, so as to meet all three of the following requirements (based on the performance objectives from Table 3.1):

1. One-engine inoperative (OEI) requirement,

2. Max. cruise in ISA, two engines @ MCP: 160 knots at 4000 ft and 153 knots at 8000 ft

3. Max. cruise in ISA+20, three engines @ MCP: 150 knots at 4000 ft and 150 knots at 8000 ft

(Note that the engine sizing is based on the desired maximum cruise speed, instead of the nominal 150 knot cruise speed. Furthermore, at 8000 ft (ISA) the flight speed is limited to by the RFP tip Mach number, see Figure 3.1).

In addition the aircraft must have sufficient power margin and thrust margin to execute a Rate 1 turn in cruise (corresponding to a nominal 30 keg bank). In this manoeuver, the engine setting can be increased to intermediate power. For the present design, the twin engine cruise requirement is the worst case condition: for the 7000 kg (15430 lb) maximum take-off mass, three engines with a nominal rating (dry, un-installed) of 932kW (1250 hp), each, are required. Based on this cruise sizing, the engines are oversized for the OEI requirement, and the 1250 ft/min rate of climb limit for an un-pressurized cabin. The engine model includes several standard power losses that are incurred between the engine shaft and the rotor/fan shafts, including: installation loss (1.0%), compressor bleed (2.5%, no pressurization), engine accessories: (2.0%), and gearbox losses (3.5%).

Figures 9.2 and 9.3 show the total power required by the helicopter and available power curves as a function of airspeed, for different altitude and ISA+ conditions. The variation of the trim control settings with flight speed and the resultant fuselage pitch attitude are shown in Figure 9.4. The fuel consumption in cruise flight is shown in Figure 9.5.

Considering that the helicopter cruises on 2 engines, with the third engine shut-off, it is important to demonstrate that flight safety is not jeopardized in the event of an engine failure in cruise. The power curves in Figure 9.2 show that in the event of an engine failure during the twin engine cruise, it is possible to maintain level flight at 4000 ft and the minimum power speed (approximately 80 knots). The pilot needs to apply contingency power (with a 2 minute time limit), decelerate to 80 knots (and if necessary descend to 4000 ft). In the interim the full authority digital flight control system (FADEC) automatically restarts the the third engine (that was originally switched-off for the cruise segment). As soon as straight and level flight is established, the pilot then diverts to the nearest airport/vertiport for a precautionary landing.

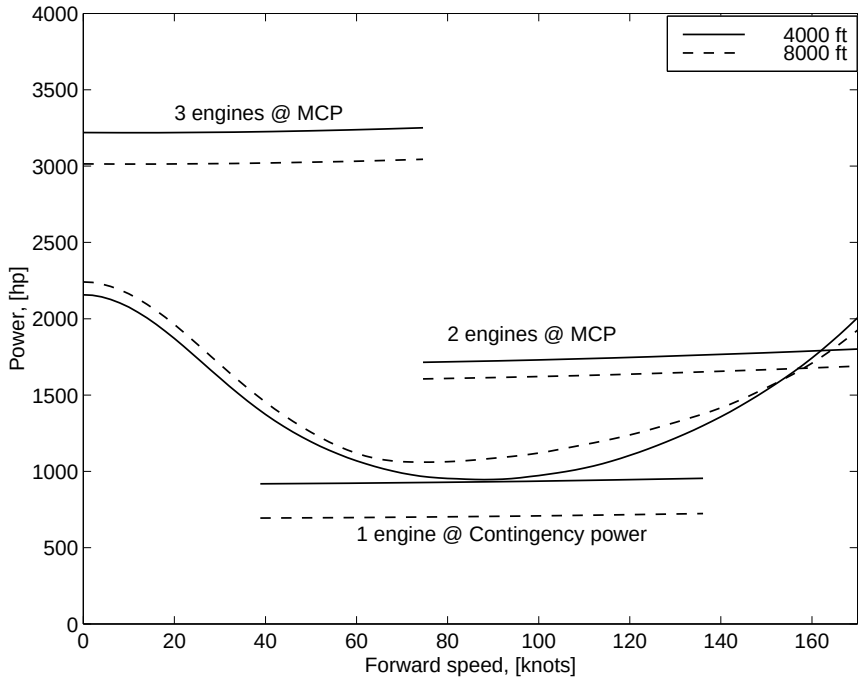

Figure 9.2: Required and available power curves: ISA, TOW=7000 kg (15430 lb)

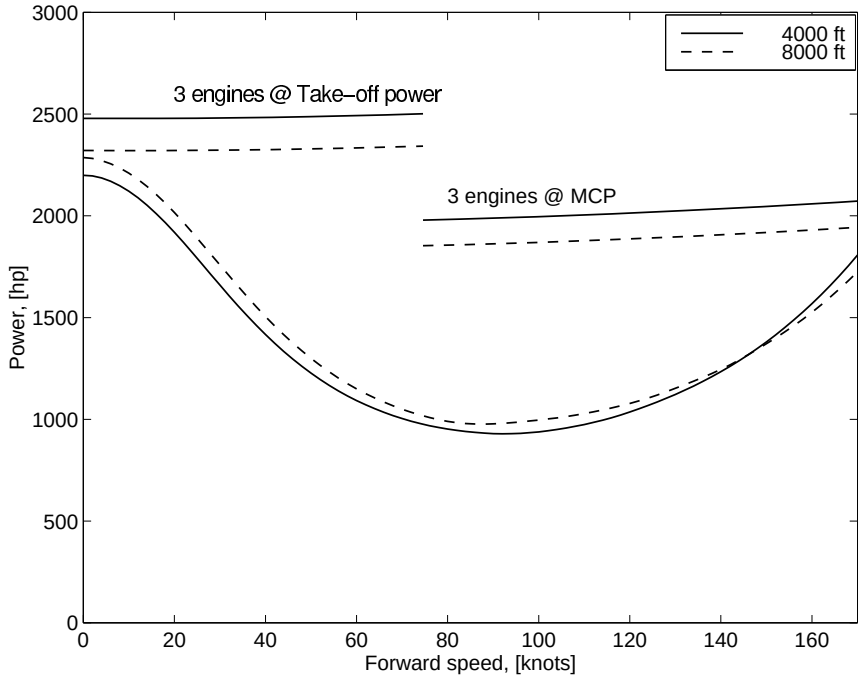

Figure 9.3: Required and available power curves: ISA+20, TOW=7000 kg (15430 lb)

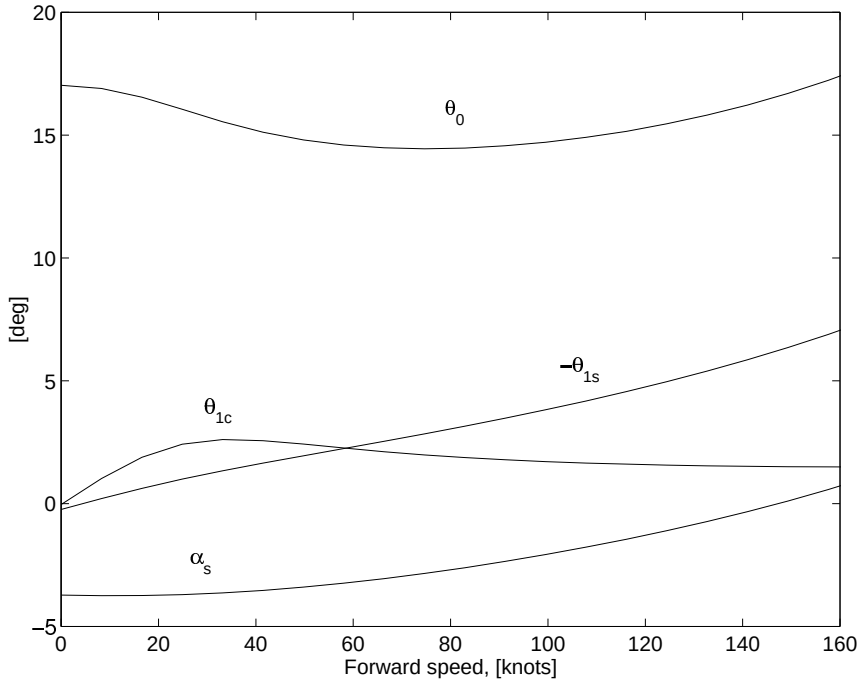

Figure 9.4: Control settings (θ_0: collective, θ_{1S}: longitudinal cyclic, θ_{1C}: lateral cyclic) and fuselage pitch attitude (α_s): ISA, 4000 ft, TOW=7000 kg (15430 lb)

Figure 9.6 shows the hover performance, in terms of the Figure of Merit vs. various C_T/σ. Within the operational hover C_T/σ range (0.06-0.075), the Chesapeake exhibits a reasonable Figure of Merit, despite the fact that the rotor is designed to generate sufficient thrust for a Rate I turn in cruise, at 8000 ft in ISA+20. Figure 9.7 shows the climb speed in ISA and ISA+20 conditions. Figure 9.8 shows hover ceiling and OEI ceiling (out of ground effect) as a

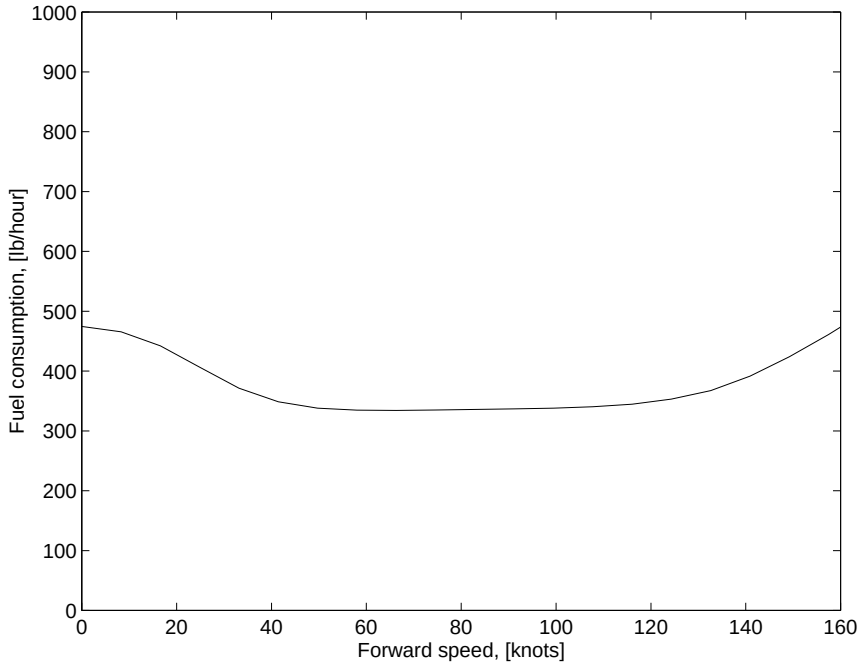

Figure 9.5: Fuel consumption: TOW=7000 kg (15430 lb), nominal cruise (ISA, 150 knots, 4000 ft, 2 engines)

function of take-off weight.

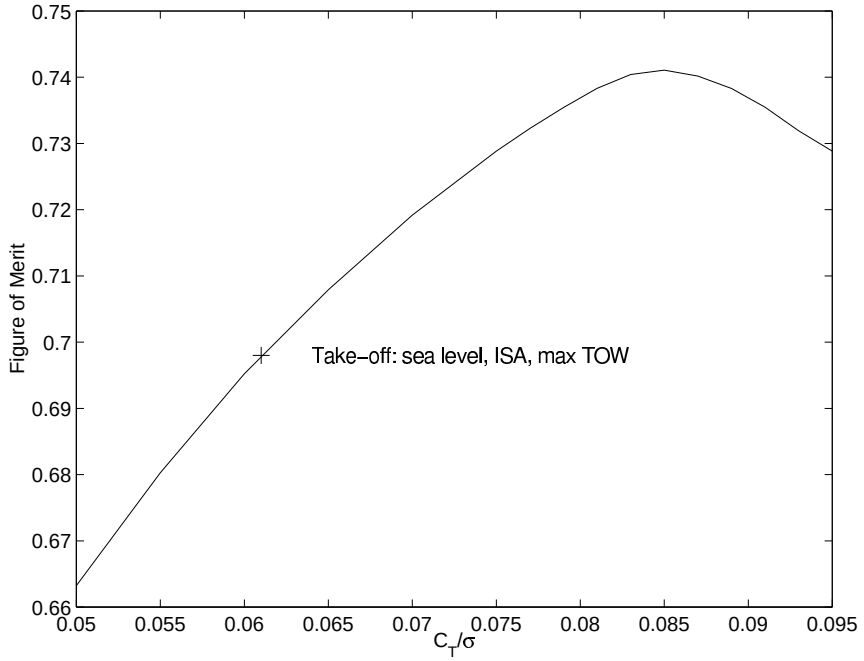

Figure 9.6: Figure of Merit

The fuel sizing is based on a un-refueled, 2x200 nm mission (with standard reserves), as stipulated by the RFP (see Figure 1.1). The standard reserves are defined as fuel for 30 minutes nominal cruise plus an additional 25 nm. Table 9.3 shows the required fuel to complete the mission profile under different cruise conditions.

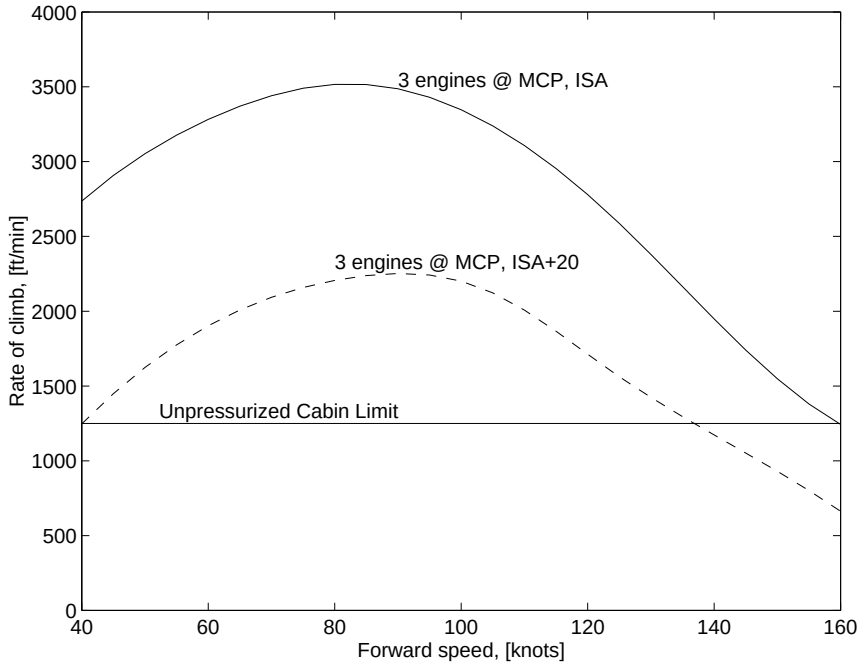

Figure 9.7: Rate of climb vs. flight speed: sea level, TOW=7000 kg (15430 lb)

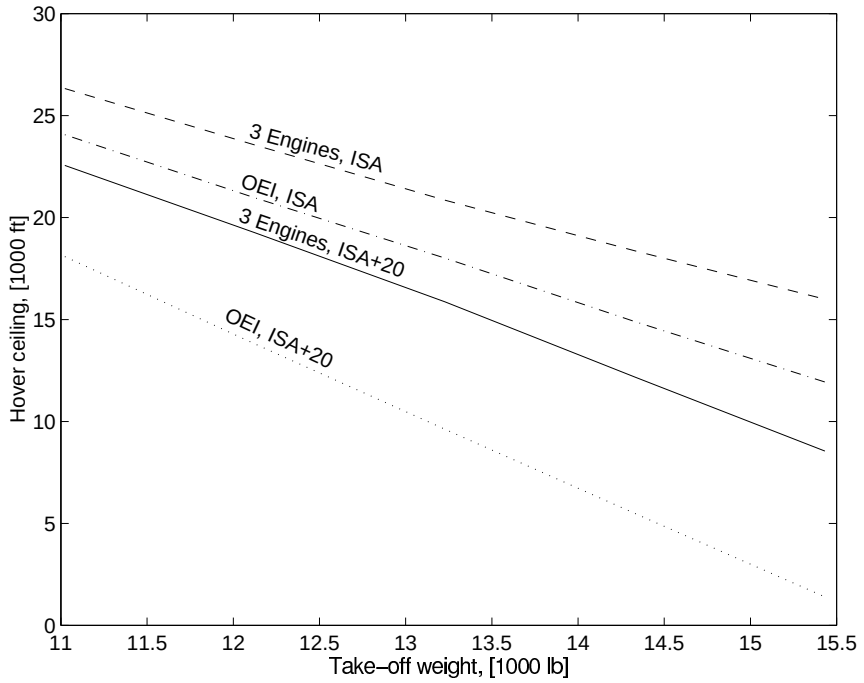

Figure 9.8: Out of ground effect hover ceiling

The fuel capacity (including standard reserves and 1.3% unusable fuel) is set at 1080 kg (2381 lb, 366 US gallons). This fuel capacity is considerably lower than that of the similarly sized S-92, and is attributable to the outstanding fuel economy of the IHPTET engine.

From the fuel consumption curve (Figure 9.5), the maximum endurance speed is between 60 and 100 knots, and the best range speed is 140 knots. The flat region in the fuel consumption curve is related to the fact that

Table 9.3: 2x200 nm Roundtrip Fuel Requirement (including standard reserves)

Cruise Temperature	Altitude, ft	Fuel, kg (lb)
ISA+0	4000	1028 (2270)
ISA+0	8000	1002 (2210)
ISA+20	4000	1066 (2350)
ISA+20	8000	1043 (2300)

between 60 and 100 knots the increase in required power, and the associated reduction in specific fuel consumption are approximately equal (refer also to Fig. 8.1). The endurance and range are obtained by integrating the specific endurance and range respectively, over the total fuel quantity, for a given initial gross aircraft weight and flight condition. This analysis accounts for the fact that the aircraft weight decreases as fuel is consumed, and thus the required engine power is reduced, to maintain a steady cruise speed. Figures 9.9 and 9.10 show the range and endurance as a function of payload. For a nominal cruise configuration (ISA, 4000 ft, 150 knots, full payload) the single leg range is 980 km (529 nm). At the best range speed of 140 knots the maximum range is 1033 km (558 nm). Figure 9.11 shows the required fuel load vs. range, for a fixed maximum take-off weight of 7000 kg (15430 lb).

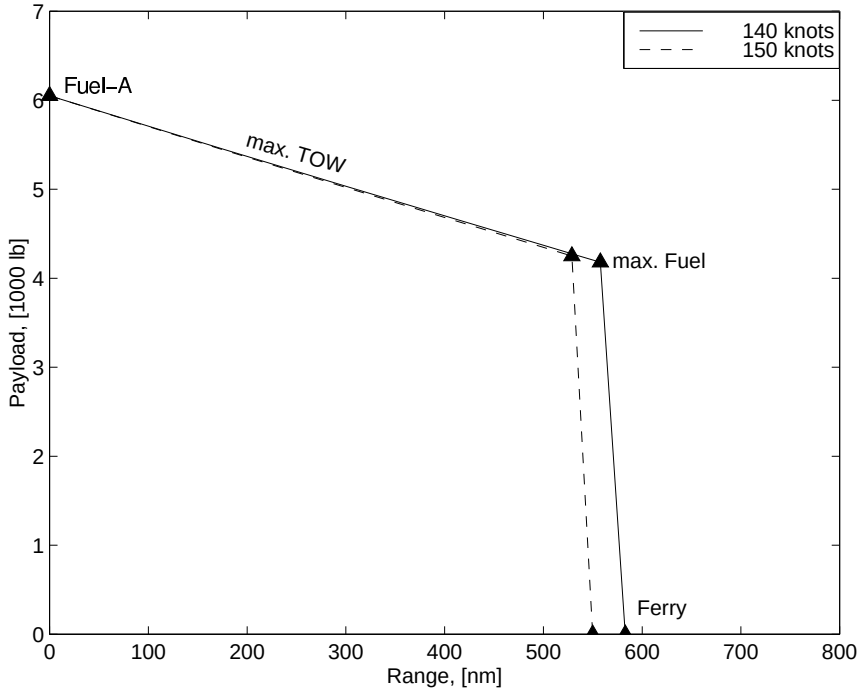

Figure 9.9: Payload-range capability (ISA, 4000 ft, 2 engines): best range speed is 140 knots, Fuel-A = standard reserve fuel plus fuel for take-off and landing

9.3 CRUISE MANOEUVER CAPABILITY

In accordance with the RFP (based on FAR) it is required to demonstrate that the aircraft has sufficient thrust and power margin to sustain a standard Rate 1 turn (180 deg/min) in cruise. The Rate 1 turn corresponds to a 30 deg bank, with a 1.155 load factor. Table 9.4 shows the thrust loading and required power at maximum flight

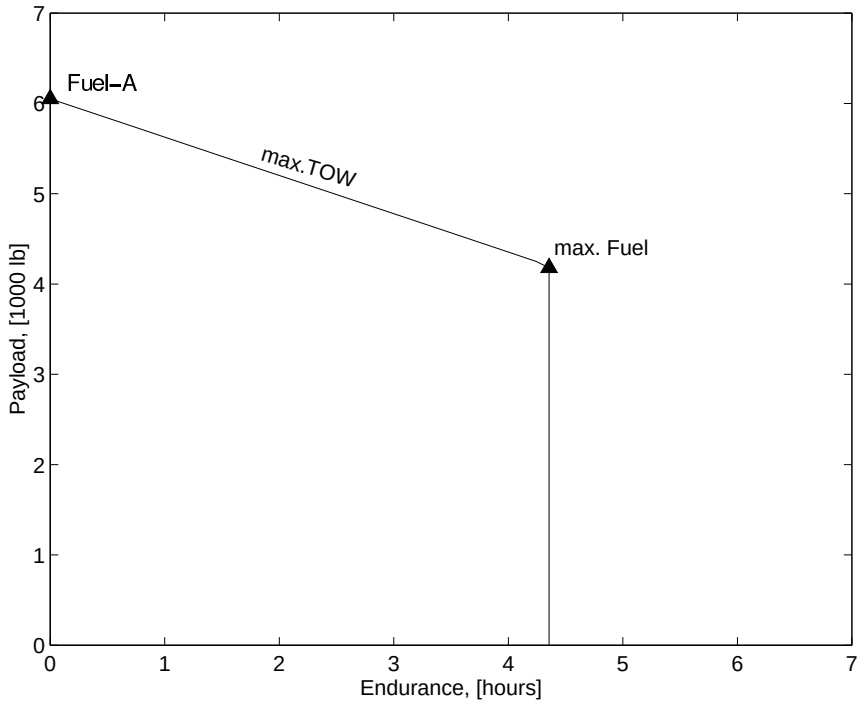

Figure 9.10: Payload-endurance capability (ISA, 4000 ft, 2 engines): best endurance speed is 80 knots, Fuel-A = standard reserve fuel plus fuel for take-off and landing

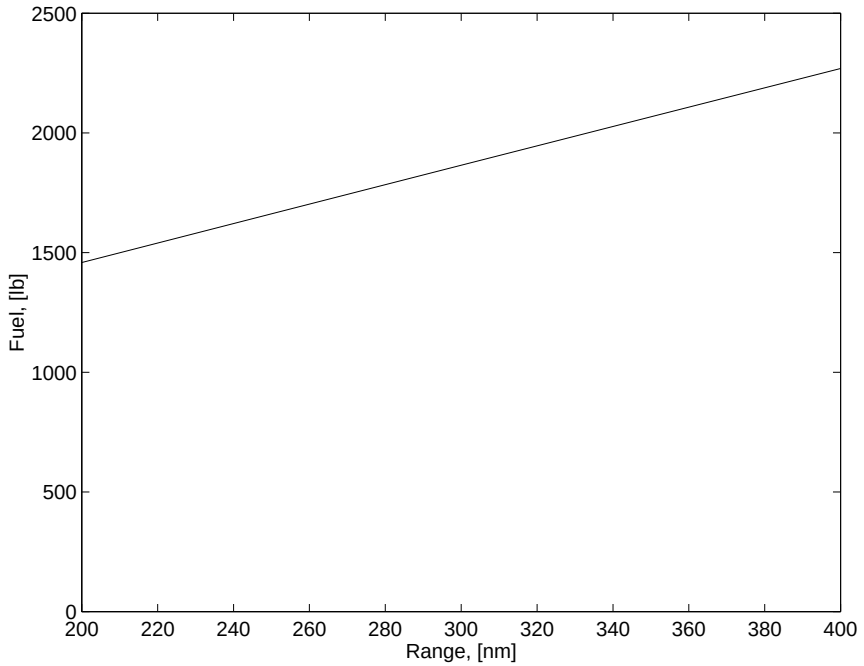

Figure 9.11: Required fuel (including standard reserves) vs. range chart: TOW=7000 kg (15430 lb), nominal cruise (150 knots, 4000 ft, 2 engines)

speed for different cruise altitudes and ISA+ conditions. In all cases the rotor thrust, C_T/σ, is below the 0.10 limit (Section 3.2), and the required power is less than the available intermediate power.

Table 9.4: Thrust Loading and Power Margin in a Rate I turn: TOW=7000 kg (15430 lb)

Height ft	ISA+ K	Max. cruise speed knots	C_T/σ	Required Power hp	Available Power hp
4000	0	160	0.079	1880	2090 (2 eng. @IRP)
8000	0	153	0.089	1897	1959 (2 eng. @IRP)
4000	20	160	0.085	1700	2405 (3 eng. @IRP)
8000	20	153	0.096	1709	2255 (3 eng. @ IRP)

ISA: cruise on 2 engines, ISA+20: cruise on three engines
Required and available power refer to power to the main-rotor and fan-in-fin

10 MAIN ROTOR AND HUB DESIGN

During the preliminary design of a new helicopter, the main rotor design is of critical importance. The design of the main rotor must consider many key factors such as the hub configuration, number of rotor blades, rotor diameter, tip speed, solidity, airfoil section, planform, autorotation characteristics, blade dynamic characteristics, and material selection. This section outlines the structural and dynamic design of the main rotor. The helicopter performance analysis is discussed in Section 9.

10.1 ROTOR TYPE

Rotor designers are constantly looking for design concepts aimed at reducing the number of parts, increasing the fatigue life and reducing the maintenance and operating costs of the rotor system. Advanced composites have enabled designers to develop bearingless rotors, which eliminate the mechanical hinges and bearings used in fully articulated systems. Another important development that has made it possible to design and develop advanced rotor concepts are elastomeric dampers. Composite materials have high strength-to-weight and stiffness-to-weight ratios, exhibit superior fatigue characteristics and increase operational safety by the inherent load path redundancy. They also have a slow and inspectable crack propagation and damage tolerance and better impact resistance. Secondly, the classical solution to avoid aeromechanical instabilities has been to include mechanical lag dampers at the root of each blade. While this solution has proven satisfactory for articulated rotors, that have significant lag motion at their hinge, their effectiveness in hingeless and bearingless rotors is greatly reduced. Elastomeric dampers, in conjunction with an advanced hub design, can provide the required level of damping.

Bearingless rotors offer simpler hubs by removing the hinges and bearings, which reduces total weight and the number of parts (about 75% reduction compared to articulated rotors and 15% reduction compared to hingeless rotor) [Hube92]. Manufacturing efforts and costs are reduced while reliability and maintainability are improved. From the available bearingless rotor design data, hub simplicity could achieve 15% to 25% reduction in the rotor system weight compared to hingeless rotors [Hube92]. In addition, bearingless rotors have greater control power compared to fully articulated rotor designs, thereby achieving better handling qualities.

10.2 BEARINGLESS MAIN ROTOR SYSTEM

The main rotor is a five-bladed soft-inplane bearingless rotor manufactured of composite materials. The blade tips exhibit both sweep and taper. Figure 10.1 illustrates the main rotor hub schematic and shows the assembly of the torque tube, flexbeam, and main-blade. The hub extends 15 inches (5% of rotor radius) from the center of rotation. A bearingless rotor consists primarily of a flexbeam and a torque tube. The flexbeam carries the centrifugal force, the lift and drag forces, and flapping and lead-lag moment of the blade. The pitching moment is carried by primarily by the torque tube. The flexbeam, which permits flap, lag and pitch motions, is rigidly bolted and cantilevered to the hub at its root end. It has 3 degrees of pre-cone angle and is connected to the blade at the outboard end. Blade flap and lag motions are achieved via a single flexbeam with rectangular cross section. The chord and thickness vary non-linearly along the length of the flexbeam and are optimized to achieve the desired strength and stiffness properties and location of the virtual flap and lag hinges. The flexbeam, with a thin rectangular cross-section, is soft in torsion. The torque tube, which surrounds the flexbeam, is connected to the blade at its outboard end at 20% radius and to the pitch link at its inboard end (at 5.5% radius). The graphite-epoxy, elliptical torque tube has a significantly higher torsional stiffness than the flexbeam. Thus, a vertical motion of the pitch link pitches the rotor blade via a rigid rotation of the torque-tube and elastic twist of the flexbeam. A combined snubber and elastomeric damper element is installed at the inboard section of the flexbeam/torque tube assembly to provide lag damping.

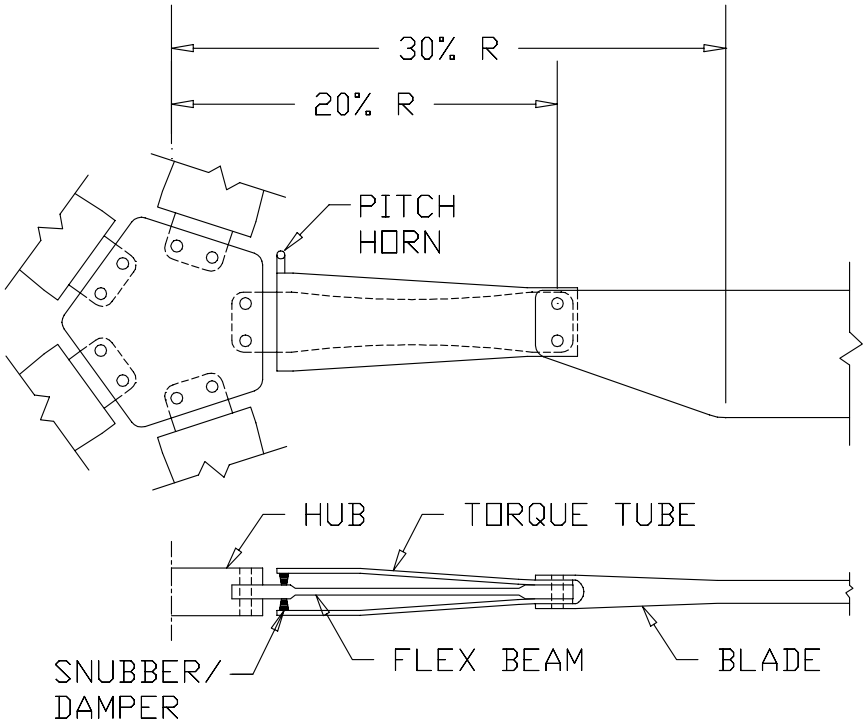

Figure 10.1: Main rotor hub schematic

10.3 AIRFOIL SELECTION

The performance of the main rotor largely depends on the aerodynamic characteristics of the airfoil. Unlike fixed wing airfoils, a helicopter blade operates in a time periodic rotating aerodynamic environment. A suitable airfoil

distribution for a helicopter rotor blade must have such properties:

1. High lift coefficient
2. Low drag (everywhere along blade)
3. High drag divergence Mach number (near the tip), to achieve high speed flight
4. Low aerodynamic pitch moment (lower control system load)
5. Good lift to drag ratio (lower power consumption)
6. Good unsteady stall properties

In high forward speed flight, an increasing portion of the retreating side of the rotor disk will be in stall and as the blade rotates about the azimuth it experiences periodic stall. Therefore, the airfoil must have good unsteady stall properties. It has been found that good static stall properties indicate good dynamic stall characteristics, so the airfoil selection can be based on static data if unsteady measurements are unavailable [John80]. No single airfoil can satisfy all these requirements. Hence, different airfoils are used along the blade span to achieve optimum aerodynamic performance.

For the Chesapeake, three types of airfoils are used: RAE 9648 (inboard of 65%), VR-7 (from 65% to 85% radius) and VR-8 (from 85% radius to the tip), see Figure 10.2. There is a 5% transition region between two adjacent airfoil sections. The VR-8 profile, at the tip, is a 8% thin cambered airfoil, selected primarily for its low Mach-drag-divergence number. The mid-section VR-7 profile provides most of the blade lift and is a 12% thick cambered airfoil with a high maximum lift coefficient, a high lift/drag ratio and good stall properties. The strong nose down pitching moment of both the outboard cambered profiles and the swept tip is reduced by the reflex cambered airfoil used on the inboard section (where its lower stalling angle is not important).

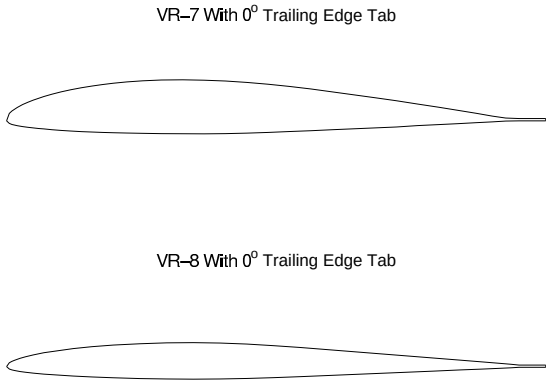

Figure 10.2: Main rotor-blade airfoil sections

10.4 MATERIALS AND MANUFACTURING

The selection of materials requires a detailed data base (generated by testing and experience) to examine life cycle costs, reliability, maintainability, and other factors. The selection is also affected by tool design and manufacturing technology. Thus, the materials from existing helicopters are referenced to decide the appropriate materials for the main rotor and hub designs.

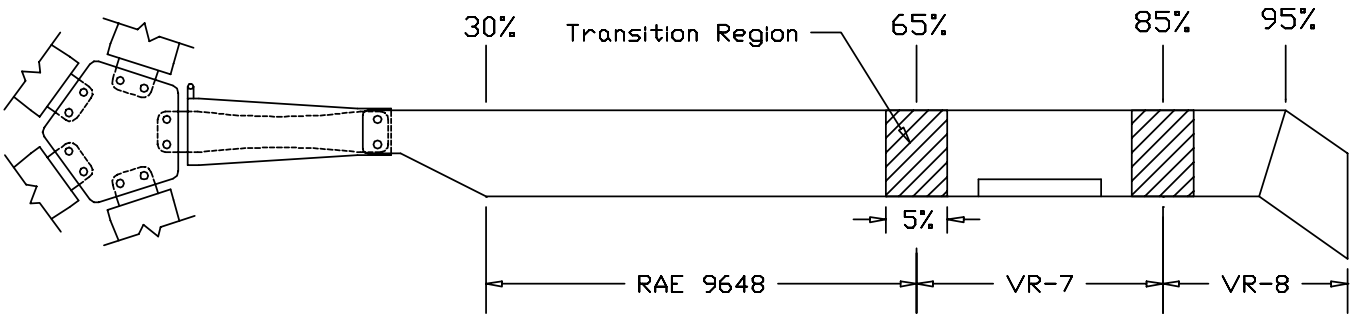

Figure 10.3: Blade planform

Titanium alloy, TIMETAL 6-4 (Ti - 6%Al - 4%V), is selected for the rotor hub. Titanium exhibits good tensile properties at normal temperatures, creep resistance up to 325 deg and excellent fatigue strength. The mechanical properties for the hub are given in Table 10.1.

Table 10.1: Titanium-Hub Material Properties [Timet98]

0.2% proof stress GPa	Tensile strength MPa	Max. Elongation %	Tensile modulus GPa	Fatigue limit % of TS	Density kg/m^3
1075	1205	14	105 - 120	55 - 60	4427

The flexbeam is constructed using unidirectional fiberglass/epoxy and its cross-section is tailored such that it provides the desired flap, lead-lag and torsional frequencies and the strength to carry the rotorblade loads with a long fatigue life.

The torque tubes are fabricated primarily of carbon fiber filament wound over the mandrels using a NC (Numerical Control) filament winder. Unidirectional tape is added to provide higher bending stiffness.

The blade cross section is shown in Figure 10.4. The basic structural materials of the blade are fiberglass, carbon/epoxy and a Nomex honeycomb core. The blade spar is made of a unidirectional fiberglass composite 'D' spar with a torsion-wrap of graphite/epoxy. Nomex honeycomb is selected for the core, since it has a lower weight compared to a foam core and presents fewer problems in producing a satisfactory bond to the skin. Furthermore, it exhibits low moisture absorption.

Rotor blade fabrication consists of three major cure cycles: first the spar assembly is laid-up and cured and second, the cured spar, the fairing skin, and the core are assembled and cured. Pre-impregnated tapes are used in the design of the rotor blade components because of the accurate orientation of unidirectional tape and excellent control of the resin-to-fiber ratio. Finally the de-icing heating pads and the leading edge erosion strip are bonded into place.

10.5 NUMBER OF BLADES

A trade-off study was conducted between a 4- and 5-bladed rotor system. Their characteristics are shown in Table 10.2. The radius and tip speed of each blade and solidity of the rotor system were decided based upon performance characteristics. Vibration, noise and weight were considered in the selection the number of blades.

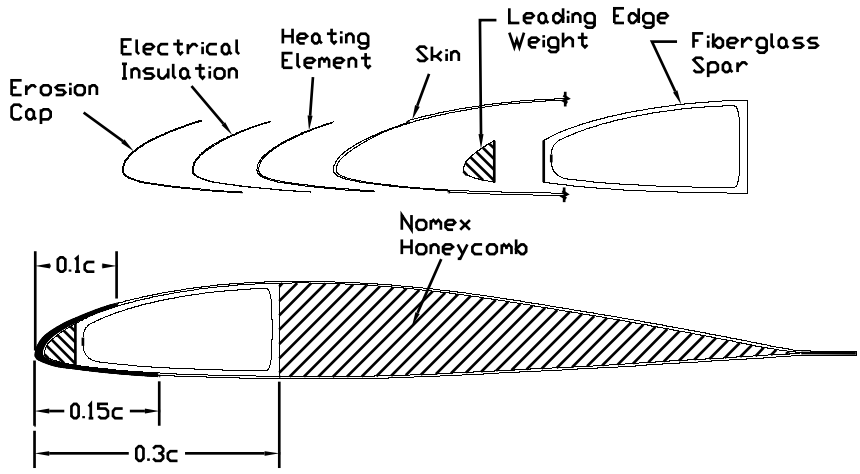

Figure 10.4: Blade cross section

Table 10.2: 4 vs. 5 Blades

	4 blades	5 blades
Solidity	0.11	0.11
Radius	25 ft	25 ft
Tip speed	700 ft/sec	700 ft/sec
Chord	2.19 ft	1.75 ft
Aspect ratio	11.4	14.3

Vibration of the main rotor is an important factor in the decision of how many blades to use. Helicopter vibration is characterized by harmonic excitation in the non-rotating frame, primarily at 1/rev and N_b/rev (where N_b is the number of blades). A 1/rev vibration of the frequency occurs due to rotor imbalance, which may be caused by a blade out of track or physical differences between individual blades. An ideal rotor system with perfectly balanced blades only transmits rotor forces at harmonics of the number of blades per revolution. By increasing the number of blades, the vibration frequency is increased, but the vibration amplitude is decreased because of the lower loading on each blade. $(N_b \pm 1)$/rev harmonic loads in the rotating frame are transmitted to the fuselage producing N_b/rev harmonic vibration in the fuselage. In the rotor design, the second flap frequency, approximately 3/rev, creates 4/rev inplane fuselage vibrations for a 4-bladed rotor, whereas the second lag frequency, approximately 4/rev, creates 5/rev vibration in a 5-bladed rotor. But, the second flap frequency (2.67/rev) is much lower than the second lag frequency (4.23/rev), and thus the magnitude of the load is much higher. Usually, the second flap frequency cannot be placed far from 3/rev and thus the 5-bladed rotor has less vibration.

The weight of main rotor blade and hub is calculated using the following equations [Prou90]:

Main rotor blade: $W_{bM} = 0.026 N_b^{0.06} c R^{1.3} V_T^{0.67}$, hub: $W_h = 0.003 N_b^{0.28} R^{1.5} V_T^{0.43} (0.67 W_{bM} + \frac{g I_\Omega}{R^2})^{0.55}$

Where I_Ω is the polar moment inertia and g is gravity. The weight estimates are in Table 10.3.

The 5-bladed rotor increases hub weight by 2%, but decreases rotor weight by 7.4% because of the reduced chord, resulting in a net 3.9% reduction of total hub and blade weight, compared to that of the 4-bladed system. Although the above equations do not give exact weights, the 5-bladed rotor has no significant weight penalty compared to the 4-bladed rotor. In addition, the 5-bladed system transmits less vibration to the fuselage, therefore a lighter vibration

Table 10.3: 4 vs. 5 Blades Weight Estimates

	4 blades	5 blades
Rotor weight	100 %	92.6 %
Hub weight	100 %	102 %
Total weight	100 %	96.1 %

reduction system is required. Additionally, the low weight of each blade in the 5-bladed rotor facilitates the manual blade folding process. Thus, the 5-bladed rotor is preferable compared to the 4-bladed rotor.

From an aerodynamic point of view, a small number of blades results in a stubby shape where the tip loss region covers a significant portion of the blade area. Furthermore, the wake left by a rotor with small number of blades is pulsating, which generates a higher induced power than the smoother wake created by a multi-bladed rotor. A larger number of blade leads to weaker tip vortices for the same overall rotor thrust, thus reducing blade-vortex interaction airloads and noise, as well as vibration. Also, from a noise point of view, a higher number of blades results in a smaller chord and therefore less "thickness" noise.

Now, the 5-bladed rotor requires more parts (blade, flexbeam, torque tube, pitch link, snubber, and damper, *etc*) than the 4-bladed rotor thereby increasing manufacturing, purchase and maintenance costs. The cost increase will be offset to an extent by the lower weight of the 5 bladed system. The direct impact of the number of rotor blades on the aircraft price and the maintenance costs is beyond the scope of the present cost model (see Section 15).

Overall there are advantages and disadvantages with both rotor systems. However, providing passengers with smooth and comfortable flight is one of the primary design objectives. Thus, the 5-bladed rotor, with the associated lower vibration and noise levels, is selected.

10.6 ROTOR DESIGN PARAMETERS

The rotor characteristics, including structural and inertial distributions, are initially based on an existing five-bladed bearingless rotor. These have subsequently been iteratively adjusted to achieve the desired performance values. Table 10.4 summarizes the pertinent parameters for the main rotor design (see also Section 9).

10.7 ROTOR DYNAMICS

A very important consideration during the development of a rotor system is the blade dynamics. It is necessary to avoid resonance conditions between the coupled blade frequencies and the exciting rotor harmonics. Figure 10.5 depicts the rotor-blade fan diagram. An accurate determination of the blade structural modes must be accomplished to insure that the blade natural frequencies are separated from the rotor harmonics at the operating speed.

The blade rotating natural frequencies are calculated using UMARC (University of Maryland Advanced Rotorcraft Code). The blade, flexbeam, and torque tube are divided into nine beam finite elements with the flexbeam cantilevered to the hub. Flapwise, chordwise and torsion stiffness distributions are shown in Figures 10.6, 10.7 and 10.8.

Four flap, two lag, and one torsional frequency are shown in Figure 10.5. The blade frequencies (at operating speed) are shown in Table 10.5. The first in-plane frequency is a key parameter, that has a direct influence on ground

Table 10.4: Main Rotor Design Parameters

Radius, R	7.06 m (25 ft)
Number of blades, N_b	5
Disk area	156.6 m^2 (1963.5 ft^2)
Chord, c	0.533 m (1.75 ft)
Tip speed	213 m/s (700 ft/s)
Nominal operating speed	267 rpm
Solidity	0.11
Twist	-10 deg(Linear)
Blade area	20.32 m^2 (218.75 ft^2)
Aspect ratio	16.11
Blade flapping moment of inertia, I_b	1271 Nm^2 (937.2 slug-ft^2)
Polar moment of inertia, I_Ω	6597 Nm^2 (4866.0 slug-ft^2)
Effective flap hinge offset	8.24%
Airfoils	RAE 9648 (30%R to 65% radius), VR-7 (65% R to 87.5% radius) and VR-8 (87.5% radius to the tip)
First flap frequency	1.06/rev
First lag frequency	0.7/rev (soft-inplane)
First torsion frequency	6.76/rev
Damper type	Fluid-elastomeric damper

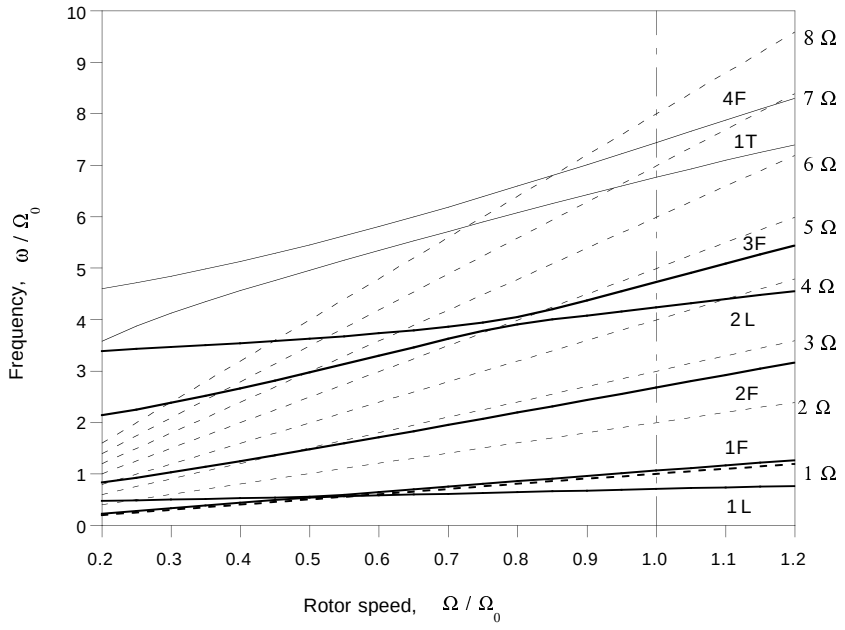

Figure 10.5: Fan diagram (F: flap, L: lag, T: torsion, Ω_0: operating speed)

and air resonance instabilities and requires special attention.

The relation between the lag frequency, the required damping and the blade in-plane loads is shown in Figure 10.9. For lower in-plane frequencies, higher in-plane damping is required. On the other hand, the first in-plane frequency cannot be increased beyond 0.8/rev, due to resonance amplification of the blade in-plane loads. Hence, an in-plane frequency of 0.7/rev is chosen at the operation RPM.

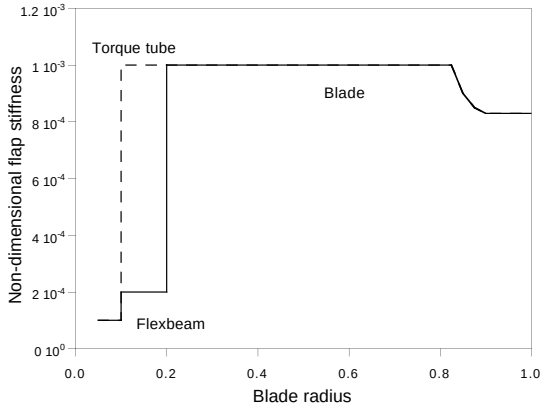

Figure 10.6: Flapwise stiffness distribution

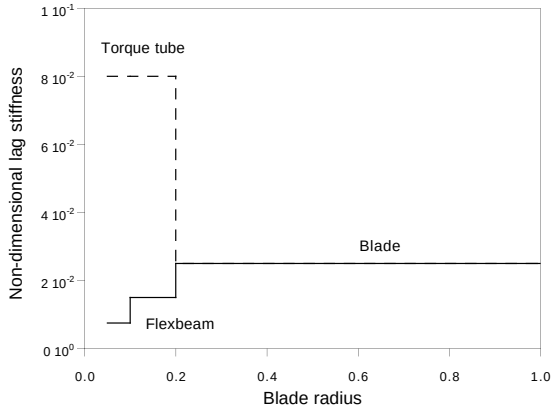

Figure 10.7: Chordwise stiffness distribution

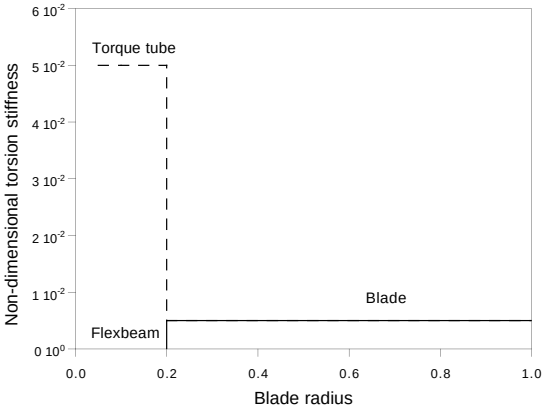

Figure 10.8: Torsional stiffness distribution

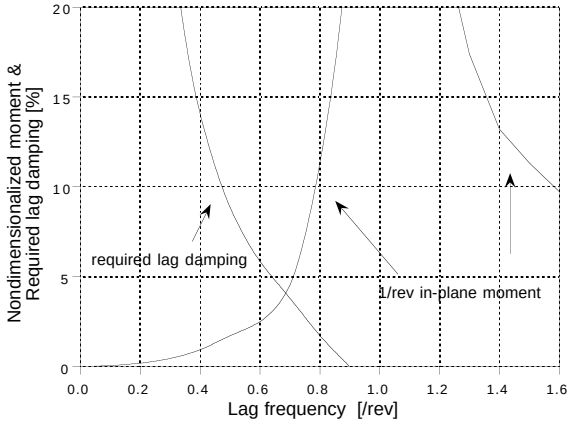

Figure 10.9: Torsional stiffness distribution

10.8 AUTOROTATION CHARACTERISTICS

Autorotation performance depends on several factors including the rotor disk loading (which affects the descent rate) and the stored kinetic energy in the rotor system (which influences the entry and completion of the autorotation). An Autorotation Index (AI) is often used in the main rotor design. Although the absolute value of the AI is not significant by itself, but it provides a means of comparing the autorotative performance of a new helicopter design with existing helicopters that exhibit acceptable autorotative characteristics. The index used by Sikorsky [Whit82], is a factor that is defined as the kinetic energy of the main rotor divided by the gross weight of the helicopter and disk loading.

Table 10.6 lists the autorotative index of the Chesapeake with that of several other helicopters with maximum take-off weight over 10000 lbs. The Chesapeake has good autorotation characteristics compared to the other helicopters. Furthermore, irrespective of the autorotation index, the fact that the Chesapeake has three engines improves its safety compared to twin engine helicopters.

Table 10.5: Main Rotor Blade Natural Frequencies

Mode shape	Frequency
1st lag	0.70 (/rev)
1st flap	1.06 (/rev)
2nd flap	2.67 (/rev)
2nd lag	4.23 (/rev)
3rd flap	4.72 (/rev)
1st torsion	6.76 (/rev)
4th flap	7.44 (/rev)

Table 10.6: Autorotation Index Comparison: $AI = \frac{1}{2}\frac{I_\Omega * \Omega^2}{W * DL}$

Helicopter	Max. TOW (lb)	Polar moment of inertia $I_\Omega(slug - ft^2)$	Rotor speed Ω (rad/sec)	Disk loading DL (lb/ft^2)	Autorotation index AI (ft^3/lb)
Chesapeake	15470	4866	28	7.88	15.6
Bell 412	11900	2760	33.9	7.16	18.6
MD AH-64	17650	3800	30.25	9.75	10.1
Sikorsky UH-60A	22000	7060	27.02	9.73	12
Sikorsky CH-53E	69750	51800	18.53	14.23	8.96
Sikorsky S-76A	10300	1890	30.68	6.77	12.8
Westland Model 30	12800	2175	34.13	8.55	11.6

10.9 MANUAL BLADE FOLDING MECHANISM

As required by the RFP, a manual blade folding mechanism was designed to minimize hangar requirements. The folding mechanism includes:

- a hinge point at the end of the flexbeam with a locking bolt
- an indexing mechanism for proper alignment of the rotor blades prior to folding
- a support arm to be used by the ground personnel to move the folding blades
- a support device to be fixed to the top of the rotor hub that supports the folding hinge.

There are two possible blade folding positions without increasing the structural complexity. These are at the hub-flexbeam attachment position and flexbeam-blade attachment position. The hub-flexbeam attachment position is not desirable, due to geometric constraints and the requirement to remove the pitch-links. Thus, the flexbeam-blade attachment position is chosen as the blade folding axis.

To prevent high stresses in the hub and the flexbeams due to the folded blades, a support mechanism was designed to protect the flexbeam and torque tube, and to hold the folded rotor blade. This is a graphite-epoxy truss-type system, with 5 arms, that attaches to the top of the hub. Each arm holds a blade in place from above by locking it within a holder and a clamp. The support truss is designated as ground equipment and is not carried by the helicopter. Figure 10.11 shows the side view of blade support mechanism.

The process for folding the rotor blades will require at two ground personnel. The rotor blades are rotated until the index stop is reached and the blades are locked in position. The support device is fixed to the top of the rotor hub and attached to each of the blades to be folded. Each blade is then manually moved into the folded position by

removing the locking bolt and moving the blade with a support arm operated by a person on the ground. The support arm has an airfoil shaped clamp and is used to rotate the blade into the stowed position. Special consideration must be given to protecting the elastomeric dampers and hub and avoiding overloads in the flexbeam while preparing the helicopter for hangar storage. This is achieved by the support frame, which unloads the flexbeam and torque-tube, prior to folding of the blades. In addition, when the aircraft is prepared for flight, each locking bolt must be installed with the correct torque rating and lock wire.

In the stowed position, one non-folded blade is indexed parallel above the tail boom. The other four blades are then folded. Two blades are folded backwards and parallel to the reference blade and the remaining two blades are folded forward. The length of the vehicle is 17.97 m (59.0 ft) and the width of the vehicle is 4.25 m (13.9 ft). Figure 10.11 depicts the blade support mechanism and Figure 10.10 shows the top view of the vehicle after blade folding.

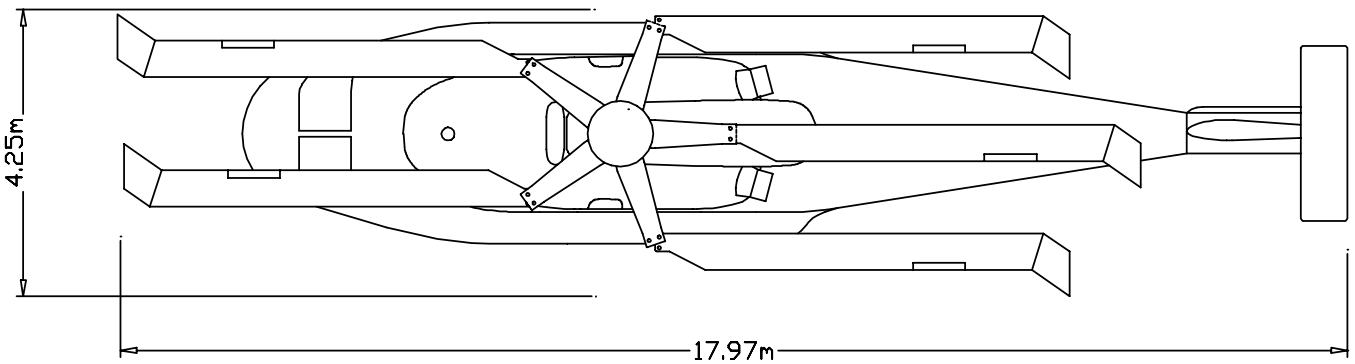

Figure 10.10: Top view of helicopter with blades folded (support frame not shown)

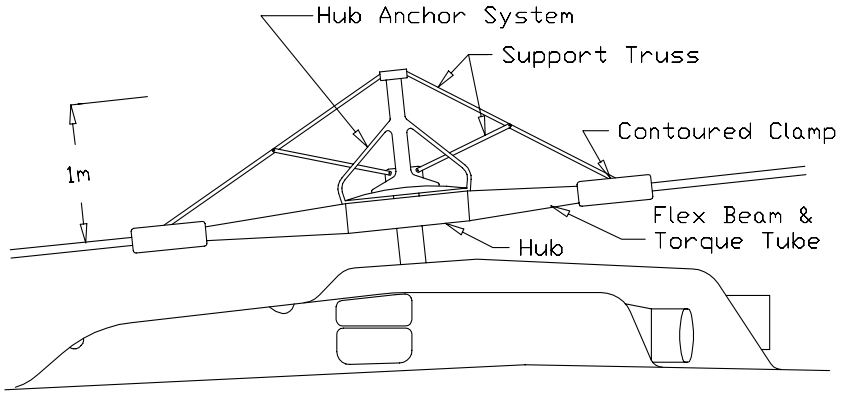

Figure 10.11: Blade-folding support mechanism

10.10 ACTIVE VIBRATION CONTROL USING TRAILING EDGE FLAP

Helicopters are characteristically susceptible to high vibration levels because of the unsteady aerodynamic environment in which the flexible main rotor blades operate. High vibration loads result in accelerated fatigue of structural components and reduced ride quality. This structural fatigue impacts reliability and maintenance costs, while the poor ride quality reduces the marketability as a commercial commuter aircraft. Even though Chesapeake has five

blades and the blade frequencies are well placed to minimize vibration levels, an active vibration control system is installed to offer the customers a near jet-smooth ride. The active vibration system will buy its way onto the aircraft via the overall reduced maintenance costs and improved reliability. In this conceptual stage, the financial impact, in terms of acquisition costs vs. reduced structural fatigue, is not quantifiable and needs to be carefully considered in the subsequent design iterations. In addition, it is essential to ensure that a failure of the active vibration control system does not compromise the flight safety of the aircraft.

There are two main approaches: one is to use active support struts to cancel the vibration from the combined rotor and transmission system. The other is use a direct excitation of the rotor blades to cancel the undesirable unsteady airloads on the rotor blades. The former system has been implemented on the EH101 while the active on-blade technology is being investigated by both Boeing [Stra97, Derh96] and Sikorsky. With the advent of smart structures, active on-blade systems appear attractive. The advantage of the on-blade activation systems, compared to the active support struts, are that they are potentially able to simultaneously address in-flight tracking, vibration reduction, noise reduction and performance enhancement. In addition, reducing the blade vibratory loads, reduces the loads in the hub dynamic components (swashplate, pitch links, etc). The primary disadvantage of the on-blade systems is the increased rotor blade complexity and the requirement to transfer power from the fixed to the rotating frame.

It should be noted that active rotor control, via higher harmonic control of the swashplate (HHC) or via individual blade control (IBC) are not considered as candidates. Both these systems have been shown to be inferior to the active on-blade systems.

There are a variety of on-blade activation concepts. These include active integral twist, discrete trailing edge flaps (or servo-flaps) and active rotor blade tips. Of these, presently the trailing edge flaps are the most promising option, for near term implementation. Chopra[Chop97] presents a recent overview of the state of the art in the application and feasibility of smart structures for rotorcraft systems.

10.10.1 Installation and Actuation Scheme

The University of Maryland has developed extensive analytic and experimental experience in the field of active rotor systems. Based on this, it is proposed to use a discrete plain-trailing edge flap, driven by a piezo-stack actuator, using a mechanical lever-arm amplification system [Lee98]. Figure 10.12 shows a schematic of the flap and actuator system.

The flap sizing (chord and span) and location are based on the parametric flap performance study performed by Milgram and Chopra, on a typical 5-bladed bearingless rotor [Milg97]. The flap has a 10% span, 20% chord and is centered at 75% radius of a blade (to maximize flap effectiveness and minimize power required for actuation), see figure 10.13. The length of flap is chosen as 10% of blade radius to enhance the localized nature of the flap input. The flap chord is set at 20% to limit flap deflections and rates. Lower flap amplitudes and rates reduce the actuator requirements and reduce trailing edge separation.

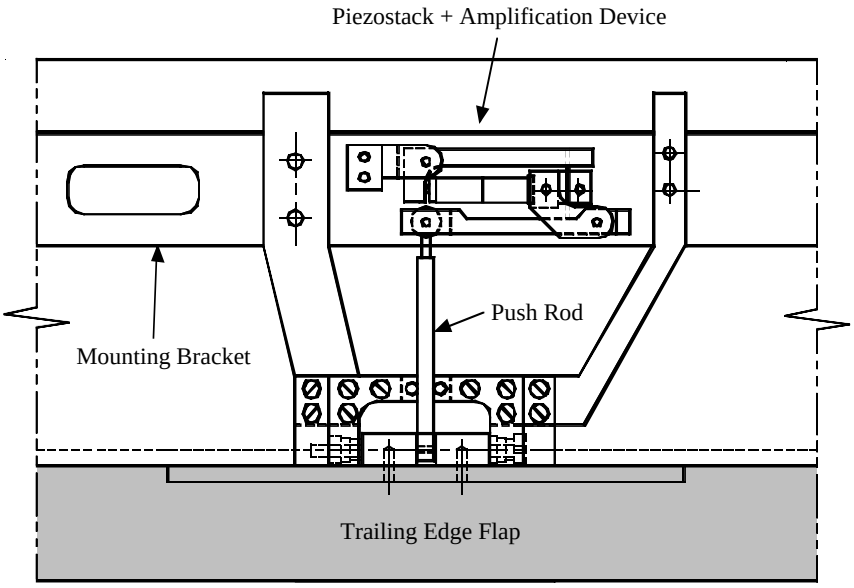

Figure 10.12: Trailing edge flap actuation mechanism

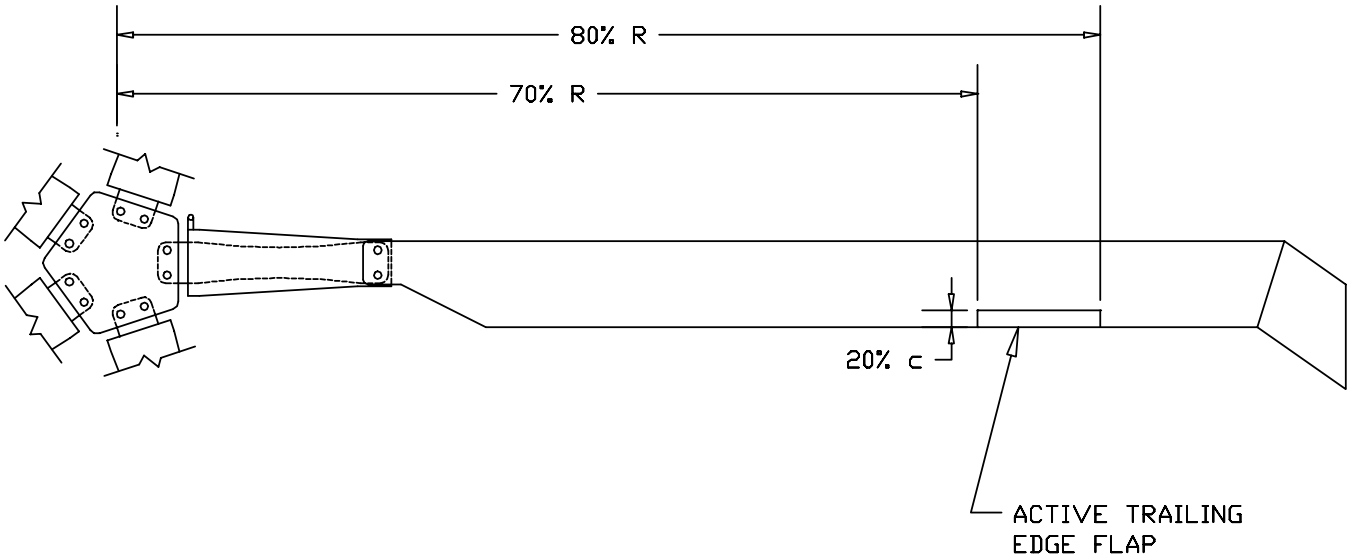

Figure 10.13: Trailing edge flap location

10.10.2 Mutlicyclic Control Algorithm

As a first estimate for this design stage a mulitcyclic control algorithm is used to demonstrate the potential vibration reduction of the active flap system. This controller is designed to reduce the N_b/rev rotor loads that are filtered through the hub into the fuselage.

In implementing the mulitcyclic control algorithm, a scalar vibration objective function J is defined as:

$$J = z_n^T W_z z_n + \theta_n^T W_\theta \theta_n + \Delta\theta_n^T W_{\Delta\theta} \Delta\theta$$

where z_n is a hub loads vector containing the sine and cosine coefficients of the 5/rev hub loads at time step n. θ_n

and $\Delta\theta_n$ represent the harmonics of the control inputs and control rates, respectively. The diagonal matrices W contain weights for different harmonics of the vibration (W_z), the control inputs (W_θ) and the control rates($W_{\Delta\theta}$).

10.10.3 Vibration Reduction Capability

The vibration reduction capability of a trailing edge flap at the cruise speed is investigated. Chesapeake has five blades, thus dominant vibratory hub loads which are transmitted to the fuselage and produce fuselage vibration are 5/rev components.

Figure 10.14 shows non-dimensional 5/rev hub loads at the cruise speed. The active trailing edge flap reduced longitudinal and lateral hub forces by 75 %. Active trailing edge flap reduced blade vibratory loads as well as hub loads. Figures 10.15 and 10.16 show non-dimensional half peak-to-peak vibratory blade beam bending moment and chord bending moment distribution along the blade. Active trailing edge flap reduced vibratory root beam bending moment by 70% and chord bending moment by 60%.

In subsequent design iterations, a neural network based adaptive controller would be implemented, with distributed blade sensors, hub and cabin accelerometers, for enhanced vibration reduction. Numerical simulations have shown that the controller exhibits good robustness for on-line implementation in rotor-systems [Spen98].

It would also be of interest to investigate the BVI noise reduction potential, as demonstrated by Straub [Stra95]. At present, true blade-vortex-interaction (BVI) noise control via plain flaps is in the early development stages. However, with advances in actuator materials it is envisaged, that the trailing edge flaps will achieve the amplitudes and rapid deflection rates required for BVI control. Using multiple discrete flaps it is then potentially possible to achieve active in-flight tracking, vibration reduction and noise reduction.

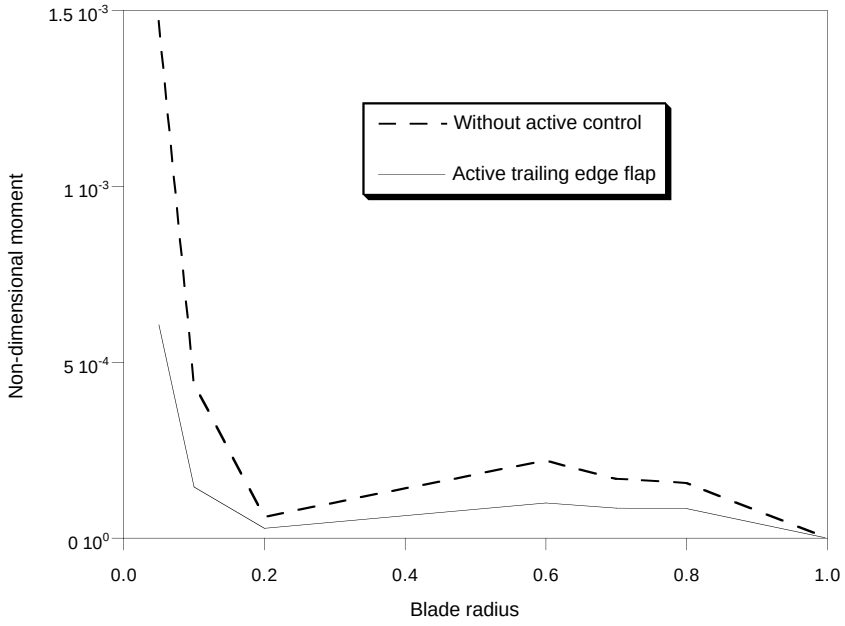

Figure 10.15: Half peak-to-peak vibratory beam bending moment in cruise

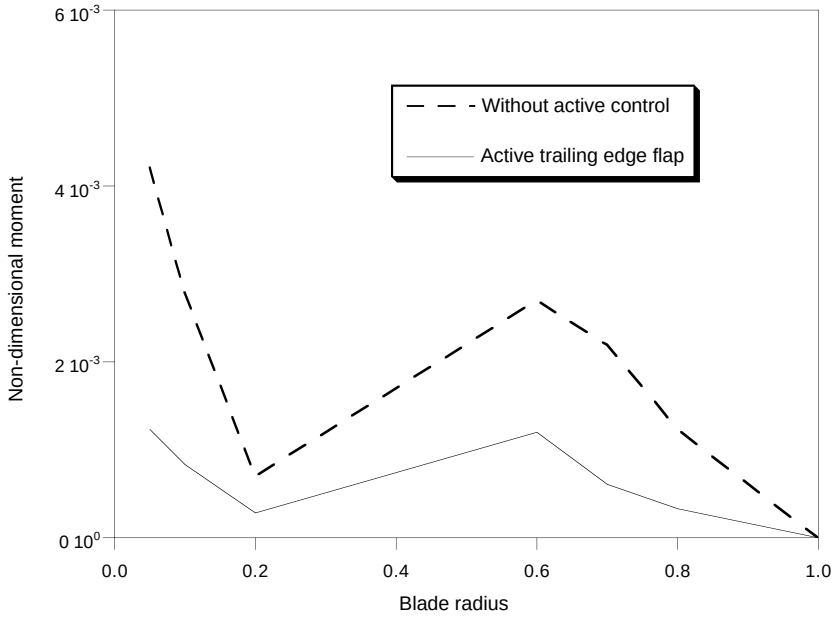

Figure 10.16: Half peak-to-peak vibratory chord bending moment in cruise

10.11 AEROMECHANICAL STABILITY ANALYSIS

Ground resonance is a dynamic instability caused by the coupling of the blade lag motion and the hub in-plane motion. At the instability condition, one of the lag frequencies in the fixed frame coalesces with the support frequency. This is the reason that the landing gear and the supporting structure characteristics are important for stability. Air resonance is caused by the coupling of the low frequency blade flap and lag modes and rigid body airframe modes. Ground resonance is a violent instability and could result in a catastrophe. On the other hand, air resonance is

normally a weak instability and often results in limit-cycle oscillations. One major design concern is to avoid these instabilities.

The aeromechanical stability analyses for both ground and air resonance, are performed using UMARC (University of Maryland Advanced Rotorcraft Code). The rotorcraft structural model is a non-linear representation of elastic rotor blades coupled to a rigid fuselage. The blade is modeled as an elastic beam undergoing flap bending, lag bending, elastic twist, and axial deflection. Finite element methods in space and time are used to solve non-linear periodic equations of motion. For ground resonance, the characteristics of landing gear (i.e. stiffness and damping) are also included in the body equations. Dynamic inflow modeling is used to include the low-frequency wake effect.

First, a coupled-vehicle trim solution is solved to obtain fuselage attitudes, pitch control angles, and blade steady deflections for a given thrust level. Then, the coupled rotor/fuselage/dynamic inflow equations are linearized about the deflected position of the blade. Finally, the perturbation equations are solved using Floquet transition matrix theory to calculate damping of the different modes.

Non-dimensional fuselage properties are shown in Table 10.7.

Table 10.7: Fuselage and Landing Gear Properties (non-dimensional)

Fuselage roll inertia (I_ϕ/m_0R^3)	1.77
Fuselage pitch inertia (I_α/m_0R^3)	14.18
Fuselage roll damping ($2\zeta\omega_\phi/\Omega$)	.0197
Fuselage pitch damping ($2\zeta\omega_\alpha/\Omega$)	.0118
Fuselage roll stiffness ($K_\phi/m_0\Omega^2R$)	.43
Fuselage pitch stiffness ($K_\alpha/m_0\Omega^2R$)	1.24

Figures 10.17 and 10.18 show the ground resonance results. Figure 10.17 presents the variation of the damping of a regressing lag mode with increasing main rotor RPM. Lag damping was investigated up to 110% of the operational RPM. Lag damping increases with rotor RPM. The Chesapeake is stable for all regions. Figure 10.18 illustrates the variation of the damping of a regressing lag mode for the collective angle. Figure 10.19 shows air resonance results with forward speed. The Chesapeake is stable at all forward speeds.

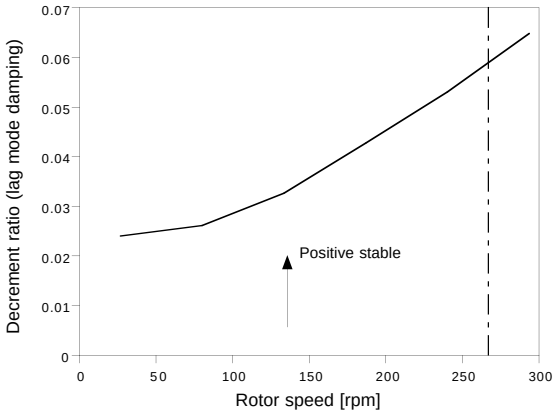

Figure 10.17: Ground resonance: lag mode damping with rotor speed

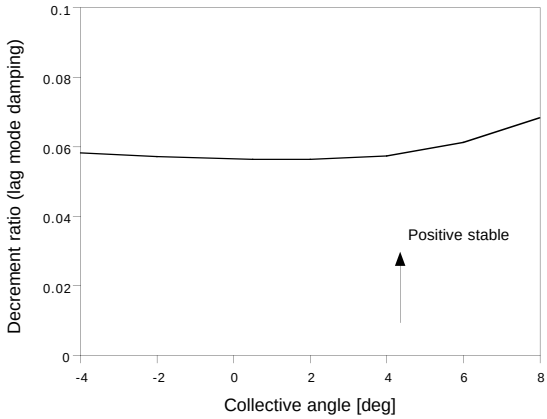

Figure 10.18: Ground resonance: lag mode damping with collective angle

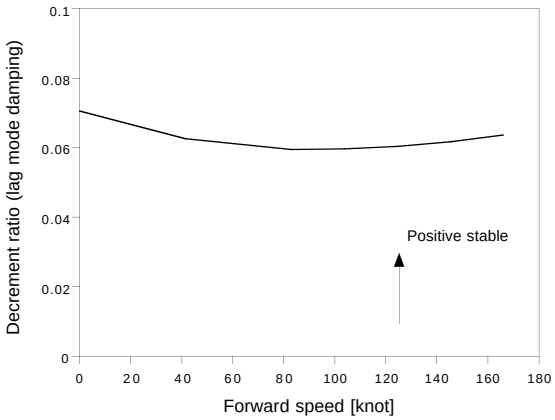

Figure 10.19: Air resonance: lag mode damping with forward speed

11 THE ANTI-TORQUE SYSTEM

11.1 INTRODUCTION

The anti-torque system must meet the manoeuver and control requirements throughout the flight envelope. In addition to efficient performance and low weight, it should exhibit good reliability and maintainability and should not present an undue danger to ground-personnel and passengers. A configuration trade-off study is conducted between a conventional tail rotor and a fan-in-fin design. The circulation control tailboom (NOTAR) design was not considered, because the high gross weight of the Chesapeake would require an excessively large diameter tailboom. The fan-in-fin design is based on the Boeing-Sikorsky FANTAIL system.

11.2 REVIEW AND ANALYSIS OF EXISTING DATA

A literature survey of helicopters with a fan-in-fin system was conducted to guide the trade off-study and subsequent preliminary design of an anti-torque system and empennage assembly.

Table 11.1: Characteristics of existing Fan-in-Fin/Fenestron Systems

Helicopter	TOW (lb)	Main Rotor				Fan-in-Fin				Cruise (knots)
		Radius (m)	Chord (m)	Blades	RPM	Radius (m)	Blades	Chord (m)	RPM	
SA330	14110	-	-	-	-	1.95	13	-	2542	140
Ka62	14880	13.50	0.25	4	-	-	11	-	-	140
SA342	4630	10.50	-	3	-	-	-	-	-	140
SA365	9370	11.94	0.39	4	350	1.10	11	-	3665	154
SA565	9369	11.94	0.39	4	350	1.10	11	-	3665	154
EC135	5952	10.20	-	4	-	1.00	11	-	3533	146
EC120	3417	10.20	0.26	3	-	0.75	8	0.06	-	130
G2	1212	6.50	0.16	3	597	0.54	7	0.04	5734	97
RAH66	17174	11.90	-	5	314	1.37	8	0.17	-	177
S76	10500	13.41	0.39	4	0	1.20	8	0.16	2935	145

11.3 TRADE-OFF STUDY OF FAN-IN-FIN AND CONVENTIONAL TAIL ROTOR

The anti-torque configuration selection study was conducted with regard to the following aspects.

11.3.1 Operational Comparison

Safety on Ground and In-Flight For the anti-torque system used in a civil helicopter, safety is an important consideration. On the ground, the fin and the shroud of the fan-in-fin design house the rotor blades preventing the rotor from injuring personnel and passengers. Furthermore, the shroud of a fan-in-fin design prevents the rotating fan blades from striking the ground during landings or take-offs. In flight, it is less likely, for the fan to be struck by debris detached from the airframe or main rotor blades. The vertical tail of the fan-in-fin design can be made larger than that of a conventional tail rotor, where blockage considerations limits the size of the vertical tail. The larger fin permits significant unloading of the fan in cruise.

Housed in the fin, the fan is not directly exposed to sand, snow, rain, ice, etc. From the experience of Aerospatiale and their fenestrons, a de-icing system for the fenestron is not necessary thereby reducing acquisition and maintenance costs for the fan design [Moui79].

Manoeuverability Good yaw manoeuverability and smooth handling are reported for helicopters installed with a fan-in-fin anti-torque system. The higher induced velocity in a fan-in-fan, delays the onset of the left side wind effect (due to the fan entering the vortex ring state) [Moui79].

Noise A fan-in-fin normally has more blades than a conventional tail rotor. Therefore, the noise of the fan-in-fin, which is related to the tip Mach number, is at higher frequencies and attenuates faster over distance than conventional tail rotor noise. In order to reduce noise further, it is proposed to use asymmetrically spaced fan blades (also known as the phase modulation technique [Niwa98]). The Chesapeake fan-in-fin will be quiet by virtue of its low tip speed and asymmetric blade spacing.

Weight and costs The use of composite materials ensures that the fan-in-fin has similar weight and cost characteristics are comparable to those of a conventional tail-rotor configuration, manufactured from composites.

11.3.2 Power Efficiency

Hover The fan-in-fin normally has a much smaller fan diameter due to structural and weight concerns. Therefore the fan-in-fan has a higher induced power consumption than a conventional tail rotor. The fin blockage effect and interaction between main rotor and tail rotor must be considered when comparing the power efficiency of an anti-torque system. The anti-torque thrust is typically reduced by 10% as a result of the fin blockage effect in a conventional tail rotor. The fan-in-fin configuration eliminates the fin-blockage and also reduces the interaction with the main rotor wake. The high induced power, associated with the high disk loading is offset by the fact that approximately half of the thrust of the fan-in-fin is provided by the diffuser and the shroud lip surfaces which do not consume power. Consequently, the fan-in-fan has a power efficiency comparable to that of a conventional tail rotor.

Forward Flight The power efficiency of a fan-in-fin is better in forward flight than in hover. Noting that fin blockage is not a consideration for a fan-in-fin, a larger vertical fin can be incorporated in the design. This permits fin-sizing to carry the full anti-torque side-force in cruise, thereby unloading the fan. In this condition, the fan only requires power to overcome the profile drag of the blades and consequently has a low cruise power consumption. In addition, the fan-in-fin drag is typically less than that of the conventional tail rotor. It should be noted however, that the power reduction achieved via the unloaded fan is offset to a certain extent by the increased induced drag of the fin.

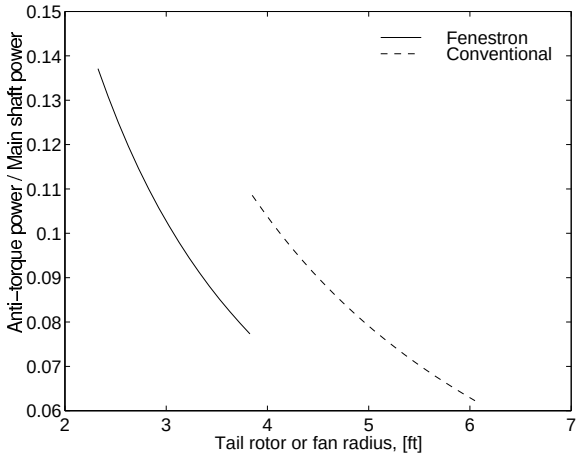

Figure 11.1: Induced power vs. fan / tail-rotor radius, in hover

11.3.3 Final Configuration Selection of Anti-Torque System

The trade-off study shows that the fan-in-fin offers distinct safety and flight performance advantages compared to the conventional tail-rotor. The Chesapeake helicopter thus will incorporate a fan-in-fin anti-torque system.

11.4 FAN-IN-FIN DESIGN

The fan-in-fin assembly is comprised of a small rotor housed in a shroud and and a large vertical fin with a T-tail horizontal stabilizer. The shroud, together with the fan nose and tail cone provide a ducted intake and conical exit diffuser. The tail cone houses the fan gearbox and the pitch control system. The fan hub is supported by two sets of support arms on the exit side. The fan-in-fin design is divided into three parts: fan, duct and stabilizers design. Figure 11.6 shows a schematic of the final empennage configuration.

11.4.1 Fan Design

The fan design focuses primarily on achieving high aerodynamic efficiency. Research results from Aerospatiale's helicopter division [Vuil86, Vuil89] and Boeing-Sikorsky fan-tail design [Desj91, Wrig91, Keys91, Raja97] are used in this design. From historical data, the rotor diameter is about one half the equivalent conventional tail rotor diameter and the rotor solidity is roughly twice the value of present tail rotors. The pertinent design parameters are summarized in Table 11.2.

Table 11.2: Fan Design Parameters

Attribute	Duct
Length between fan and main rotor hub	8.96 m (29.4 ft)
Fan diameter	1.576 m (5.17 ft)
Fan tip Mach number	0.55
Number of blades	8
Fan direction of rotation	aft at top
Fan blade twist	-7 deg
Fan solidity	0.63
Fan blade airfoil	NACA63A312
Fan root cutout	40%

Fan Diameter: the selection of the diameter represents a compromise between power consumption in hover and weight and structural concerns. The fan diameter was initially estimated using momentum theory, Figure 11.1. For the same rotor diameter and thrust, the fan-in-fin consumes only 71% of the power consumed by a conventional tail rotor. This power efficiency is due to the extra thrust produced by the duct in shrouded fan configuration.

The fan diameter is selected such that it has a rotor disk which is large enough to give good hover power efficiency and small enough to avoid the "heavy tail" effect. In addition, the fan diameter should be large enough to make the tip Mach number as small as possible which is the key point to noise reduction. Upon deciding the fan diameter, the length between the main rotor shaft and the fan center is determined.

Fan Tip Mach Number Selection: the fan tip Mach number selection was primarily based on the noise produced by the fan. The current design has a tip Mach number of 0.55 which is similar to other helicopters of the same gross weight.

Fan Blade Spacing: as noise is a very important concern in the overall design, unequal spacing of the fan blades is used in the fan design by applying the phase modulation technique. This technique is reported in reference [Niwa98] and is shown to reduce the noise level compared to that of an equal spaced fan. The XOH uses an 8-bladed fan with an asymmetry angle of 35/55 deg [Niwa98]. It is important to ensure that there is no mechanical interference of the pitch-links in such a scissored configuration. The Chesapeake fan will thus be an 8-bladed fan, with a 35/55 deg asymmetry angle.

Other Parameters Selection: an untapered fan planform was chosen to simplify manufacturing and improve the maximum thrust capability. The number of blades is based on acoustic, reliability and durability considerations. A NACA63A312 profile is selected, based on the Comanche FANTAIL.

11.4.2 Duct Design

Due to approximately half of the anti-torque thrust being provided by the duct, the fan duct design is critical in achieving the anti-torque system performance goals. The duct thrust is produced by negative static pressure on the duct inlet and diffuser area. This additional thrust of the duct allows the fan diameter to be smaller than a conventional tail rotor for the same required hover power.

Since the fin is sized to unload the fan in cruise, the duct geometry is chosen mainly to maximize hover and low speed performance with the smallest duct size in order to minimize forward flight parasite drag. The theoretical

analysis and results of wind tunnel tests that are available in the literature are reviewed. The pertinent duct design parameters include: inlet and exhaust lip radii, duct width and the duct aft closure shaping. Wind tunnel test data [Keys91] indicates that the largest lip radii produced the highest figure of merit. It was found that in order to obtain maximum hover performance, an inlet lip radius to diameter ratio greater than 0.065-0.075 is required. A ratio of 0.075 is selected for the Chesapeake, based on the Comanche FANTAIL. A sharp exit radius is required for hover good performance, but this degrades forward flight performance. A 0.005 ratio of exit radius to diameter is selected. A small ducted width is beneficial from a parasite drag point of view. The final width of 0.518 m (1.7 ft) is based on fan performance and acoustic considerations. The duct divergence angle is chosen in order to increase the flow stream expansion in duct, while preventing premature flow separation from the duct walls. Two stator blades are included in the duct design which straighten the axial flow. As the velocity slightly decreases, the stator blades directly create additional axial force and some pressure recovery.

Table 11.3: Duct Design Parameters

Attribute	Units	Duct
Inlet radius / diameter	-	0.075
Exit radius / diameter	-	0.005
Divergence angle	deg	5
Width	m (ft)	0.518 (1.7)

11.5 VERTICAL STABILIZER DESIGN

To achieve the best lift-to-drag ratio of the tail assembly in cruise flight, it is preferable to fully unload the fan. Thus, the full required anti-torque thrust has to be supplied by the cambered fin, which is set at a given angle of attack with respect to the aircraft centerline. In contrast, for a conventional tail rotor empennage, such a fin size is not practical due to fin blockage effect.

The main advantage of unloading the fan is that the dynamic loads on the rotating parts of the fan-in-fin are significantly reduced, reducing maintenance requirements and extended the flight life.

11.5.1 Vertical Fin Area

Several aspects are considered in selecting the fin size. Structural design, weight, and the size of the fan to be accommodated were the most important considerations. Figure 11.2 shows the fin-effectiveness as a function of fin area and flight speed. As a compromise between fin size (and weight) and fully unloading the fan in cruise, a fin area of 2.787m^2 (30 ft^2) is selected. This yields a 80/20 ratio for the respective anti-torque side force contribution of the fin and the fan. Vertical fin thrust versus forward flight speed is plotted in Figure 11.4 and the power required by the fan is shown in Figure 11.5.

11.5.2 Vertical Fin Airfoil, Aspect ratio and Incidence

A NASA633A618 airfoil is selected for the vertical tail due to its superior drag performance at the relatively high design lift coefficient. In addition, it provides sufficient thickness to house the support structure for the T-tail. The

Table 11.4: Horizontal and Vertical Fin Data

Attribute	Units	Horizontal	Vertical
Area	m^2 (ft^2)	1.8 (19)	2.8 (30)
Span	m (ft)	2.6 (8.4)	1.7 (5.7)
Mean chord	m (ft)	0.7 (2.3)	1.2 (3.9)
Aspect ratio	-	3.75	1.4
Sweep	deg	0	37.5(@ 1/4 chord)
Incidence	deg	-3	4.0
Airfoil	-	SU3015	NASA633A618

aspect ratio is based on the structural boundary with the fin that shrouds the fan and the fin area. The vertical fin span is large enough to make the horizontal fin higher than the main rotor disk in order to keep the horizontal fin out of main rotor wake. The effective incidence angle was selected to provide the required 80% anti-torque thrust in cruise.

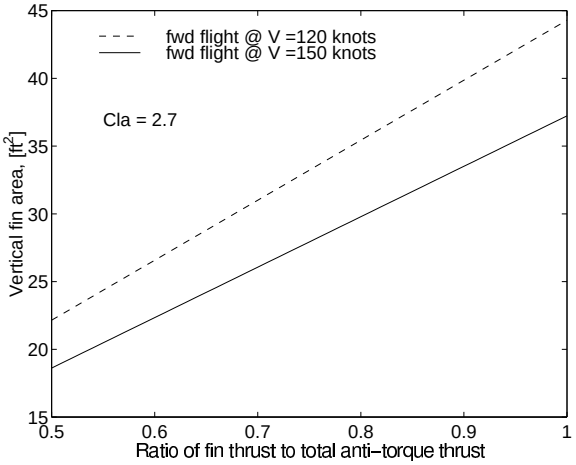

Figure 11.2: Vertical fin area selection

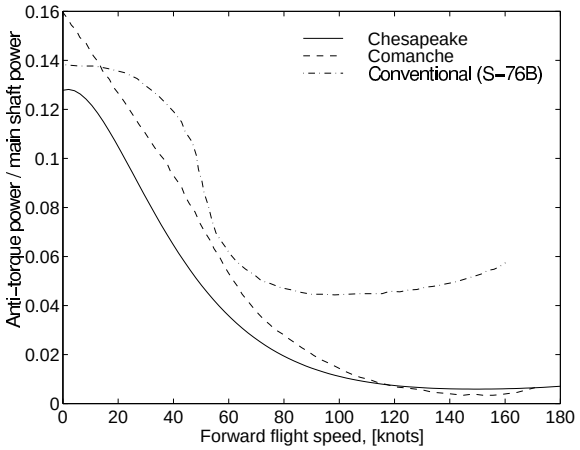

Figure 11.3: Comparison of required fan power with existing helicopters

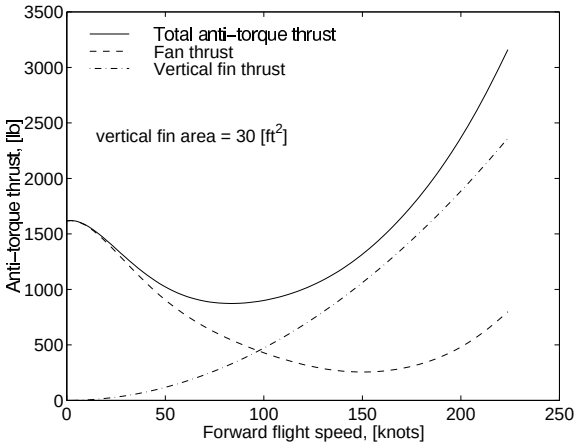

Figure 11.4: Vertical fin thrust in forward flight

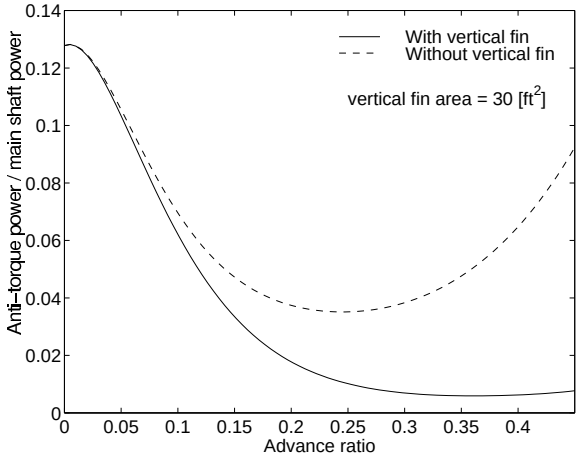

Figure 11.5: Fan power vs. advance ratio

11.6 HORIZONTAL STABILIZER DESIGN

In this design iteration, the horizontal stabilizer is designed based on the Comanche, which has a similar take-off weight. In subsequent design iterations the handling-qualities analysis will fine-tune the exact sizing and location. The final result of empennage design is showed in figure 11.6.

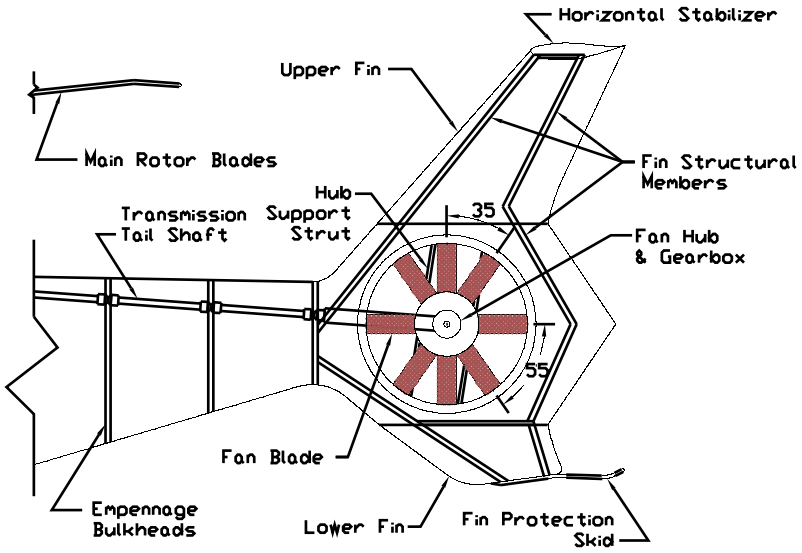

Figure 11.6: Empennage detail (side view)

12 TRANSMISSION DESIGN

12.1 MAIN ROTOR TRANSMISSION DESIGN

The output from the three turboshaft engines is transferred through a three-stage main transmission to drive the rotors. The main gearbox is rated to transmit a power of 3x932 kW (3x1250 hp), corresponding to the maximum nominal output from all three engines. The transmission components linking each engine and the main gear box are individually rated to carry the maximum emergency rating of 1165 kW (1563 hp). A schematic of the transmission can be seen in Figure 12.1.

The first stage consists of beveled or helical gears with a reduction ratio of approximately 1.5:1. This stage is also used to rotate the shafts of the outboard engines by ninety degrees. By placing the bevel gear on the outside of the transmission, all three inputs to the collector gear are rotating in the same direction thereby eliminating the need for an idler gear in the helical stage of the center engine. Spring clutches are included in the transmission, just before the collector gear, to disengage the engines from the rotor system in the event of an engine failure.

The power from all three engines is then supplied to a face gear with a reduction ratio of 3.75:1. The main transmission shaft from the face gear then powers the sun gear of a four-planet planetary gear system. A reduction of 4.0:1 is achieved in the planetary system as the main rotor torque is transferred via the planetary carrier to the main rotor. This gives an overall gear reduction of 22.5:1, which enables the input speed of 6016 RPM to be reduced to 267.4 RPM that is required by the rotor system.

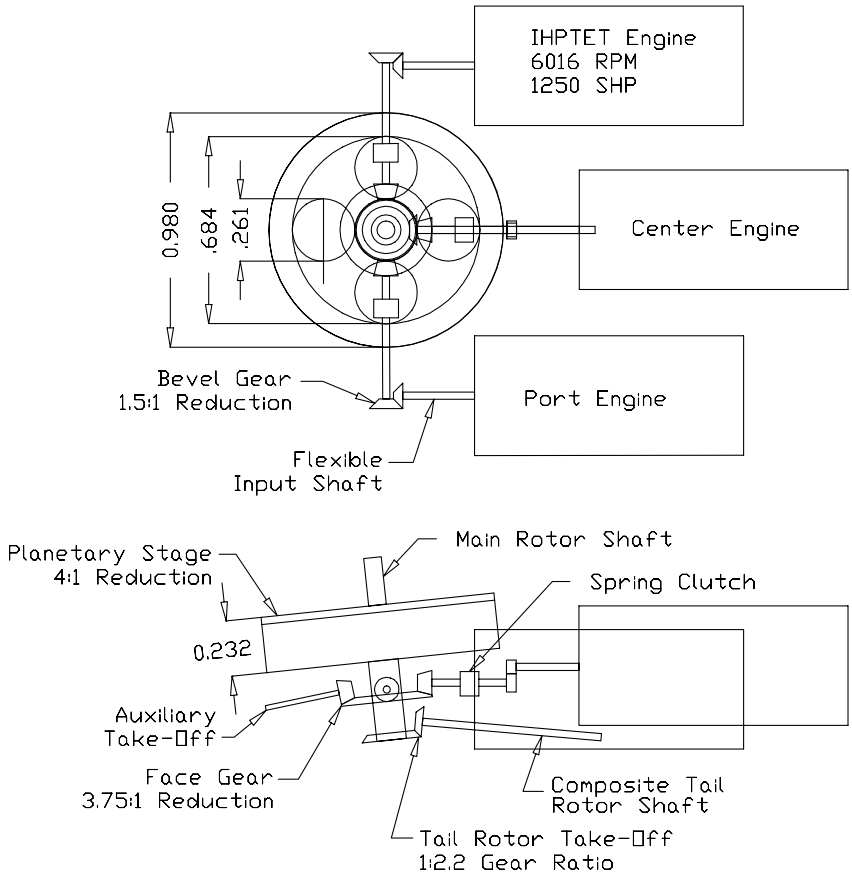

Figure 12.1: Main transmission

The gearbox planform is defined by geometric constraints of the triple engine installation. The thickness of the planetary gears is determined via gear tooth strength limits.

12.2 TAIL ROTOR TRANSMISSION DESIGN

The transmission take-off for the tail rotor is located on the main rotor shaft below the face gear system. A beveled gear with a reduction ratio of 1:2.05 provides the anti-torque fan with the necessary speed of 2200 RPM. Power is transmitted from the main gearbox to the fan-in-fin via sub-critical composite tail rotor shafts. The overall tail rotor shaft is 9.0 meters long and is divided into 6 segments of 1.5 meters each. By choosing a uniform shaft length, commonality between each segment is maintained. In addition, maintainability is improved as the segments are a manageable length for maintenance personnel. The shaft is constructed of graphite-epoxy weave with a 3 cm radius and a thickness of 0.5 cm Each segment is supported by a set of bearing blocks and flexible couplings are incorporated between each section to accommodate shaft misalignment and fuselage bending.

Finally, a small tail gearbox is needed to rotate the tail transmission shaft by 90 deg to power the fan. A pair of self-lubricating bevel gears is employed for this stage with no reduction in the shaft RPM.

Table 12.1: Transmission Stages

Stage	Input RPM	Output RPM	Transmitted Torque, Nm	Reduction Ratio
Engine	-	6016	1663.1	-
Spiral Bevel/Helical	6016	4010.7	2495	1.50:1
Collector Gear	4010.7	1069.5	28064 (3 Engines)	3.75:1
Planetary Gear	1069.5	267.4	112260 (3 Engines)	4.00:1
Tail Rotor	1069.5	2200	1631.9 (12% of Pmax)	1:2.2

12.3 AUXILIARY SYSTEMS

The power for the main auxiliary systems is provided by a take-off from the face gear stage of the main transmission. Power from this take-off is used to run the electric generators for instrumentation and de-icing as well as the hydraulic pumps. There are three separate hydraulic systems. Two provide redundant control power to the rotor system while the third is used solely for retracting and extending the landing gear.

12.4 GEAR BOX DESIGN

The main gearbox supports and drives the rotor shaft and encloses the main transmission components. The cast magnesium-zirconium gearbox is equipped with cored-passages to facilitate lubrication of the gear meshes. Each engine output shaft provides power to an oil pump. In the event of an oil pump failure, there would still be two pumps to provide the necessary oil flow. The size of the oil pumps and volume of oil is reduced by using advanced lubricants and materials that can tolerate higher operating temperatures.

The gearbox is mounted to the aircraft frame via two A-frame structures mounted fore and aft of the gearbox. The top of the gearbox is attached with pins to the top of the A-frame.

12.5 ADVANCED TECHNOLOGIES

A number of advanced gear-train technologies will be incorporated to provide a stronger and lighter transmission compared to current helicopter systems. These technologies include:

1) High Strength/Temperature alloys for increased allowable stresses and higher temperatures in the gear teeth.

2) An advanced spring clutch design over conventional sprag clutches for smaller and lighter weight.

3) Advanced high-contact ratio gear tooth geometry for longer life and a reduction in noise and vibrations.

4) Ceramic spherical roller bearings for longer life.

5) Advanced alloys for reducing the weight and size of the planet carrier and gearbox.

6) Composite tail drive shaft for increased reliability and lower weight.

13 MAINTENANCE/RELIABILITY

13.1 GENERAL MAINTENANCE

Ease and low cost of maintenance of the helicopter is of prime importance for it to be an economically viable product. Maintenance costs are a major driver of the DOC. For the Chesapeake, the $400/flight-hour maintenance costs constitute approximately 20% of the DOC per air-seat-mile. By incorporating more durable components, the helicopter will be more reliable, thereby reducing down time and missed flights. All portions of the helicopter are easily accessible via removable maintenance panels. Furthermore, a high commonality of fasteners and a very limited number of tools needed to change the Line Replaceable Units (LRU's) facilitates maintenance of the helicopter. The high number of composite components gives the helicopter superior fatigue life characteristics.

13.2 HELICOPTER HEALTH AND USAGE MONITORING

The reliability of the engines and transmission system is greatly improved by the installed HUMS (health and usage monitoring) system. The HUMS system, monitoring rotor hub and blade integrity, the transmission system and overall vibration levels, will alert pilots in the case of flight critical problems in the rotor hub and the transmission. In addition, the HUMS will provide a data base, that can be down-loaded after each flight for on-condition monitoring.

Health monitoring of the transmission is provided by two separate systems. The first is a chip detector placed in the sump at the bottom of the gearbox. The chip detector will detect any loose metallic particles in the lubrication. A second more advanced system is based on of the vibration signature of the gearbox. Three accelerometers are mounted to the ring gear of the planetary gear stage and one accelerometer is mounted to the bearing blocks of each of the input shafts to the collector gear and the output shaft of the tail rotor take-off. Vibration data from each of the accelerometers is individually processed using a harmonic wavelet-based algorithm which produces output in the form of the Normalized Energy (NE) metric [Samu98]. Both the chip detector and NE results are fed to a Neuro-fuzzy classification system which determines the type of damage, if any, present in the system and its extent. This information is subsequently used to provide a prognosis of the remaining useful life of the transmission.

The health monitoring system significantly increases the Time Between Overhaul (TBO) requirement for the transmission, thereby greatly reducing the transmission maintenance costs. In addition, transmission reliability is increased. It is expected that within three years, subsequent refinements will allow the transmission maintenance to be placed on entirely condition, thereby further reducing maintenance costs.

13.3 TRANSMISSION MAINTENANCE

Easily removable panels above the main gearbox facilitate maintenance of the transmission. The gearbox is comprised of four sections. The bottom half of the gearbox is one continuous casting with oil sight gauges to check the oil levels and cored-passages to facilitate lubrication oil flow. The top portion of the gearbox is split into three sections with each section accessible through a separate service panel. Similarly each section of the tail drive shaft is accessible through removable panels.

14 AIRCRAFT OPERATION

In the trade off study (Section 2), it was shown that a triple engine helicopter with twin engine cruise offers a distinct advantage. For the relatively low disk loading selected for this design, the engine power is dictated by the requirement for twin engine cruise (at maximum continuous power, MCP, and ISA+0), rather than the OEI requirement. This results in engines that are oversized for the nominal OEI condition, however, due to the improved cruise fuel efficiency, the fuel consumption, and hence take-off weight are lower compared to a regular triple engine helicopter. Within the limited resolution of the cost analysis, the additional cost for the oversized engines is offset by the improved fuel efficiency and lower take-off weight. The subsequent discussion is focussed on the 19-seat aircraft.

In the performance analysis, it is shown that the OEI capability exceeds the stipulated hover (out of ground effect) with full passenger load, 60% fuel, at sea level and in ISA+20. The OEI hover ceiling (in ISA+20), as a function of take-off weight, is shown in Figure 9.8. For example, it is possible to achieve an ISA+20 OEI (hover out of ground effect) of 1500 ft, at maximum take-off weight, or 5000 ft with 60% fuel.

Furthermore, for a standard helicopter designed for ISA+0 cruise, the available engine power will be inadequate to maintain the desired cruise speed in ISA+ conditions. This implies, that in ISA+ conditions, the operator sacrifices on-time arrival, and will have to refuel after each mission leg. However, for the present design, it is possible to compensate for the reduced engine performance in ISA+ conditions by using all three engines in cruise (see Figures 9.2 and 9.3. The aircraft can achieve the maximum cruise speed and complete the 2x200 nm round-trip mission in ISA+20 (without refueling after one leg). The Chesapeake thus greatly expands the deployment flexibility for the operator, allowing on-time, full payload operations in conditions up to ISA+20 and airfield elevations up to 5000 ft. This improved performance, is achieved with no measurable increase in operating cost, compared to a standard triple engine design configuration (as discussed in Section 2.5.4).

14.1 ISA and ISA+ MISSION PROFILES

The RFP stipulates a mission profile, to be flown in nominal ISA+0 conditions. However, considering hot daytime conditions during the summer months, it is to be expected that flight conditions will exceed ISA+0. For this reason, the aircraft has been designed and sized with sufficient thrust, power margin and fuel capacity to complete the 2x200 nm round-trip mission in ISA+20 conditions. The OEI requirement will affect the ISA+20 range and payload, depending on the take-off elevation.

Table 14.1 shows the flight profile details for ISA+0 and ISA+20 conditions, and Table 14.2 lists the take-off elevation OEI limitations. Figure 14.1 is added for reference.

The aircraft takes off on three engines. Depending on the airfield elevation, and the ISA+ condition, the aircraft fuel and payload are restricted to meet the RFP stipulation that HOGE can be maintained in a OEI situation.

After take-off and having cleared the vertiport terminal area, the helicopter accelerates to 150 knots and enters a 1250 ft/min en-route cruise-climb. In ISA+0 this can be achieved with the engines set below MCP, while in ISA+20 intermediate power is required. Intermediate power is limited to 30 minutes, however, the climb to 8000 ft only takes 6.4 minutes (at 1250 ft/min). The climb rate is limited to 1250 ft/min, since the cabin is not pressurized. The reason for climbing at the cruise speed rather than at the slower best-rate-of-climb speed, is that the total travel time has a

Table 14.1: ISA+0 and ISA+20 Flight Profile Details

Segment	ISA+0	ISA+20
Take off	3 engines, take-off power	3 engines, take-off power
Climb	1250 ft/min, 150 knots, 3 engines (MCP)	1250 ft/min, 150 knots, 3 engines (IRP)
Cruise	150 knots, **2** engines (MCP)	150 knots, **3** engines (MCP)
Descent	3 engines, partial power	3 engines, partial power
Landing	3 engines, HOGE	3 engines, HOGE

Nominal cruise: 4000 ft, bad weather cruise: 8000 ft

Max cruise: 160 knots at 4000 ft, 153 knots at 8000 ft

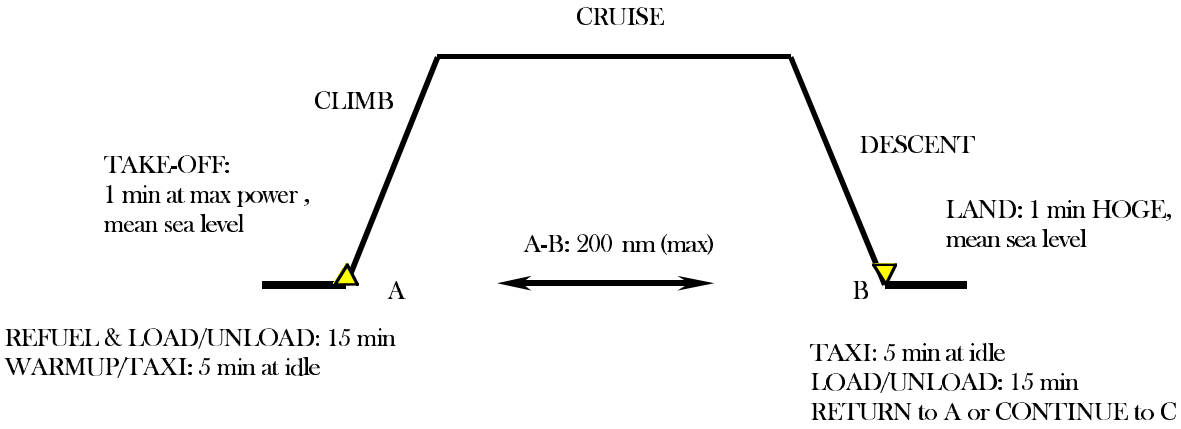

Figure 14.1: Civil short-haul VTOL mission profile

more dominant impact on the operating costs per air-seat-mile and the rentability index than the fuel consumption (as discussed in Section 2).

The nominal cruise altitude is 4000 ft and bad weather cruise is set at 8000 ft (the altitude limit for an un-pressurized cabin). These altitudes are based on cloud-cover and airfield elevation information in the Northeast corridor (see Section 2.4.2). In ISA+0, one of the three cruise engines is switched off, to ensure that the remaining two engines are operating close to optimum efficiency at MCP. The in-flight engine shut-down is slaved into the FADEC system, which determines, which engine is next in the shut down rotation. (Each engine is switched-off for one flight leg every third time). In the presence of headwinds the cruise speed can be increased to the maximum cruise speed of 160 knots (4000 ft and ISA), which allows for on time arrival despite 10 knot headwinds. In ISA+20, all three engines are required to achieve the 150 knot cruise speed.

Table 14.2: ISA+20 OEI Restrictions

Take Off Elevation	Restriction
0 - 1500 ft	none
1500 - 5500 ft	reduce fuel load (up to 40%), refuel after one flight leg
$>$ 5500 ft	60% fuel, reduce payload at a rate of 260 lb per 1000 ft

Prior to starting the en-route descent, the third engine is restarted, for safe flight operations as the aircraft descends and enters the vertiport terminal area for landing. The fuel tanks are sized such that the aircraft can complete the 2x200 nm round-trip mission without refueling. If the OEI restrictions require reduced fuel, then refueling is required after each flight leg.

14.2 OEI PROCEDURES

The OEI procedures are separated into two categories: first, engine failure during take-off and landing and second, engine failure in cruise. The procedures for the take-off and landing engine failure are based on the procedures developed during the development and qualification of the S-76C+ [Cole97]. It is only recently that engines have been developed that are capable of bestowing viable one-engine-out capability on multi-engine helicopters, for operation at or near gross weight. The key advances have been the development of small, compact, efficient engines with 125% 30-second emergency and 100% 2-minute contingency ratings, with precise engine control provided by the FADEC. The high, short term emergency power allows for better matching of the engines for cruise requirements, which improves engine efficiency.

14.2.1 Landing and Take-Off OEI Procedures

In the event of an engine failure during vertical flight mode, the following sequence takes place: the FADEC automatically detects the one-engine-inoperative condition, and accelerates the remaining two engines to the 30-second emergency setting. If the engine failure is below a minimum altitude (to be established after flight tests) the pilot will enter a OEI hover and execute an emergency landing within the 30 second window. If the engine failure is above the threshold altitude the pilot lowers nose and accelerates to the minimum power speed (approximately 80-90 knots). Once this speed is reached the pilot initiates a climb and go-around. The pilot then returns for an emergency landing. During the above OEI flight procedures the FADEC cues the pilot when it is necessary to de-select from the emergency setting (30-second time limit), to the contingency setting (2 minute limit) and then to the continuous power setting.

During the entire emergency the FADEC's OEI control logic is such that the engine attempts to accelerate the main rotor to its maximum speed. This relieves the pilot from having to continuously work the collective, apart from lowering it, as each time-limit expires. The pilot's main workload in this critical phase is to fly airspeed with pitch attitude, while maintaining rotor rpm with collective and remaining alert to the engine setting limit in use, and its time expiry.

For both OEI and normal flight operations, the FADEC monitors the engine parameters for routine on-line maintenance purposes. If the emergency setting is ever used, the engine has to be removed and dismantled for inspection. Further details on the FADEC system and the OEI procedures can be found in reference [Cole97].

14.2.2 OEI Procedures in Twin-Engine Cruise

In the event of an engine failure during twin engine cruise, the FADEC automatically sets the remaining engine to the 2-minute contingency rating and initiates re-start of the third engine. The pilot decelerates to the minimum power speed (80 knots), and descends to and maintains 4000 ft (see Figure 9.2). The third engine will be online before the

two-minute contingency limit expires. After two minutes (with a visual cue from the FADEC) the pilot de-selects to the maximum continuous power setting and initiates a precautionary landing at the nearest airfield. The FADEC does not select emergency power in the event of a cruise engine failure, since this is not necessary. Nonetheless, there is a provision for the pilot to manually select the 30 second emergency setting, if required. Again, if an engine is run-up to emergency power it subsequently needs to removed, disassembled and inspected.

The above OEI discussions give a brief overview of the envisaged emergency operation in the event of an engine failure during take-off/landing or in cruise.

15 COST ANALYSIS AND FLEET SIZING

In this section the aircraft cost analysis and the fleet sizing are described. Although the maximum design range is 2x200 nm, the average round-trip flight will be shorter. In Section 2, it is shown that the average distance between existing airports in the Northeast corridor is 125 nm. This is not strictly appropriate for estimating the average flight distance, which will be weighted by the dominant flight routes. In the absence of detailed market information and flight routes, it will be assumed that the average flight distance, for fleet sizing and cost analysis purposes, is 150 nm.

15.1 COST ANALYSIS

The helicopter cost analysis is based on historical data and empirical models. All cost calculations are in 1997 Dollars. Table 15.1 shows a breakdown of airline operating costs, as defined in the NASA Rotorcraft Economics Workshop [Lesl96]. The direct operating costs are essentially incurred per flight hour of the aircraft, whereas the indirect operating costs are independent of the fleet flight hours.

Table 15.1: Operating Cost Breakdown

Direct Operating Costs (DOC)	Cash DOC	Fuel and lubricants, maintenance, flight crew
	Ownership DOC	Depreciation, hull insurance, financing
Indirect Operating Costs (IOC)	Airplane Related	Ground property, facilities, control and communication, landing fees, ground handling, ground power, etc
	Passenger Related	Amenities, liability insurance, passenger handling, baggage handling, reservations and sales, commissions, advertising and publishing, etc

It will be assumed that, for a given passenger mile requirement, the indirect fleet operating costs are independent of the aircraft and hence, will not be included in this comparative analysis. Table 15.2 outlines the ingredients for the present cost model.

Table 15.2: Cost Analysis Summary (applicable to both Helicopter and Tiltrotor, all prices in 1997 $)

Cost	Description
Aircraft Price [Harr97]:	f(empty weight, installed rotor power, no. of blades per rotor, no. of engines, no. of main rotors)
Residual Value	10% (with an aircraft life of 10000 flight hours)
Maintenance [Olso93]	$0.052/fh/lb (per flight hour per lb empty weight)
Insurance [Scot96, Olso93]	Helicopter: 5% per year Tiltrotor: 6% per year
Financing [Scot96]	8% per year
Crew Cost	$62 per flight per crew member
Fuel	$0.667/gal

The aircraft price is estimated via an empirical model based on a multivariable linear regression analysis of historical aircraft price data (including twin and triple turbine engine helicopters and the V-22 tiltrotor [Harr97]). For investment accounting, several depreciation methods exist. For simplicity, a linear depreciation per flight hour with a 10% residual value is used, based on the RFP data of an aircraft life of 10000 flight hours and a utilization of 2000 flight hours per year. The finance costs are heavily dependent on the method of purchase, the total fleet size ordered and the rate of acquisition. As a first estimate, the aircraft is assumed to be 90% financed, at 8.5% per year. The details of hull insurance costs are based on factors beyond the scope of this analysis. The hull insurance will be assumed to be 5% per year for a helicopter and 6% for the tiltrotor. The 1% increase reflects the higher risk associated with the new technology tiltrotor.

Olson [Olso93] reports an average maintenance cost of $0.067/fh/lb (empty) for helicopters and $0.008/fh/lb (empty) for turboprop aircraft. This is within 10% of the quoted maintenance costs of the Bell Model 212, 412 and 430[Bell98], the Sikorsky S-76 and the Eurocopter AS-365N Dauphin. In order to account for advanced health monitoring and on-conditions systems, the maintenance cost used in this trade-off study is reduced by 25% to $0.052/fh/lb (empty).

Crew cost per flight hour is based on a nominal helicopter pilot salary of $65,000/year [USDL96] and the FAR maximum number of 1200 pilot flight hours per year [FAR Part 121.481]. Assuming a 90% deployment factor the effective average cost is $62/fh per crew member. The fuel pricing varies considerably based on where the fuel is purchased geographically and whether it is purchased in retail or in bulk. In this analysis, a cost of $\$_{95}0.63$/gal will be used, as defined in the NASA Rotorcraft Economics workshop [Scot96]. This is less than 50% of the average retail price quoted by Bell [Bell98].

For the mission analysis, three distinct time intervals are defined:

- "engines-on": this is the total time from engine start to engine shut down
- "flight-time": this is the total effective flight time and includes the total time from take-off to landing, and only 20% of the time for warm-up and taxiing [Tish98]
- "travel time": this is the total travel time for a customer, from boarding to disembarking

Only 1/5 of the actual warm-up and taxi interval is used in computing the "flight-time", to reflect that during this period the aircraft does not encounter any significant loading.

The crew compensation is referenced to "engines-on" time; depreciation, insurance, financing and maintenance costs are based on the "flight-time"; and the rentability index (discussed in Section 2.5.2) is based on the "travel time". The fuel consumption is calculated directly. The definitions for costs per flight hour, cost per air seat mile and rentability are given by:

$$\text{DOC/fh} = \frac{\text{DOC per flight}}{\text{flight time}}$$

$$\text{DOC/asm} = \frac{\text{DOC per flight}}{\text{flight distance \#seats}}$$

$$\text{RI} = \left(\frac{\text{travel time}}{\text{flight distance}}\right)^{0.4} \frac{1}{\text{DOC/asm}}$$

The above economic model has several important limitations that need to be considered. The effect of the production rate and total production quantity on the aircraft price and maintenance costs is ignored. The impact of new advanced technologies, high automation manufacturing and quality control techniques (especially for composite components) is not reflected in historical price trends. The number of installed engines is not directly captured in the price and maintenance estimates. The software development costs, which are independent of aircraft weight, are not explicitly included. For an advanced technology aircraft with a glass cockpit, digital flight control and health-and-usage monitoring systems, the software development costs can be high. In addition, the lower maintenance costs of a modern aircraft with a high composite structural content are not accurately predicted by historical data of predominantly metal airframes. In addition, the indirect costs have not been included. The ground facilities (including hangar space, maintenance facilities and apron space) do scale with the fleet size, which will impact the total fleet-operation expenses. However, in the absence of a detailed cost data base and a high definition detailed design, the above economic model will be considered as a first estimate of the aircraft price and operating costs.

15.2 FLEET SIZING

The fleet sizing, for a specified daily passenger-mile requirement is dictated by two constraints: first, the 16 hours maximum flight operations per day, and second, the aircraft utilization limit of 2000 flight hours per year. In addition, it will be assumed that the aircraft has to return to the base airport at the end of the working day.

Based on the 16 hour day and using the "travel-time" definition, one aircraft can complete 5 round-trips. However, based on the yearly utilization limit (in conjunction with the "flight-time" definition) the aircraft will average only 2.28 round-trip flights per day. Ideally, based on projected market demand (including variations between weekdays and weekends), considering after hours maintenance operation and ignoring a yearly utilization limit, it is possible to define the minimum fleet size. A smaller fleet size yields reduced indirect costs (such as hangar space, apron space, maintenance operations). Since this marketing information is not available at present, the yearly utilization limit will be used to define the fleet size.

15.3 PURCHASE PRICE AND OPERATING COSTS OF THE 19 SEAT AIRCRAFT

Table 15.3 summarizes the fleet size and aircraft costs for the 19-seat Chesapeake. Figure 15.1 shows the breakdown of the direct operating cost (per air-seat-mile). Typically for rotorcraft, the fuel and crew compensation account for about 10% of the direct operating cost. The largest portion is related to the depreciation, which in turn is proportional to the aircraft value and lifespan.

Table 15.3: Chesapeake Fleet Sizing and Cost Estimates*

Fleet Size (700,000 passenger miles/day)	77
Fleet Size (1,100,000 passenger miles/day)	121
Aircraft Price, million $	9.03
DOC/flight hour, $	2089
DOC/asm**, $	0.855

* Based on a 2x150 nm round trip, all prices in 1997 $
** DOC/asm = direct operating cost per air-seat-mile, includes: depreciation, financing, insurance, maintenance, fuel and crew compensation

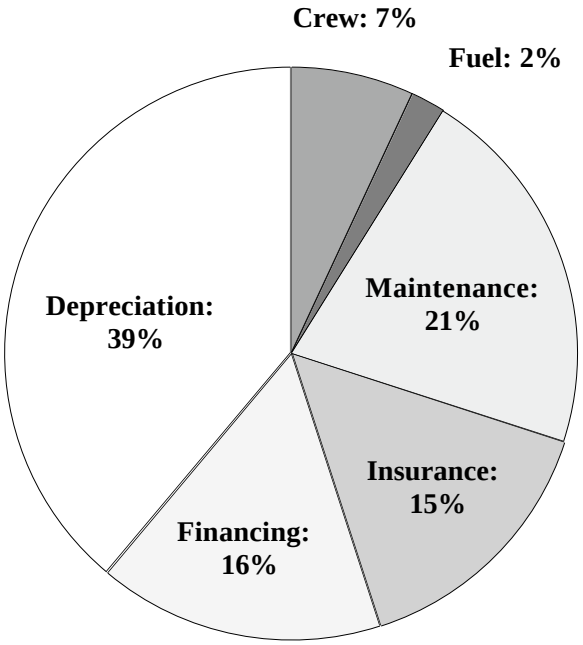

Figure 15.1: Breakdown of Direct Operating Costs (per air-seat-mile)

For a VTOL aircraft, the fuel and crew costs are secondary compared to the aircraft-value related ownership costs (depreciation, insurance and financing) and the maintenance, which is directly the opposite of the turboprop economics [Olso93].

16 12-SEAT CONFIGURATION

The RFP requires a 12-seat derivative of the 19-seat aircraft as a "lead-in" product to establish the civil short haul VTOL commuter airline. According to the RFP Addendum (11 March, 1998), it is anticipated that delivery of the 12-seat configuration will start in 2007, with launch of the 19-seat version in 2012. This implies that the 12-seat aircraft is expected to meet the 700,000 passenger-miles/day requirement (per fleet).

16.1 REQUIREMENTS FOR THE 12 SEAT DERIVATIVE

The 12-seat and 19-seat versions are required to have the same dynamic components (including main rotor, engines, transmission, fan-in-fin), and substantial commonality of subsystems, including the hydraulics, electrical system and avionics, but excluding the the fuselage structure [RFP98]. This is to minimize the additional investments (such as tooling *etc*) and the costs associated with certification and qualification.

The requirement of dynamic component commonality for a 12- and 19-seat VTOL aircraft is not very cost-effective. The reason is that for a VTOL aircraft it is necessary to carefully optimize the match between the dynamic components and the payload. However, in this case, the 12-seat aircraft is required to fly with a rotor, main gearbox and engine set that have been configured and optimized for a 58% larger payload. Consequently, the rotor is significantly oversized and the aircraft will be severely over-powered. This translates into a poor empty weight fraction, a very low hover figure of merit and inefficient fuel consumption in cruise. In addition the large main rotor results in an excessively long tail section, which also contributes to a high empty weight fraction. Also, the layout of a 12-seat derivative cabin is limited by the CG travel and stability/control limits of the main rotor. Thus the main difference between the 12- and 19-seat variants will be the smaller fuselage structure and reduced number seats, interior furnishings, baggage compartment and fuel capacity. These weight savings only constitute a 7% reduction of the empty weight, compared to the original 19-seat aircraft.

Now, in the cost analysis, Section 15.1, it is shown that the primary cost drivers for a VTOL aircraft (helicopter or tiltrotor) are the empty weight and the installed power. Since the empty weight only drops by 7% and the installed power is unchanged, it is evident that the aircraft operating costs per flight hour will be similar to those of the 19-seat aircraft. Consequently there will be a significant increase in the direct costs per air-seat-mile for the 12-seat aircraft. Although it is possible to design efficient and cost-effective fixed wing aircraft families (using fuselage expansion plugs and a matched family of engines), this design flexibility is not available for the much more restrictive VTOL design requirements.

16.2 12 SEAT CONFIGURATION OPTIONS

Nevertheless, to satisfy the requirements of the RFP, it was attempted to convert the 19-passenger design to a 12-passenger design retaining the same main rotor, main gearbox, engines, transmission and fan-in-fin. There are essentially three options: 1) retain the exact same aircraft and alter the passenger cabin from a high density 19-seat configuration to a more spacious 12-seat configuration, 2) shorten the cabin by two rows (and lengthen the tail to maintain the clearance from the main rotor), 3) narrow the fuselage by eliminating one seating row in the cabin (this results in a 25% reduced width).

The first option is the simplest solution. Eliminating 7 seats (accounting for approximately 70 kg), and reducing the payload by 58% has a negligible impact on the aircraft empty weight and the fuel consumption. Hence, the total operating price per flight hour is essentially unchanged, and it follows that the direct cost per air-seat-mile is increased by a $\frac{19}{12} = 58\%$ to \$1.354/asm. The second option is not viable, since the shortened cabin length results in an excessive rear-ward cg shift, that exceeds the rotor limits. The third option circumvents the cg-envelope problem and derives an additional benefit over the first option, in that the fuselage structural weight is reduced, and the fuselage drag is reduced, via the narrower fuselage. Considering the high composite content of the aircraft structure, the narrower fuselage will not yield a significant empty weight savings. The small reduction in empty weight and the negligible impact of the fuel costs on the total operating costs (see Section 15.1) implies that the narrow body 12-seat helicopter will not offer a significant reduction in total operating cost per flight-hour compared to the 19-seat aircraft. It should be noted, that it is expected that there will be similar difficulties in deriving a 12-seat tiltrotor from the baseline 19-seat vehicle, since commonality of the main rotors (and hence the wing span), transmission and engines is required.

It is possible to make the 12-seat aircraft slightly more cost competitive, if the RFP requirements are relaxed, so as to allow the 12-seat version to have smaller engines (while retaining the same rotor and transmission system). Although the different engines will require separate certification, the lower installed power will reduce the price and operating expenses. In order to further try and improve the cost-effectiveness of the 12-seat derivative, it is proposed to reduce the maximum speed cruise from 160 to 155 knots and to reduce the range to one-mission leg. The halved fuel requirement results in a lower take-off weight and even smaller engines. The main disadvantage is that the helicopter needs to be refueled after each mission leg.

Table 16.1 summarizes the weight, price and direct operating costs for three 12-seat configurations: version 12-S is the 19-seat aircraft configured for a spacious 12-seat layout, version 12-N is the narrow body version (with full commonality of all dynamic systems). The third variant is the 12-Ne, a narrow body 12-seat derivative that retains the dynamic systems of the 19-seater (including rotor and transmission), but has 3 smaller engines. This aircraft has a reduced fuel capacity for only one mission leg. All three 12-seat aircraft are designed to the same performance criteria and mission requirements as the 19-seat baseline version.

The required full payload (12 passengers) and 2 crew members is 1379 kg (3040 lb). Fuel sizing is for a maximum trip distance of 200 nm (one or 2 legs, depending on the configuration) and the direct operating costs are evaluated for an average flight of 150 nm. As with the 19 seat design, the 12 seat design includes a 2.5% weight growth factor, that is incorporated in the empty weight.

Table 16.1 clearly shows the poor cost effectiveness of the 12-seat narrow-body derivative. It is evident that in all three cases the high empty weight fraction and high power/weight ratio result in a very high price and operating costs. Compared to the baseline 19-seater the narrow body 12-N and 12-Ne have a 7.3% lower parasite drag, and a 6.5% weight reduction associated with the smaller cabin. The 12-Ne has a further 2% weight saving due to the smaller engines. All three 12 seat variants have a empty-weight fraction (We/TOW) greater than 60%, compared to the 55% of the 19-seater. The 12-N price is 3.2% cheaper, whereas the 12-Ne, with the smaller engines, is 15.7% cheaper than the \$9.03 million baseline version. The 12-Ne has the lowest DOC/asm of \$1.15, which is still 34% more expensive than the 19-seat DOC/asm of \$0.86. In considering the 12-Ne design, it should be noted, that there

Table 16.1: 12 Seat Chesapeake Helicopter Derivatives

	Units	12-S	12-N	12-Ne
Range	nm	2x200	2x200	1x200
Take-off weight	kg (lb)	6231 (13737)	5880 (12963)	5375 (11850)
Payload + 2 Crew	kg (lb)	1379 (3040)	1379 (3040)	1379 (3040)
Empty weight	kg (lb)	3786 (8347)	3590 (7915)	3513 (7745)
Fuel capacity (usable)	kg (lb)	1066 (2350)	911 (2008)	484 (1067)
Installed power	kW (hp)	3x930 (3x1250)	3x930 (3x1250)	3x745 (3x1000)
Empty weight fraction	-	0.608	0.611	0.654
Power/weight ratio	kW/kg (hp/lb)	0.449 (0.273)	0.476 (0.289)	0.416 (0.253)
Fleet size[1,2] *	-	122	122	122
Aircraft price	million $\$_{97}$	9.03	8.74	7.61
DOC[2,3]/flight hour	$\$_{97}$	2089	2000	1777
DOC/asm	$\$_{97}$	1.35	1.30	1.15

1) Fleet size based on 700,000 passenger-miles/day
2) Fleet sizing and DOC are based on an average mission leg of 150 nm 3) DOC = direct operating cost, includes: depreciation, financing, insurance, maintenance, fuel and crew compensation

will be additional certification costs for the smaller engine, that need to be taken into account.

In comparison, the Bell 412-HP, a 130 knot, 400 nm, 13 passenger helicopter, has a base price of $4.74 million. Using the quoted fuel and maintenance costs of $671/fh [Bell98], and the depreciation/financing/insurance/crew costs listed in Section 15.1 and considering a 150 nm mission leg, it is estimated that the DOC/asm is $1.07. The 12-Ne version has a 10% higher DOC/asm, although it will achieve a better rentability as a result of the higher cruise speed.

The results substantiate the above arguments that indicate that it is not feasible to design a 12-seat derivative of a 19-seat helicopter (with complete dynamic component commonality). Based on this configuration study, it is recommended that the commonality requirement be relaxed to exclude the engines. This allows the engines to be matched to the aircraft, thereby reducing the acquisition price and DOC/asm. It would also be of interest to investigate the market response to direct introduction of the 19-seat variant, rather than the less cost-effective 12-seat derivative, or to consider a dual size fleet. For this fleet the 12- and 19-seat aircraft would be separate designs, sharing only subsystem commonality.

16.3 THE CHESAPEAKE 12-Ne

Despite the above arguments against a 12 seat derivative, the Chesapeake 12-Ne is presented in order to satisfy the RFP specifications. The detailed performance curves for the 12-Ne variant are not shown, however, the pertinent performance specifications are summarized in Table 16.2. Figures 16.1 and 16.2 show a general layout of the narrow body, 12-seat version.

Table 16.2: Performance Summary for the Chesapeake 12-Ne: Max TOW, ISA, unless otherwise specified

Max. Take-off Weight (TOW)	kg (lbs)	5400 (11900)
Nominal cruise speed	km/h (knots)	278 (150)
Max. cruise speed (4000 ft)	km/h (knots)	287 (155)
Nominal cruise altitude	m (ft)	1219 (4000)
Bad weather cruise altitude	m (ft)	2438 (8000)
Engines used in cruise*	-	3
HOGE ceiling: ISA (3 eng. @ take-off power)	m (ft)	6357 (20857)
HOGE ceiling: ISA+20 (3 eng. @ take-off power)	m (ft)	4048 (13281)
Max. climb rate (sea level, 80 knots, MCP)	m/s (ft/min)	20.3 (4000)
Max. climb rate (sea level, ISA+20, 83 knots, MCP)	m/s (ft/min)	15.2 (3000)
Max. vertical climb rate (sea level, MCP)	m/s (ft/min)	9.5 (1875)
Best range speed	km/h (knots)	260 (140)
Best endurance speed	km/h (knots)	148 (80)
Range (w. standard reserves, 150 knots)	km (nm)	485 (262)
Endurance (w. standard reserves, 80 knots)	hours	2.2
One Engine Inoperative: TOW with 60% fuel	kg (lbs)	5200 (11480)
HOGE ceiling: ISA (2 eng. @ emergency)	m (ft)	5007 (16412)
HOGE ceiling: ISA+20 (2 eng. @ emergency)	m (ft)	1910 (6267)

* Climb, descent is on 3 engines, cruise in ISA+20 is on 3 engines

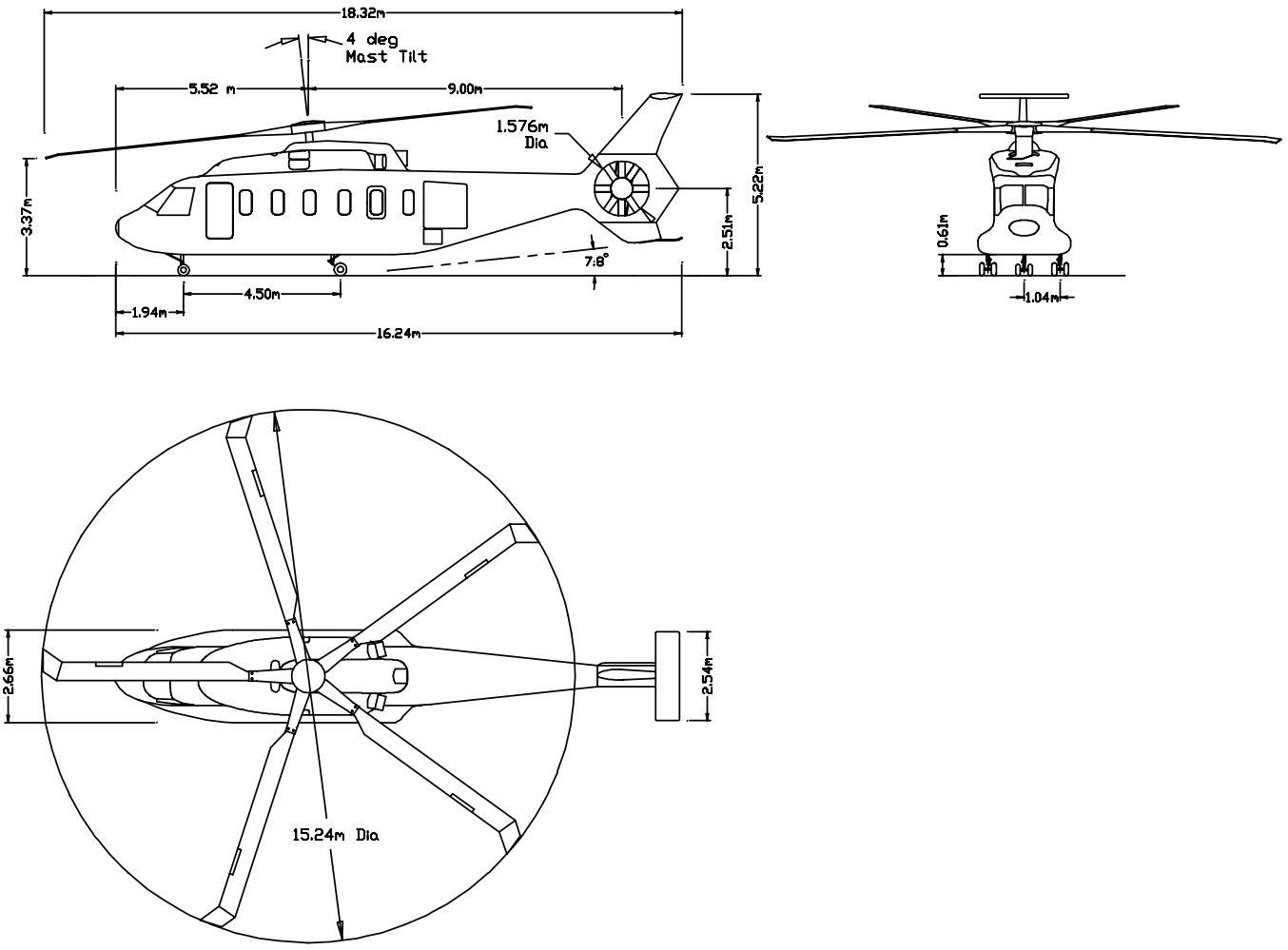

Figure 16.1: Three-view drawing of the Chesapeake 12-Ne

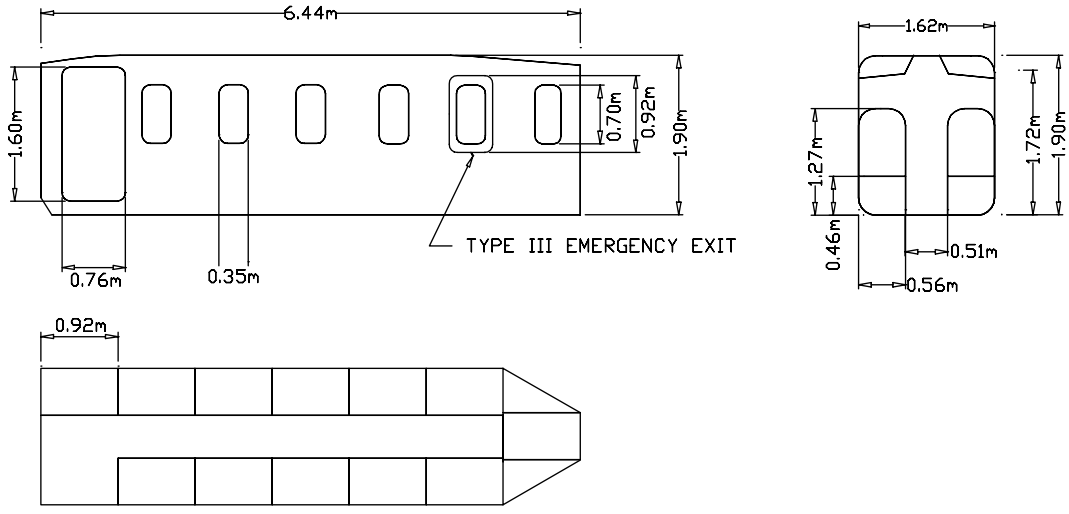

Figure 16.2: Cabin layout of the Chesapeake 12-Ne

17 SUMMARY AND CONCLUSIONS

The preliminary design of the Chesapeake 19-seat civil transport helicopter is presented. The Chesapeake meets/exceeds all of the performance objectives outlined in the Request For Proposal submitted by AHS International. After a preliminary trade-off study, that included a conventional helicopter and a tiltrotor configuration, it was determined that a conventional triple-engine helicopter is the most economical configuration to meet the requirements for a 19-seat passenger helicopter in the North-East Corridor of the United States. A detailed design study outlines the basic layout and structure of the Chesapeake.

The Chesapeake incorporates a 5-bladed, bearingless, composite main rotor. The rotorblades, with swept anhedral tips, use three different high performance airfoil sections and incorporate an active trailing edge flap. A fan-in-fin is installed as the anti-torque device, primarily for its low noise and safety qualities, compared to a conventional tail rotor. The 7000 kg (15432 lb) Chesapeake is powered by three 932 kW (1250 hp) IHPTET engines. In order to improve the aircraft cost-effectiveness, nominal cruise (150 knots, 4000 ft, ISA) is achieved on two engines, with the third engine switched-off. This reduces the required fuel load, because operating engines run closer to the optimum continuous power setting. In addition, with each engine only flying two out of three cruise legs, the engine maintenance requirements are reduced. The transmission is a three-stage, single planetary system, rated to deliver a maximum of 2800 kW (3750 SHP) to the rotors, the fan-in-fin and auxiliary systems.

The helicopter has a nominal cruise of 150 knots at 4000 ft with a bad weather cruise of 150 knots at 8000 ft. In ISA conditions one engine is switched-off in cruise to improve fuel efficiency, while in ISA+ conditions all three engines are required to achieve the 150 knot cruise speed. The aircraft exceeds the stipulated engine failure requirement and can maintain an OEI hover out of ground effect up to 5500 ft in ISA+20, with full payload and 60% fuel. Consequently the operator does not need to reduce payload or the range (of one mission leg) during hot and high operations. The Chesapeake has a price of $9.03 million and total direct operating costs of $2089 per flight hour and $0.86 per air-seat-mile.

Several innovative advanced features are incorporated in the design. A smart trailing edge flap, installed in each blade, is used for in-flight tracking and vibration reduction. Low noise levels in the spacious passenger cabin are achieved via a hybrid active-passive trim-panel noise reduction system. A comprehensive rotor and transmission health and usage monitoring system provides the pilot with real-time flight-safety related information. It also provides a down-loadable database for on-condition maintenance. The full authority digital engine control system reduces pilot workload, enhances OEI operations and is integrated with the HUMS system for engine maintenance.

A 12-passenger derivative, the Chesapeake 12-Ne, envisioned as a "lead-in" product, is also presented. This aircraft has complete commonality of the dynamic systems (including the rotor, the transmission, undercarriage, and the fan-in-fin). However, to improve the cost effectiveness, 3 smaller 745 kW (1000 hp) engines are installed, and the fuel sizing is reduced to one mission leg. The 12-seat derivative effectively has a significantly over-designed rotor and transmission system and consequently has a 34.5% higher DOC/asm compared to the 19-seat helicopter.

The Chesapeake is a civil short-haul commuter helicopter that offers the passenger a jet-smooth ride. The low maintenance design, with extensive health and usage monitoring, innovative materials, advanced "smart systems" and the all-weather capability offer the operator a VTOL aircraft with competitive operating costs and the performance capability to meet strict commercial schedules in both bad weather and under high temperature conditions.

References

[AGAR83] "Aeroelastic Considerations in the Preliminary Design of Aircraft", AGARD CP 354, April 1983.

[AlKh98] Al-Khalil, K., Phillips, D., Ferguson, T., "Improved Hybrid System Protects Airfoils Against Icing", *NASA Tech Briefs*, Vol. 22, No. 6, June 1998

[Amer92] Amer, K., Prouty, R., Korkosz, G., Fouse, D., "Lessons Learned During the Development of the AH-64 Apache Attack Helicopter", *Proceedings of the 48th Annual Forum of the American Helicopter Society*, June 1992, washington, D.C.

[Bell98] Bell Helicopter Product Data, http://www.bellhelicopter.textron.com, April 1998.

[Bill90] Bill, R.C. "Advanced Rotorcraft Transmission Program", *Proceedings of the 46th Annual Forum of the American Helicopter Society*, May 1990, pp. 227-238.

[Chop97] Chopra, I., "Status of Application of Smart Structures Technology to Rotorcraft Systems", *Proceedings of the Royal Aeronautical Society"s Innovations in Rotorcraft Technology Conference*, London UK, June 1997.

[Cole97] Cole, J.L., Evans, C.W., Greenberg, C.E, Saal, K.W., "Development and Qualification of the S-76C+ Helicopter with 30-Second/2-Minute OEI Power Ratings", *Proceedings of the 53rd AMerican Helicopter Society Forum*, Virginia Beach, VA, April 1997.

[Curr88] Currey, N. S., *Aircraft Landing Gear Design: Principles and Practices*, American Institute of Aeronautics and Astronautics, Inc., Washington, D.C., 1988.

[Derh96] Derham, R.C., Hagood, N.W., "Rotor Design Using Smart Materials to Actively Twist Blades", *Proceedings of the 52nd Annual Forum of the American Helicopter Society*, Washington, DC, June 1996.

[Desj91] Desjardins, R.A., Noehren, W.L., Bertolazzi, A.N., "Design and Flight Test Evaluation of the Fantail Anti-torque System", *Proceedings of the 47th Annual Forum of the American Helicopter Society*, Phoenix, Arizona, May 1991, pp. 857-867.

[Fala91] Falasco, T., Zachar, E., Lallo, A., "H-76B Fantail Demonstrator Composite Fan Blade Fabrication", *Proceedings of the 47th Annual Forum of the American Helicopter Society*, Phoenix, Arizona, May 1991, pp. 399-405.

[FAR27] Federal Aviation Regulations, Part 27, Airworthiness Standards: Normal Category Rotorcraft, Federal Aviation Administration, U.S. Department of Transportation, Oct. 1993.

[FAR29] Federal Aviation Regulations, Part 29, Airworthiness Standards: Transport Category Rotorcraft, Federal Aviation Administration, U.S. Department of Transportation, Nov. 1993.

[Flat91] Flater, R., "The Vertical Commuter: A Solution to Urban Transportation Problems", *Vertiflite*, Vol. 37, No. 1, January/February 1991.

[Garb92] Garbo, S.P., Rosen, K.M., "Composites Usage on the RAH-66 Comanche", *Vertiflite*, 38(2), March/April 1992, pp. 8-13.

[Gmel89] Gmelin, B., Jones, A., Philippe J., Schmidt, U., Humpherson, D., Leprêtre, A., Rauen, A., Stevens, J., "Preliminary Comparisons of TiltRotor and Compound Helicopter for Civil Applications", *Proceedings of the 45th American Helicopter Society Forum*, Boston, Massachusetts, May 1989.

[Harr97] Harris, F.D., Scully, M.P., "Helicopters Cost Too Much", *Proceedings of the 53rd American Helicopter Society Forum*, Virginia Beach, VA, April 1997.

[Heli98] Hoverview, *Helicopter World*, March 1998.

[Hube92] Huber, H. "Will Rotor Hubs Lose Their Bearings?" A Survey of Bearingless Main Rotor Development", *Proceedings of the European Rotorcraft Forum*, Avignon, France, September 1992.

[Hump88] Humpherson, D., "Compound Interest - A Dividend for the Future", *Proceedings of the 54rd American Helicopter Society Forum*, Washington D.C., May 1998.

[John80] Johnson, W., *Helicopter Theory*, Dover Publications, Inc. New York, 1980.

[Keys91] Keys, C., Sheffler, M., Weiner, S., Heminway, R., "LH Wind Tunnel Testing: Key to Advanced Aerodynamic Design", *Proceedings of the 47th Annual Forum of the American Helicopter Society*, Phoenix, Arizona, May 1991, pp. 77-87.

[Lamb94] Lambert, M. *Jane's All the World's Aircraft*, Jane's Information Group Limited, Coulsdon, Surrey, 1994.

[Lee98] Lee, T., CHopra, I., "Design and Static Testing of a Trailing-Edge Flap Actuator with Piezostacks for a Rotor Blade", *Proceedings of the 1998 SPIE 5th Annual Symposium on Smart Structures and Materials*, San Diego, CA, March 1998.

[Lesl96] Leslie, P., "Short Haul Civil Tiltrotor and Bell Model 412 Cost Drivers", NASA/Industry/Operator Rotorcraft Economics Workshop Report, NASA Ames Research Center, Moffett Field, CA, May 1996.

[Leve90] Leverton, J., "Advanced Technology Rotorcraft - Civil Short Haul Transport of the Future", *Vertiflite*, Vol. 36, No. 1, January/February 1990.

[Milg95] Milgram, J.H. and Chopra, I. "Helicopter Vibration Reduction with Trailing Edge Flaps", *Proceedings of the American Helicopter Society Northeast Region Aeromechanics Specialists Meeting*, Stratford, CT, October 1995.

[Milg97] Milgram, J.H. "A Comprehensive Aeroelastic Analysis of Helicopter Main Rotors with Trailing Edge Flaps for Vibration Reduction", Ph.D. Thesis, University of Maryland, College Park, Maryland, January 1997.

[Moui79] Mouille, R., "Ten Years of Aerospatiale Experience With the Fenestron and Conventional Tail Rotor", *Proceedings of the 35th Annual Forum of the American Helicopter Society*, Washington D.C., May 1979, p. 9.

[Niwa98] Niwa, Y., "The development of the new observation helicopter (XOH-1)", *Proceedings of the 54th Annual Forum of the American Helcipoter Society*, pages 1285–1297, Washinton, DC, May 1998

[NOAA98] National Oceanographic and Atmospheric Administration Historical Climate Data, http://www.ncdc.noaa.gov, April 1998.

[Olso93] Olson, J. R., "Reducing Helicopter Operating Costs", *Vertiflite*, January/February 1993.

[Prou90] Prouty, R. W., *Helicopter Performance, Stability, and Control,* Robert E. Krieger Publishing Company, Malabar, FL, 1990.

[Raja97] Rajagopalan, R. G., Keys, C. N., "Detailed Aerodynamic Analysis of the RAH-66 Fantail Using CFD", *Journal of the American Helicopter Society*, Oct. 1997, pp. 310-320.

[Raym92] Raymer, D. P., *Aircraft Design: A Conceptual Approach*, American Institute of Aeronautics and Astronautics, Inc., Washington, D.C., 1992.

[Reis86] Reisdorfer, Dale and Mazza, L. Thomas, "Static Test and Flight Test of the Army/Bell Advaced Composite Airframe Program Helicopter", 1986.

[RFP98] 1998 Request for Proposal (RFP) for a Civil Transport Rotorcraft, 15th Annual Student Competition, sponsored by Boeing and the American Helicopter Society.

[Samu98] Samuel, P.D., Pines, D.J., and Lewicki, D.G., "A Comparison of Stationary and Non-stationary Transforms for Early Fault Detection in the OH-58A Main Transmission", *Proceedings of the 54th AHS International*, Washington DC, May, 1998.

[Scot96] Scott, M.W. "Economic Analysis of SHCT Tiltrotor", NASA/Industry/Operator Rotorcraft Economics Workshop Report, NASA Ames Research Center, Moffett Field, CA, May 1996

[Sen84] Sen, J. K., "Designing for a Crashworthy All-Composite Helicopter Fuselage", *Proceedings of the 40th Annual Forum of the American Helicopter Society*, Arlington, Virginia, May 1984, pp. 123-134.

[Shif98] Shifrin, C.A., "Strong Passenger Demand Propels U.S. Regionals", Aviation Week & Space Technology, 18 May 1998

[Spen98] Spencer, M.G., Sanner, R.M., Chopra, I., "Development of Neural Network Controller for Smart Structure Activated Rotor Blades", *Proceedings of the 39th AIAA/ASME/ASCE/AHS/ASC Structures, Structural Dynamics and Materials Conference and AIAA/ASME/AHS Adaptive Structures Forum*, Longbeach, CA, April 1998

[Stra95] Straub, F.K., "Active Flap Control for Vibration Reduction and Performance Improvement", *Proceedings of the 51st Annual Forum of the American Helicopter Society*, Fort Worth, Texas, May 1995

[Stra97] Straub, F.K., Ealey, M.A., Schethy, L.M., "Application of Smart Materials to Helicopter Rotor Active Control", *Proceedings of the 1196 SPIE's North American Symposium on Smart Structures and Materials*, San Diego, CA, February 1996

[Stit89] Stitzelberger, K., Ramm, U., "An Advanced Structural Concept for the NH90 Composite Fuselage", *Fifteenth European Rotorcraft Forum*, No. 91, Amsterdam, Netherlands, Sept. 1989, p. 16.

[Timet98] Titanium Metals Coporation (Timet), Titanium Alloys Product Data Sheet, http://www.timet.com/, 1998

[Tish90] Tishchenko, M, "Helicopter or Tiltrotor: A Soviet View", *Vertiflight*, September/October 1990

[Tish98] Tishchenko, M., Nagaraj, V.T., Helicopter Design Lecture Notes, University of Maryland, April 1998.

[USDL96] United States Department of Labor, Bureau of Labor Statistics, "Occupational Outlook Handbook 1996-97 Edition", January 1996.

[Vuil86] Vuillet, A., Morelli, F., "New Aerodynamic Design of the Fenestron for Improved Performance", *Twelfth European Rotorcraft Forum*, Garmisch-Partenkirchen, Germany, Sept. 1986, p. 11.

[Vuil89] Vuillet, A., "Operational Advantage and Power Efficiency of the Fenestron as Compared to a Conventional Tail Rotor", *Vertiflight*, July/Aug. 1989, pp. 24-29.

[Whit82] White, G.T., Logan, A.H. and Graves J.D. "An Evaluation of Helicopter Autorotation Assist Concepts", *Proceedings of 38th Annual Forum of the American Helicopter Society*, May 1982.

[Wood68] Wood, K. D., "Aerospace Vehicle Design; Vol. 1; Aircraft Design", Johnson Publishing Company, Boulder, Co. 1968.

[Wrig91] Wright, G. P., Driscoll, J. T., Nickerson, J. D. Jr., "Handling Qualities of the H-76 Fantail Demonstrator", *Proceedings of the 47th Annual Forum of the American Helicopter Society*, Phoenix, Arizone, May 1991, pp. 123-135.

A MIL-STD-1374 WEIGHT GROUP STATEMENT

MIL-STD-1374 PART I - TAB
NAME UMD
DATE 06/18/1998

PAGE 1
MODEL Chesapeake
REPORT

GROUP WEIGHT STATEMENT

AIRCRAFT

(INCLUDING ROTORCRAFT)

ESTIMATED - CALCULATED - ACTUAL

(CROSS OUT THOSE NOT APPLICABLE)

	CONTRACT NO	N/A					
	AIRCRAFT GOVERNMENT NO	N/A					
	AIRCRAFT CONTRACTOR NO	N/A					
	MANUFACTURED BY	N/A					
				MAIN		AUX	
	ENGINE MANUFACTURED BY			N/A			
	ENGINE MODEL			N/A			
	ENGINE NO			N/A			
	ENGINE TYPE			N/A			
	PROPELLER MANUFACTURED BY			N/A			
	PROPELLER MODEL			N/A			
	PROPELLER NUMBER			N/A			
	PAGES REMOVED				PAGE NO.		
	NONE						

1	WING GROUP				
2	BASIC STRUCTURE - CENTER SECTION				
3	- INTERMEDIATE PANEL				
4	- OUTER PANEL				
5	- GLOVE				
6	SECONDARY STRUCTURE - INCL. WING FOLD WEIGHT				
7	AELERONS - INCL. BALANCE WEIGHT				
8	FLAPS - TRAILING EDGE				
9	- LEADING EDGE				
10	SLATS				
11	SPOILERS				
12					
13					
14	ROTOR GROUP				432.5
15	BLADE ASSEMBLY			311.5	
16	HUB AND HINGE - INCL. BLADE FOLD WEIGHT			121	
17					
18					
19	TAIL GROUP				55.4
20	STRUCT. - STABILIZER			15.2	
21	- FIN-INCL DORSAL			14.6	
22	VENTRAL				
23	ELEVATOR - INCL BALANCE WEIGHT				
24	RUDDER - INCL BALANCE WEIGHT				
25	TAIL ROTOR - BLADES			8.6	
26	- HUB & HINGE			17	
27					
28	BODY GROUP				794.1
29	BASIC STRUCTURE - FUSELAGE OR HULL			794.1	
30	- BOOMS				
31	SECONDARY STRUCTURE - FUSELAGE OR HULL				
32	- BOOMS				
33	- SPEEDBRAKERS				
34	- DOORS, RAMPS, PANELS & MISC				
35					
36					
37	ALIGHTING GEAR GROUP - TRICYCLE				174.5
38	LOCATION				
39	MAIN			139.6	
40	NOSE/TAIL			34.9	
41	ARRESTING GEAR				
42	CATAPULTING GEAR				
43					
44					
45	ENGINE SECTION OR NACELLE GROUP				10.7
46	BODY - INTERNAL			10.7	
47	- EXTERNAL				
48	WING - INTERNAL				
49	- EXTERNAL				
50					
51	AIR INDUCTION GROUP				7.6
52	- DUCTS			7.6	
53	- RAMPS, FLOGS, SPIKES				
54	- DOORS, PANELS & MISC				
55					
56					

57	TOTAL STRUCTURE				1474.8
58	PROPULSION GROUP				816.4
59	ENGINE INSTALLATION	103.7	103.7	103.7	
60					
61					
62	ACCESSORY GEAR BOXES & DRIVE			53.2	
63	EXHAUST SYSTEMS				
64	ENGINE COOLING				
65	WATER INJECTION				
66	ENGINE CONTROL				
67	STARTING SYSTEM				
68	PROPELLER INSTALLATION				
69	SMOKE ABATEMENT				
70	LUBRICATING SYSTEM				
71	FUEL SYSTEM			53.3	
72	TANKS-PROTECTED				
73	TANKS-UNPROTECTED				
74	PLUMBING				
75					
76	DRIVE SYSTEM			398.7	
77	GEARBOXES, LUB SY & ROTOR BRK				
78	TRANSMISSION DRIVE				
79	ROTOR SHAFTS				
80					
81	FLIGHT CONTROLS GROUP				148.3
82	COCKPIT CONTROLS			15.5	
83	SYSTEMS CONTROLS			132.7	
84					
85					
86	AUXILIARY POWER PLANT GROUP				67.9
87	INSTRUMENTS GROUP				27.9
88	HYDRAULIC & PNEUMATIC GROUP				37.8
89					
90	ELECTRICAL GROUP				205.4
91					
92	AVIONICS GROUP				295
93	EQUIPMENT				
94	INSTALLATION				
95					
96	ARMAMENT GROUP				
97	FURNISHINGS & EQUIPMENT GROUP				396.5
98	ACCOMODATIONS FOR PERSONNEL			214	
99	MISCELLANEOUS EQUIPMENT			70.3	
100	FURNISHINGS			112.2	
101	EMERGENCY EQUIPMENT				
102					
103	AIR CONDITIONING GROUP				49
104	ANTI-ICING GROUP				28
105					
106	PHOTOGRAPHIC GROUP				
107	LOAD & HANDLING GROUP				40
108	AIRCRAFT HANDLING			20	
109	LOADING HANDLING			20	
110	BALLAST				
111	MANUFACTURING VARIATION (NOTE: INCLUDES & 2.5% WEIGHT GROWTH)				203
112	TOTAL CONTRACTOR CONTROLLED				
113	TOTAL GFAI				
114	TOTAL WEIGHT EMPTY (NOTE: DRY EMPTY WEIGHT)				3790

115	LOAD CONDITION						PRIMARY
116							
117	CREW (NO. 2)						181.9
118	PASSENGERS (NO. 19)						1551.3
119	FUEL LOCATION TYPE						
120	UNUSABLE						14
121	INTERNAL						533
122							533
123							
124							
125	EXTERNAL						
126							
127							
128	OIL						
129	TRAPPED						10.4
130	ENGINE						41.6
131							
132	FUEL TANKS (LOCATION)						
133	WATER INJECTION FLUID (GALS)						
134							
135	BAGGAGE						344.7
136	CARGO						
137							
138	GUN INSTALLATIONS						
139	GUNS LOCAT FIX OR FLEX QUANTITY CALIBER						
140							
141							
142	AMMO						
143							
144							
145	SUPP'TS						
146	WEAPONS INSTALL						
147							
148							
149							
150							
151							
152							
153							
154							
155							
156							
157							
158							
159							
160							
161							
162	SURVIVAL KITS						
163	LIFE RAFTS						
164	OXYGEN						
165	MISC.						
166							
167							
168	TOTAL USEFUL LOAD						3209.9
169	WEIGHT EMPTY	(DRY EMPTY WEIGHT)					3790
170	GROSS WEIGHT						6999.9